PL ISSN 0028-3894

ASSOCIATION OF POLISH
NEUROPATHOLOGISTS
and
MEDICAL RESEARCH CENTRE,
POLISH ACADEMY OF SCIENCES

NEUROPATOLOGIA POLSKA

VOLUME 29 1991 NUMBER 1–2

WROCŁAW · WARSZAWA · KRAKÓW
ZAKŁAD NARODOWY IM. OSSOLIŃSKICH
WYDAWNICTWO POLSKIEJ AKADEMII NAUK

NEUROPATOLOGIA POLSKA

QUARTERLY

VOLUME 29 1991 NUMBER 1–2

EDITORIAL OFFICE

Medical Research Centre
ul. Dworkowa 3, 00-784 Warszawa, Poland, Phone: 49-54-10

The typescript of the present issue was delivered to the publisher 9.05.1991

Zakład Narodowy im. Ossolińskich – Wydawnictwo. Wrocław 1991.
Objętość: ark. wyd. 8,80; ark. druk. 7,38+0,25 wkł.; ark. A_1-10.
Wrocławska Drukarnia Naukowa. Zam. 1217/91

NEUROPAT. POL. 1991, 29, 1–2
PL ISSN 0028-3894

PAWEŁ P. LIBERSKI[1,2], RICHARD YANAGIHARA[2], CLARENCE J. GIBBS' JR[2], D. CARLETON GAJDUSEK[2]

EXPERIMENTAL CREUTZFELDT-JAKOB DISEASE: LIGHT MICROSCOPIC, IMMUNOHISTOCHEMICAL AND ULTRASTRUCTURAL STUDIES OF THE FUJISAKI STRAIN OF CREUTZFELDT-JAKOB DISEASE VIRUS IN NIH SWISS MICE

[1]Electron Microscopic Laboratory, Department of Oncology, School of Medicine, Lodz, Poland,
[2]Laboratory of Central Nervous System Studies, National Institute of Neurological Disorders and Stroke, National Institutes of Health, Bethesda, U.S.A.

Ultrastructural findings in mice terminally affected with the Fujisaki strain of Creutzfeldt-Jakob disease virus are reported. Spongiform vacuolation, extensive myelin and axonal lesions and neuroaxonal dystrophy accompanied by abundant astrocytic gliosis comprise the pattern of the pathological changes at the ultrastructural level. Neuronal intranuclear inclusions and swelling of the astrocytic and dendritic processes were unspecific findings also observed in control animals.

Key words: *Creutzfeldt-Jakob disease, Fujisaki strain virus, mouse, brain pathology, ultrastructure.*

The Fujisaki strain of Creutzfeldt-Jakob disease (CJD) virus passaged in mice has proved to be a useful tool in the study of the pathology of slow unconventional virus diseases, due to its short incubation time (Kingsbury et al. 1982). The development of lesions, white matter ultrastructural pathology, neuroaxonal dystrophy and the tubulovesicular structures have been previously described (Liberski et al. 1989a–d). We now report the ultrastructural findings in mice terminally affected with the Fujisaki strain of Creutzfeldt-Jakob disease virus. At this stage spongiform changes, myelin and axonal lesions accompanied by abundant astrocytic and macrophage reaction comprise the pattern of the neuropathologic changes.

MATERIAL AND METHODS

Animals, virus strain and inoculation procedures

Weanling, 4- to 6-week-old NIH Swiss mice (Animal Production Area, Frederic Cancer Research Facility, Frederick, MD) were inoculated either

intracerebrally with 0.03 ml of 10% brain homogenate obtained from mice affected with the Fujisaki strain of CJD virus, or intraocularly with 0.01 ml of the same homogenate (Tateishi et al. 1978; Kingsbury et al. 1982; Liberski et al. 1989a, b). The incubation periods were approximately 18 to 20 and 25 to 51 weeks for animals inoculated intracerebrally and intraocularly, respectively.

Histopathology

CJD-affected and sham inoculated mouse brains were fixed by perfusion (*vide infra*) or by immersion in 10% buffered formalin and embedded in paraffin. Sections 5 μm thick were stained with hematoxylin and eosin (HE). The vacuolar lesion profile was obtained by scoring (on a scale of 0–5) the severity of vacuolation in sections stained with HE and of astrocytosis with anti-GFAP polyclonal antibodies in the following brain regions according to Fraser and Dickinson (1973): 1. medulla; 2. cerebellum – gray matter; 3. midbrain; 4. hypothalamus; 5. thalamus; 6. hippocampus; 7. paratrigeminal body; 8/9. cerebral cortex. In addition, two other brain areas were assessed: 10. corpus callosum and 11. white matter of the cerebellum.

Immunohistochemistry

Representative paraffin-embedded sections adjacent to those stained with HE were stained for hypertrophic astrocytes by the avidin-biotin technique (Vector Laboratories, Burlingame, Calif.), using a 1 : 100 dilution of a polyclonal rabbit antiserum prepared against bovine glial fibrillary acidic protein (GFAP) (Dako, Calif.). Sections were incubated in 0.3% hydrogen peroxide for 30 min, followed by 20% normal goat serum in PBS for 20 min, before incubation with the primary antibody at 4°C overnight. Sections were then incubated successively with biotinylated secondary antibody and the ABC reagent of 1 h at room temperature. Color was developed using 0.05% diaminobenzidine (Sigma, St. Louis) with 0.01 hydrogen peroxide for 5 – 10 min. Following 5 min rinse in tap water, sections were counterstained with Harris' hematoxylin for 8 min.

Electron microscopy

Mice were killed by intracardiac perfusion with 180 ml of 10% paraformaldehyde and 1.5% glutaraldehyde prepared in phosphate buffer (pH 7.4). Sham-inoculated animals were used as controls. After perfusion the mice were kept at 4°C for 2 to 4 h. Brains were removed and several 1 mm^3 samples were dissected from parietal cortex and adjacent corpus callosum. Samples were postfixed in 1% osmium tetroxide, dehydrated through graded ethanols and propylene oxide and embedded in Embed (Electron Microscopy Sciences, Washington). Semithin sections were stained with methyl blue. Ultrathin sections stained with lead citrate and uranyl acetate were examined with Hitachi 11A, Philips 300 and Zeiss EM109 transmission electron microscopes.

RESULTS

Mice infected with the Fujisaki strain of CJD virus developed clinical signs 18 to 20 weeks after intracerebral inoculation and 25 to 51 weeks after intraocular injection. The clinical signs consisted of ruffled fur covered with urine and faces, rigidity, slowness and inactivity. The responses to external stimuli were delayed and "plastic" tail was observed.

Control mice

The vast majority of neurons, their processes and glial cells appeared normal in sham-inoculated mice. A careful search revealed several scattered dilated and swollen astrocytic processes and somata, located primarily around otherwise normal appearing blood vessels. Swollen dendrites showing a decrease of subcellular organelles, as well as neurites containing accumulations of normal organelles (mostly mitochondria), were occasionally seen. Several type of intranuclear, paracrystalline inclusions were observed, the most frequent being fibrillary inclusions, less often paracrystalline rods and lattices (Fig. 1). The lattices rarely formed ring-like structures.

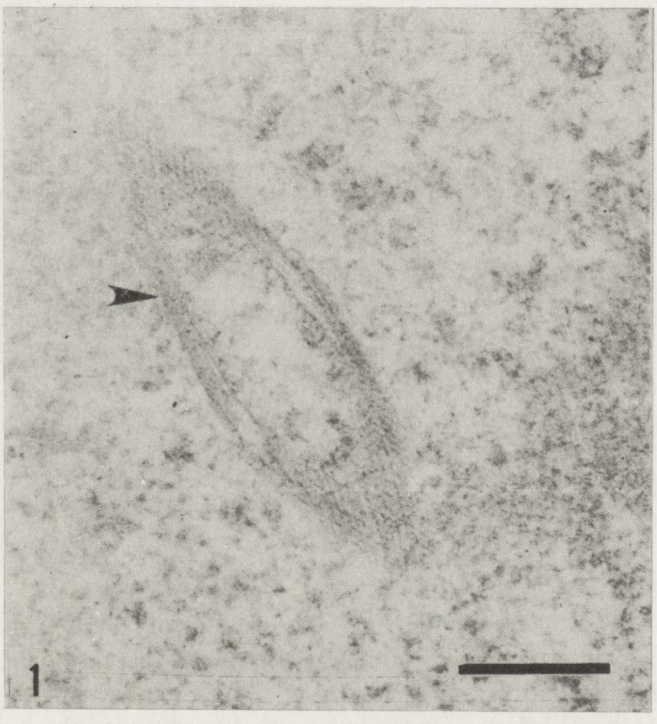

Fig. 1. Ring-like paracrystalline inclusion (arrowhead) in neuronal nucleus of sham-inoculated mice. Bar = 0.5 μm

CJD-affected mice

The lesion profile

The lesion profile for NIH Swiss mice infected with the Fujisaki strain of CJD virus is shown in Figure 2, while representative illustrations of spongiform changes and astrocytosis are shown in Figures 3a–d. Vacuolation scores revealed

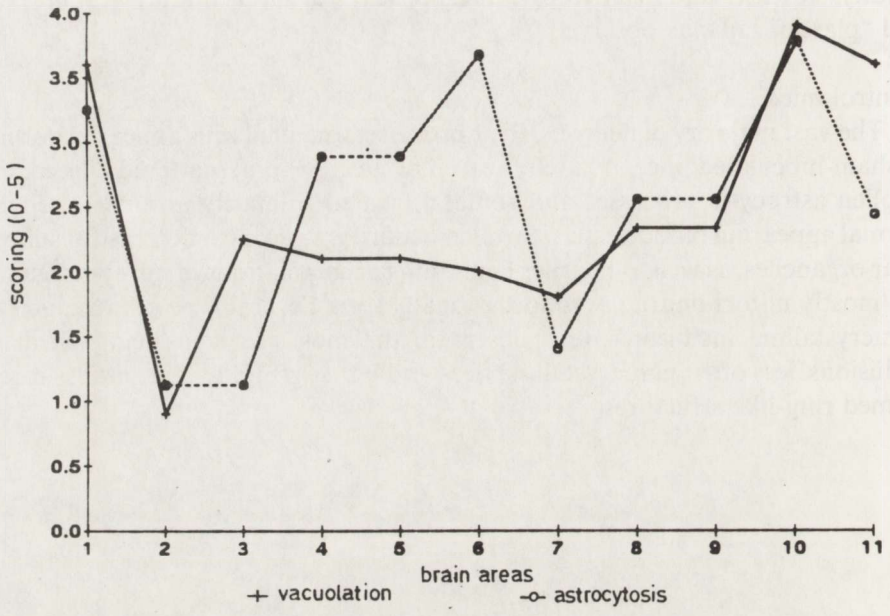

Fig. 2. Lesion profile for NIH Swiss mice infected with the Fujisaki strain of CJD virus based on assessment of spongiform changes (+) and astrocytosis (o). Note that astrocytosis surpasses the spongiform change in areas 4–6

that the most affected white matter regions were corpus callosum and cerebellum, while medulla, thalamus and hypothalamus were the most affected regions of gray matter.

The corresponding lesion profile based on a GFAP-immunopositive scoring system (Fig. 2) showed that astrocytosis, while approximately of the same magnitude as spongiosis in most regions, surpassed it in the most affected gray areas (4–6).

Electron microscopy

Two distinct types of spongiform vacuoles were observed in both parietal cortex and adjacent corpus callosum. The first type was found in myelinated axons, seen either in axoplasm (and surrounded by a narrow ring of it) or within the myelin sheath itself (Fig. 4). In the latter situation the vacuoles were the result of splitting of otherwise normal myelin at either the major dense or the intraperiod lines. Vacuoles contained secondary vacuoles (i.e. vacuoles within

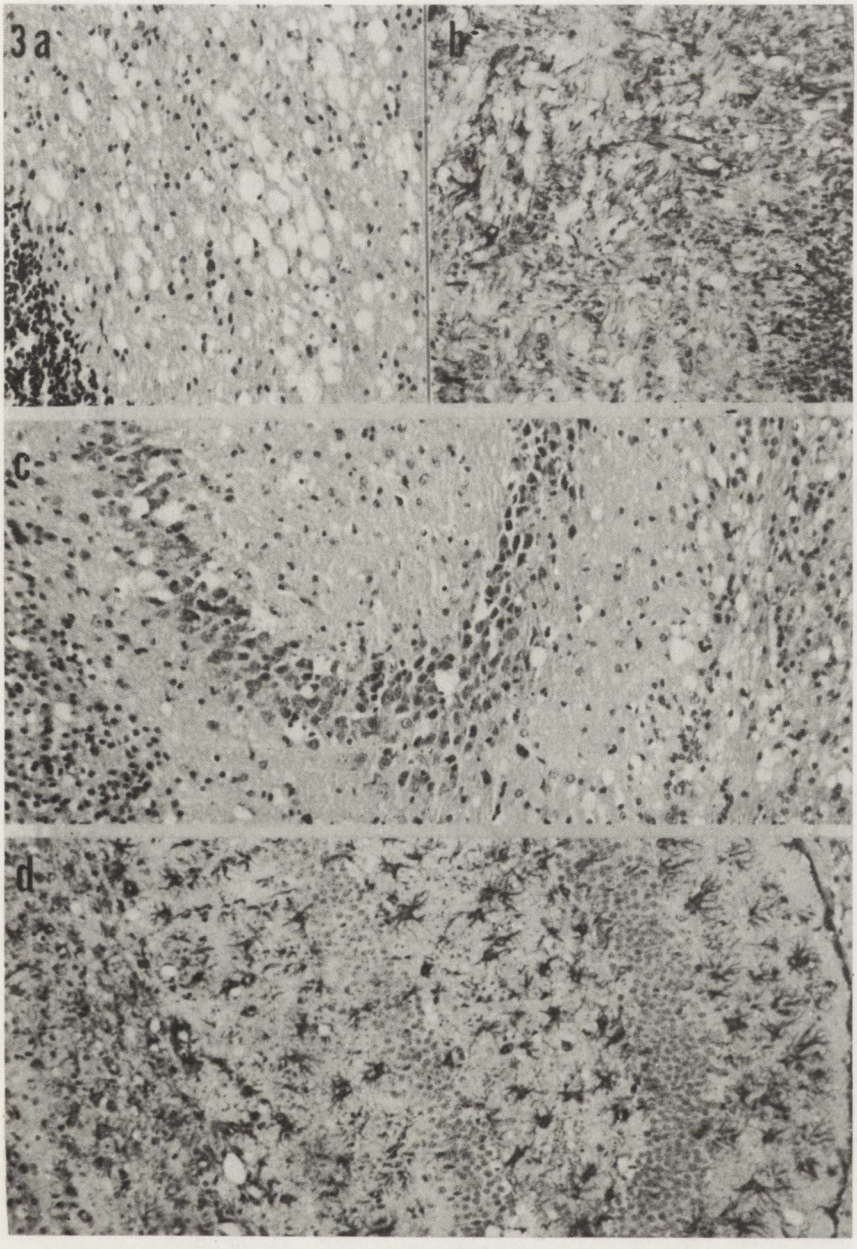

Fig. 3. Spongiform changes and astrocytosis in cerebellum (*a* – HE, *b* – GFAP immunostaining) and hippocampus (*c* – HE, *d* – GFAP immunostaining) of CJD-affected NIH Swiss mice. × 160

a larger vacuole), vesicles and curled membrane fragments. The shrunken axons with axoplasm of normal appearance were adherent to the innermost layer of the myelin sheath, occasionally by only a thin "neck". Some axons were still covered with a few layers of myelin. The myelin sheath lining the vacuole was clearly part

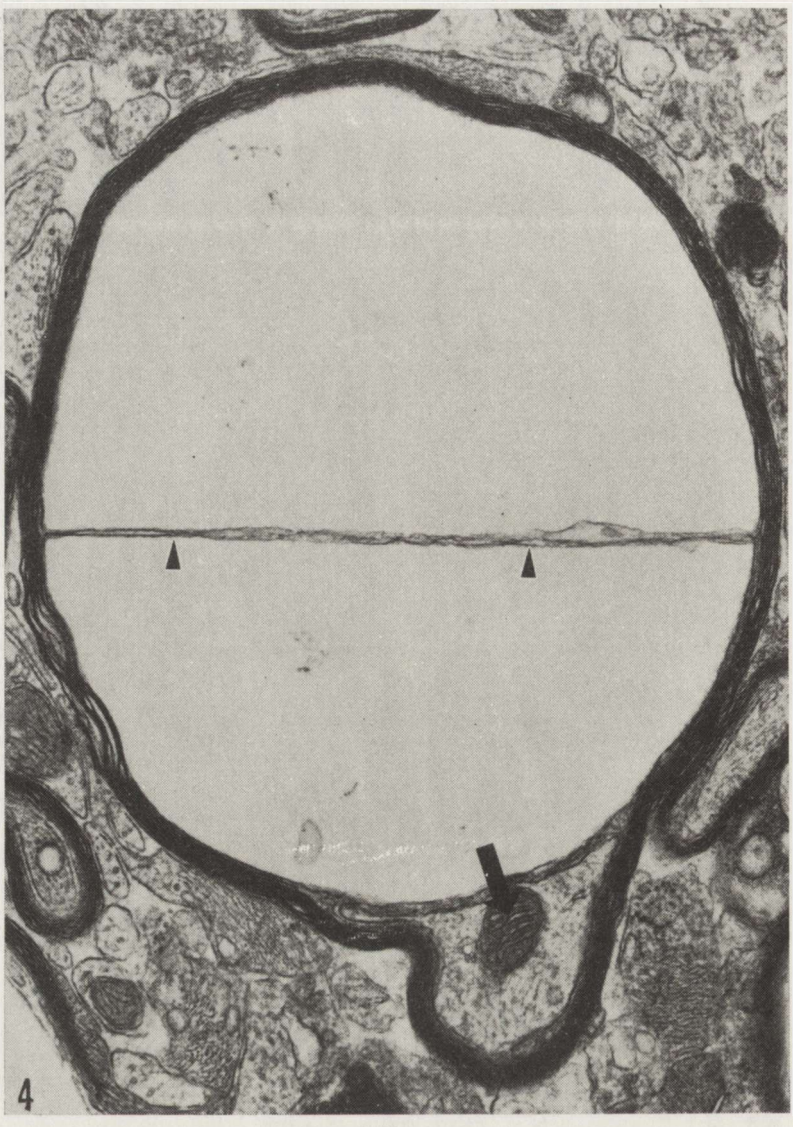

Fig. 4. Vacuole within myelinated axon in the parietal cortex of a mouse 18 weeks after intracerebral inoculation with the Fujisaki strain of CJD virus. Note the shrunken axon attached to the innermost lamella of the myelin sheath (arrow) and membraneous septum (arrowheads). × 12 500

of that covering the axon. The vacuoles within the myelin sheath were frequently ensheathed by astrocytic or macrophage processes, thus creating the impression that they were being digested by these cells (Fig. 5).

The second type of vacuole was seen within unmyelinated neurites and, predominantly, dendrites (Fig. 6). Occasionally they reached larger dimensions and several affected processes contributed to their formation. The number of

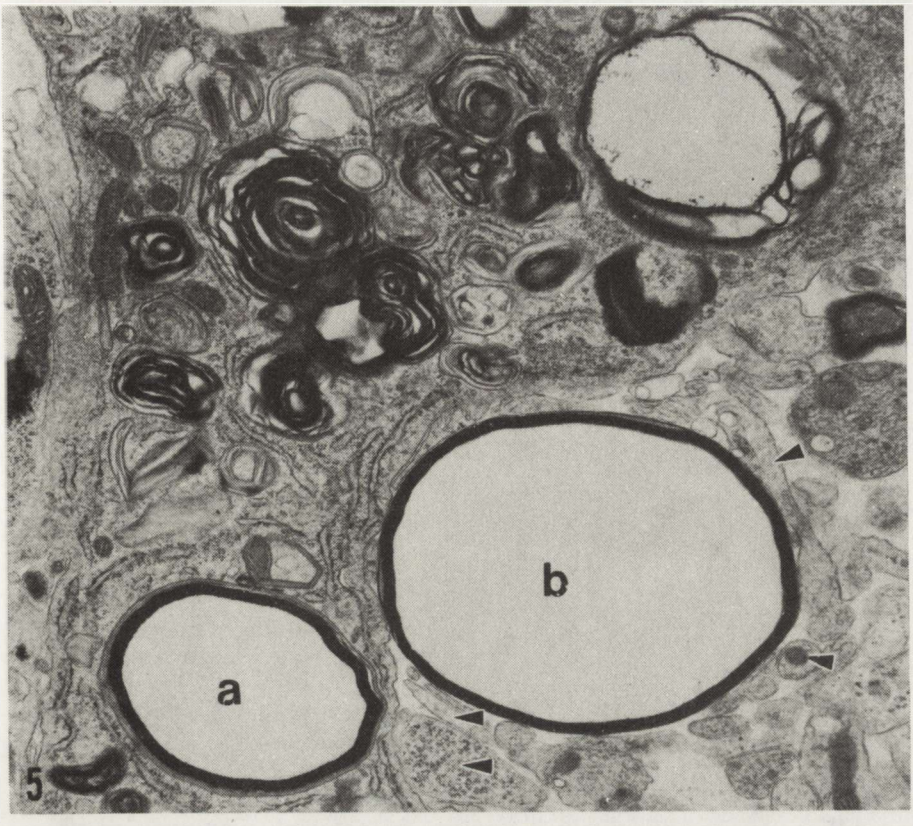

Fig. 5. Two vacuoles (a and b) within myelinated processes in the corpus calosum of a mouse 18 weeks after intracerebral inoculation with the Fujisaki strain of CJD virus. Note that vacuole "a" is completely ensheated by macrophage process and vacuole "b" is surrounded by numerous macrophage processes (arowheads). Note also myelin debris at the top of the Figure. ×9200

secondary vacuoles and curled membrane fragments were higher in these vacuoles than in those within myelinated processes.

Spongiform vacuoles were accompanied by an exuberant astrocytic and macrophage reaction. Macrophages contained numerous mitochondria, abundant rough endoplasmic reticulum and secondary lysosomes filled with digested myelin debris, electron-dense material, myelinated axon and vacuole fragments and lyre-like paracrystalline bodies (Fig. 7). Astrocytes and their processes were prominent, with a myriad of glial filaments and numerous mitochondria (Fig. 8). Astrocytes with digested cellular fragments were frequently observed. Furthermore, astrocytic processes forming a complicated network around damaged axons were seen (Fig. 9).

Neuroaxonal dystrophy (NAD) was a prominent finding. Two major categories of dystrophic axons according to previously published criteria (Lampert 1967; Liberski 1987; Gibson, Liberski 1987; Liberski et al. 1989c) were seen. The

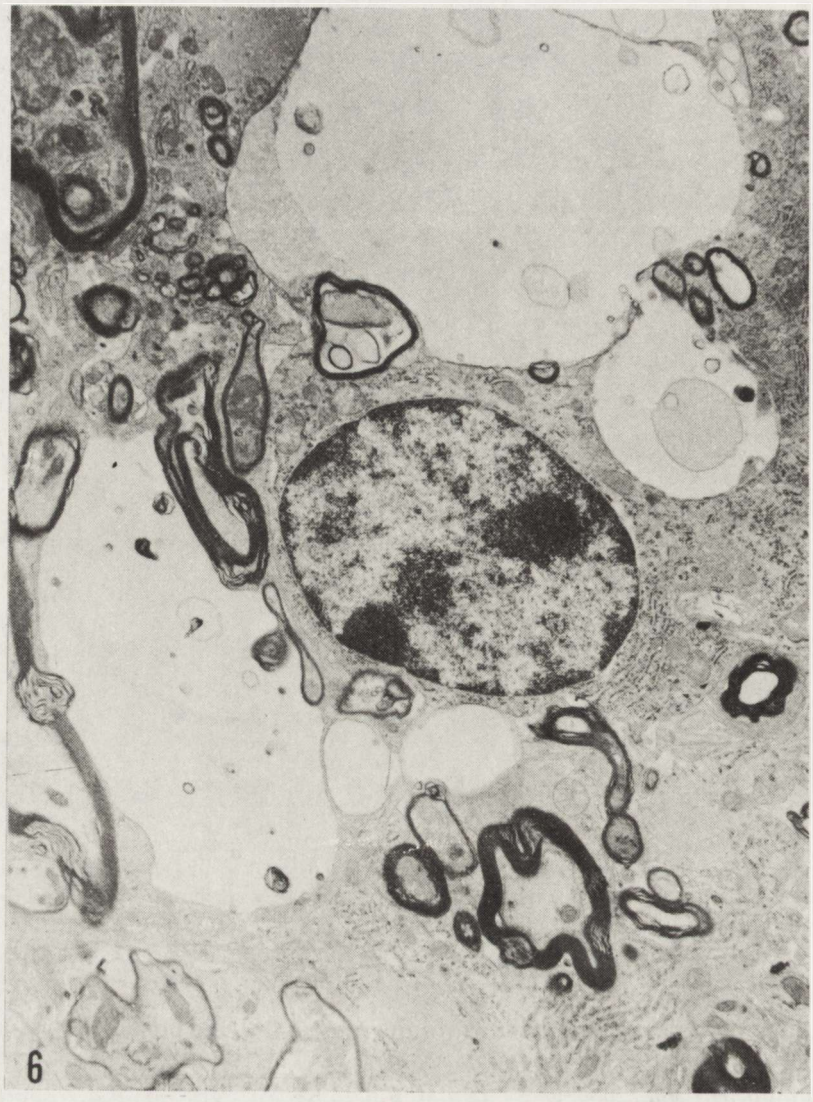

Fig. 6. Numerous vacuoles within unmyelinated processes in the parietal cortex of a mouse 18 weeks after intracerebral inoculation with the Fujisaki strain of CJD virus. Note a macrophage in a center of a Figure. × 3900

first type contained numerous pleomorphic, electron-dense bodies (Fig. 10). Occasionally, the dystrophic neurites were separated by membraneous septa into separate compartments containing subcellular organelles. The second type contained abundant masses of neurofilaments (Fig. 11). Dystrophic neurites with both electron-dense bodies and neurofilaments were occasionally observed.

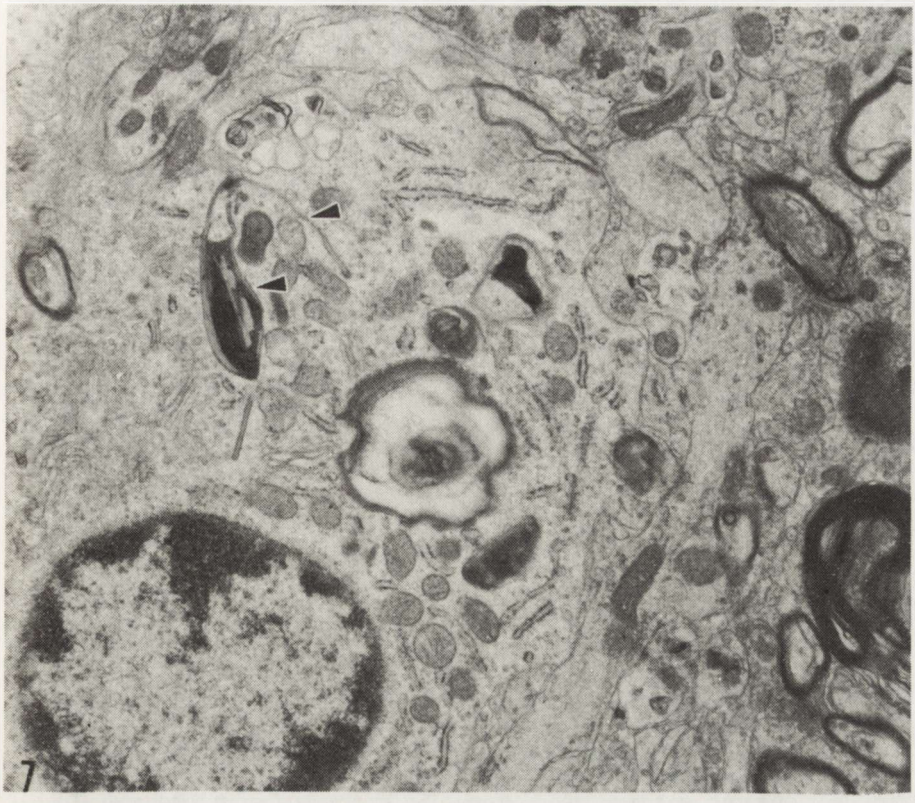

Fig. 7. Macrophage in the parietal cortex of a mouse 18 weeks after intracerebral inoculation with the Fujisaki strain of CJD virus. Note abundant mitochondria and a lyre-like paracrystalline inclusion (arrowheads). × 10 000

DISCUSSION

Spongiform changes

Two types of membrane-bound vacuoles were observed at the terminal stage of CJD-affected mice. The cellular element responsible for the spongiform changes seen at the light microscopic level is yet to be determined (Masters, Richardson 1978). Almost every cellular element of the central nervous system has been implicated. Intracellular vacuoles have been ascribed to astrocytic processes alone (Field, Raine 1964; Martin, Vial 1964), to astrocytic processes and neurons (Gonatas et al. 1965), and more recently, to dendrites, axonal terminals and preterminals (Lampert et al. 1969, 1971). In experimental CJD in guinea pigs and hamsters the vacuoles have been ascribed almost exclusively to neuronal elements (Manuelidis, Manuelidis 1979; Kim, Manuelidis 1983, 1986) and our study strongly supports that interpretation. Earlier studies showing vacuoles in astrocytes suffered from suboptimal fixation which itself causes astrocytic swelling.

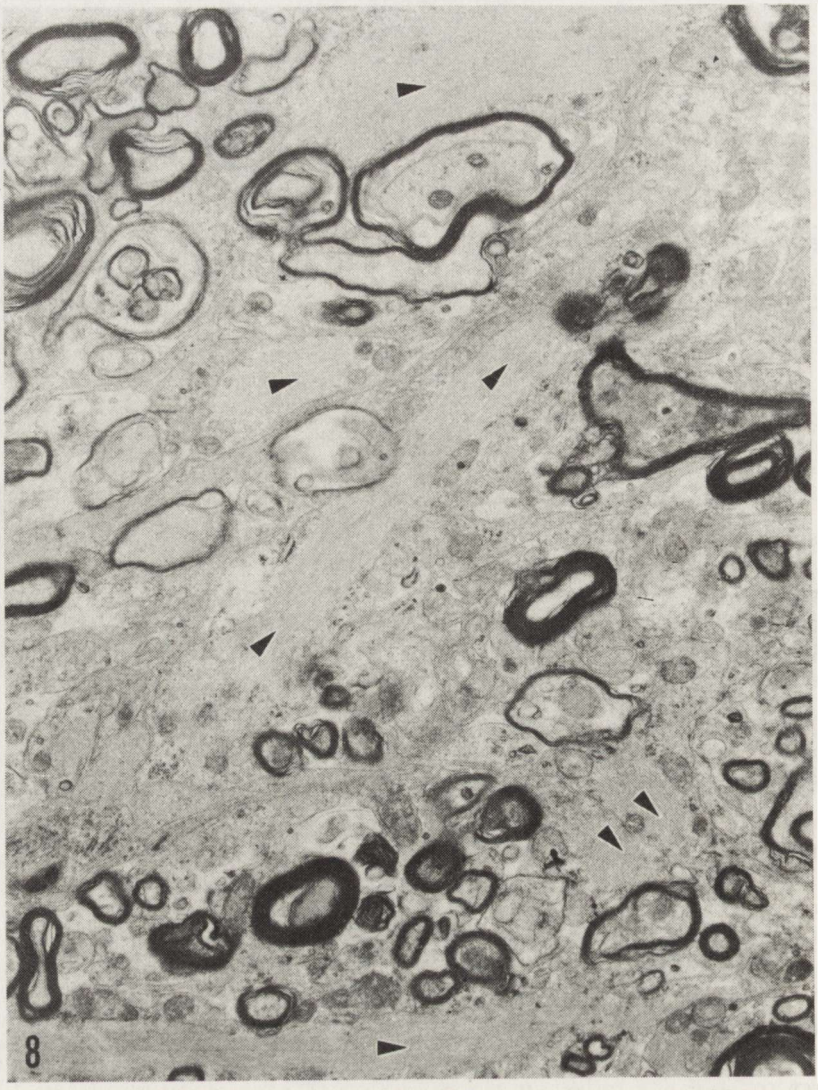

Fig. 8. Abundant astrocytic processes (arrowheads) in the corpus callosum of a mouse 18 weeks after intracerebral inoculation with the Fujisaki strain of CJD virus. × 5600

Myelin and axonal pathology

CJD has been regarded as a classic example of polioencephalopathy, i.e. a neurodegenerative disorder exclusively of the gray matter (Masters, Gajdusek 1982). While slight myelin pallor and focal accumulations of the myelin degradation products were observed in experimental kuru and CJD two decades ago (Beck et al. 1969, 1973) the vacuolation of myelinated axons attracted little attention and was regarded as a secondary phenomenon, i.e. Wallerian degenera-

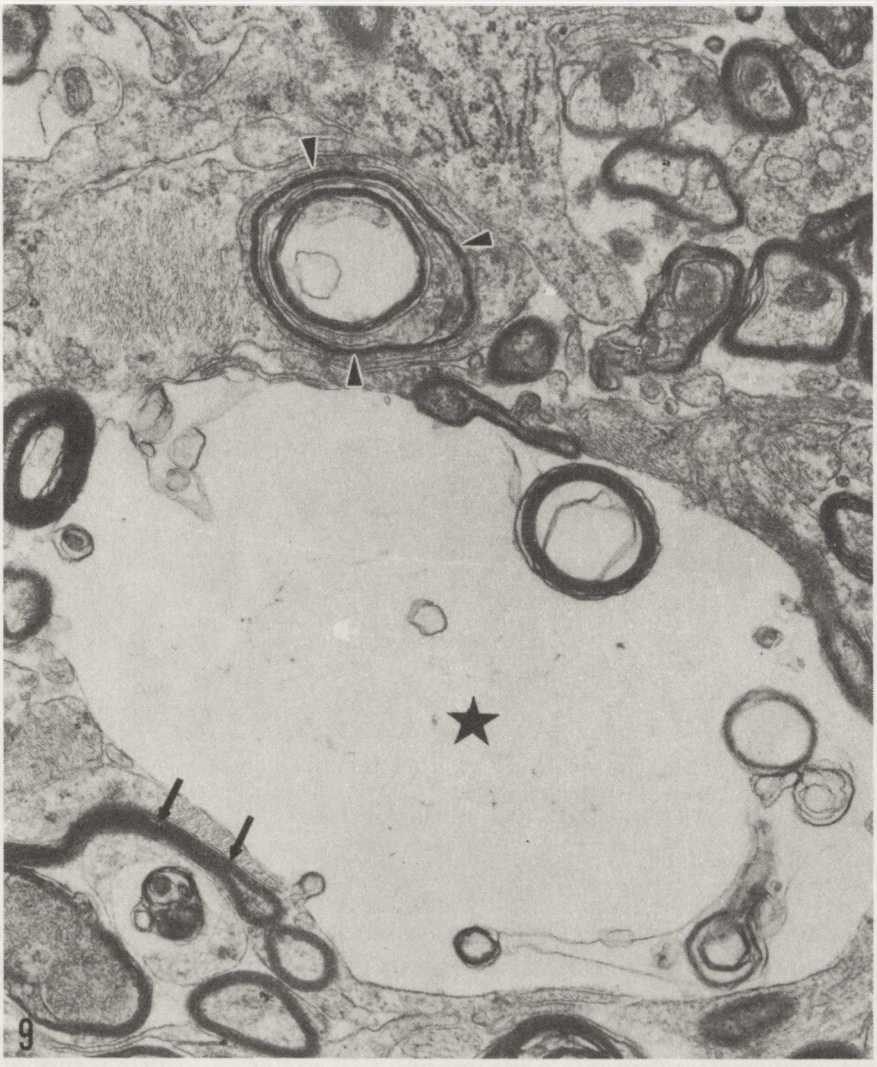

Fig. 9. Myelinated axon surrounded by a network of astrocytic processes (arrowheads) in the corpus callosum of a mouse 18 weeks after intracerebral inoculation with the Fujisaki strain of CJD virus. Note separation of myelin sheath into concentric bands by penetrating cellular processes. Note also a vacuole within unmyelinated process (asterisk) and collapsed myelin. × 10000

tion. The formation of intramyelin vacuoles (myelin balloning) is, however, a non specific phenomenon as documented by its presence in a diverse variety of naturally occurring and experimentally induced pathologic conditions (Lampert, Cressman 1966; Hemm, Carlton 1971; Watanabe, Bingle 1972; Tellez-Nagel et al. 1977; Agamanolis et al. 1978; Shehan et al. 1981). In most experimental situations the formation of intramyelin vacuoles is mostly accomplished via splitting at the intraperiod lines. However, in the model presented here splitting at both the

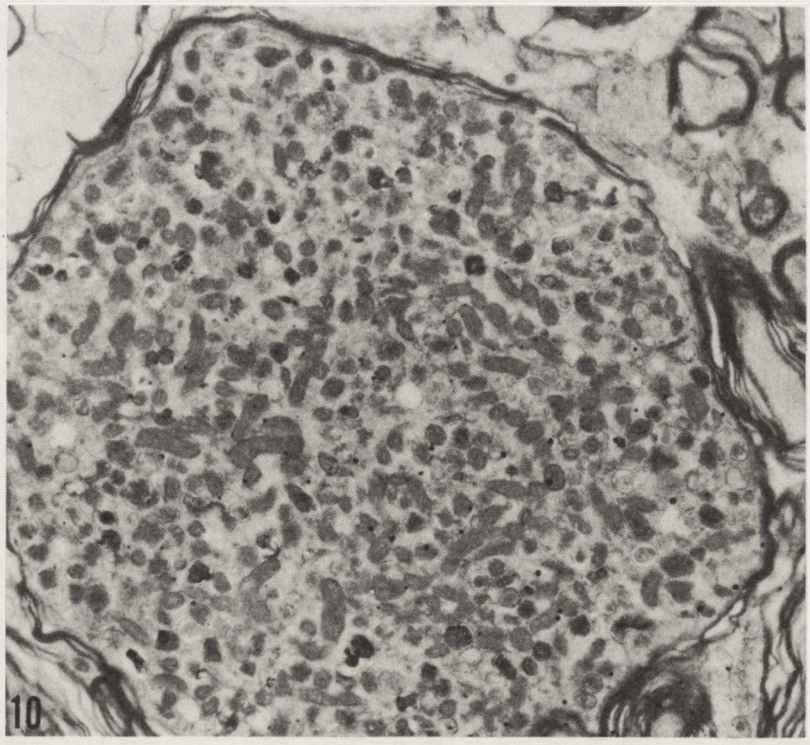

Fig. 10. Large myelinated dystrophic neurite in the parietal cortex of a mouse 18 weeks after intracerebral inoculation with the Fujisaki strain of CJD virus. Note plethora of abnormal subcellular organelles, mostly mitochondria. × 8200

major dense and the intraperiod lines was observed. Interestingly, when cultures of the mammalian peripheral nervous system were exposed to a lethal dose of sodium cyanide, the myelin split first at the intraperiod lines and later at the major dense lines (Masurovsky, Bunge 1971). Thus, the two mechanisms of intramyelin vacuoles formation are not mutually exclusive as further supported by diphteria toxin-induced demyelination in cats and rabbits (Wiśniewski, Raine 1971). Furthermore, the intramyelin vacuolation accompanied by exuberant macrophage and astrocytic reaction is a neuropathologic hallmark of certain models of experimental allergic encephalomyelitis (EAE) and multiple sclerosis (MS) (Lampert 1965; Raine 1978, 1984; Kusaka et al. 1985). The separation of myelin lamellae either at the major dense or intraperiod lines contributes to the myelin ballooning in these conditions. While the infiltration of white matter with mono- and polymorphonuclear cells obviously did not occur in mice infected with the Fujisaki strain of CJD virus reported here, the myelin ballooning and abundant macrophage and astrocytic reaction are common findings for both the EAE, MS and CJD.

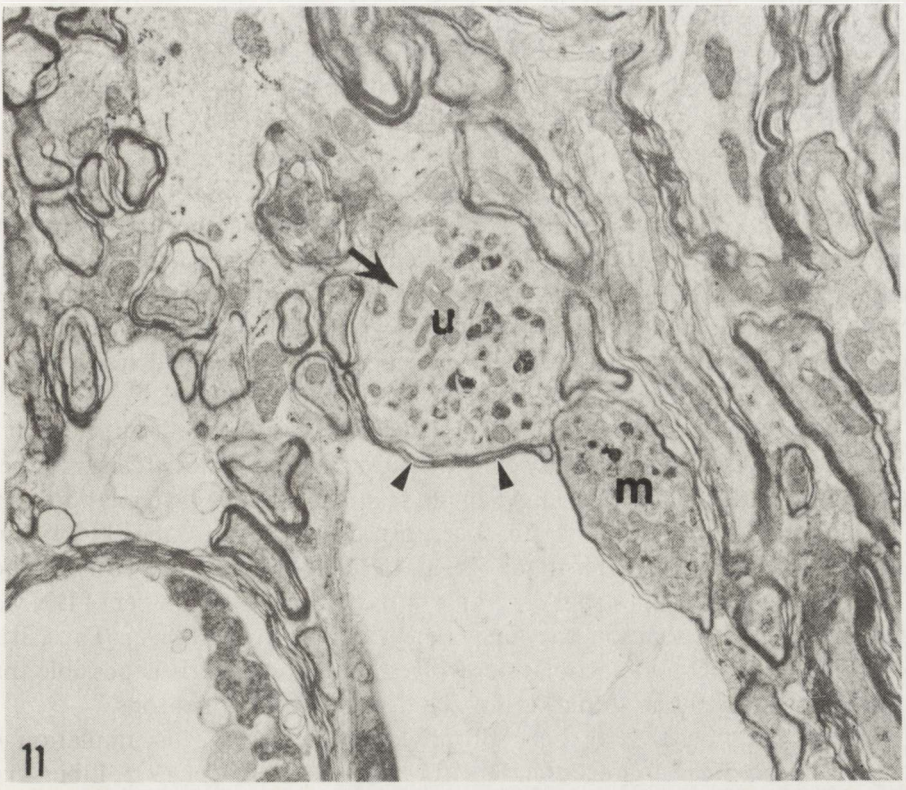

Fig. 11. Unmyelinated (u) and myelinated (m) dystrophic neurites in the corpus callosum of a mouse 18 weeks after intracerebral inoculation with the Fujisaki strain of CJD virus. Note the neurofilaments accumulated within unmyelinated neurite (arrow) and collapsed myelin sheath in close proximity to that neurite (arrowheads). × 5600

The mechanism(s) of myelin vacuolation in demyelinating diseases and CJD is unknown. Recently, Selmaj and Raine (1988) produced myelin vacuolation, ultrastructurally indistinguishable from that presented here, in mouse spinal cord culture exposed to the human recombinant tumor necrosis factor (TNF). While the biological significance of this finding is unknown these investigators proposed a hypothesis that TNF, a leukolysin released from activated macrophages and astrocytes (Robbins et al. 1987), is directly involved in myelin breakdown in several demyelinating disorders. The nearly identical ultrastructural pathology of myelinated fibers in mice infected with the Fujisaki strain of CJD virus, reanalysed against a background of previously published electronmicrographs (Field, Raine 1964; Lampert et al. 1969; Manuelidis, Manuelidis 1979; Kim, Manuelidis 1986; Liberski et al. 1989d) suggests that TNF plays a role in the pathogenesis of myelin vacuolation in subacute spongiform virus encephalopathies. Furthermore, we have shown that hypertrophic astrocytes in mice infected with the Fujisaki strain of CJD expressed the TNF.

Neuronal dystrophy (NAD)

NAD is an important feature of ultrastructural pathology of subacute spongiform virus encephalopathy (SSVE) and it probably results from impairment of slow axonal transport (Dustin, Flament-Durand 1982). The ultrastructure of dystrophic neurites (DN), which form the basis of NAD is indistinguishable in pathologic and nonpathologic conditions (Jellinger 1973; Gibson, Liberski 1987; Liberski 1987; Liberski et al. 1989b, c). DN, filled with pleomorphic inclusions, are virtually identical to the *reactive axonal enlargements* first reported by Lampert (1967). Lampert (1967) reserved this term rather for structures filled with branching tubules and proliferating plasma membranes. However, both subcategories of DN overlap, and, in our experience, they form only extreme ends of the spectrum.

The significance of NAD in transmissible brain amyloidoses is unclear. It is widespread and appears relatively early in the incubation period (Gibson, Liberski 1987; Liberski et al. 1989b, c). An increase in DN precedes vacuolation, as in mice infected with the ME7 strain of scrapie virus (Gibson, Liberski 1987) or follows it, as in mice infected with the 22C and 79A strains of scrapie virus. In mice infected with the Fujisaki strain of scrapie virus, an increased number of DN was observed when vacuolation was first seen (Liberski et al. 1989c). Thus, it is plausible that NAD and vacuolation evolved independently. It is possible that NAD is an ultrastructural marker for the depopulation of neurons.

Several hypotheses have been proposed to explain the accumulation of abnormal subcellular organelles in DN (for review see Jellinger 1973; Liberski et al. 1989b, c). Impairment of slow axonal transport has been postulated recently to be the final common pathway in SSVE, Alzheimer's disease and motor neuron disease (Gajdusek 1985). Interference with slow axonal transport is directly responsible for the formation of DN in ligated sciatic nerve, in acrylamide encephalopathy, and in transsected spinal cord axons (Pleasure et al. 1969; Kao et al. 1971; Griffin et al. 1977). In the latter situation, the electron microscopic pattern of spheroid formation is strikingly similar to that encountered in experimental CJD and scrapie. Thus, this pattern of neuronal degeneration is nearly identical, irrespective of cause.

Several conclusions can be drawn from this study. The ultrastructural pathology of CJD is more diverse than previously recognized and vacuolation is only a part of it. NAD, reflecting neuronal degeneration, is an important part of the ultrastructural pattern, and axonal and myelin damage is easily recognized, at least in this experimental model. However, more experimental work is necessary to evaluate how often the NAD and axonal and myelin pathology can be found in different models of naturally occurring and experimentally induced spongiform encephalopathies, and which structure is the primary lesion for the infectious virus.

Acknowledgements. Dr P. P. Liberski is the recipient of a grant from the Polish Academy of Sciences (VIII/40). The skilful technical assistance of Ms. Elżbieta Naganska, Ms. Leokadia Romanska and Mr. Ryszard Kurczewski is gratefully acknowledged.

DOŚWIADCZALNA CHOROBA CREUTZFELDA-JAKOBA (CJD): BADANIA HISTOLOGICZNE, IMMUNOHISTOCHEMICZNE I ULTRASTRUKTURALNE U MYSZY Z CJD WYWOŁANĄ PRZEZ SZCZEP FUJISAKI

Streszczenie

Przedstawiono wyniki badań ultrastrukturalnych wykonanych w terminalnym okresie eksperymentalnej CJD u myszy. Zmiany gąbczaste, rozległe zmiany patologiczne aksonu i osłonki mielinowej oraz dystrofia aksonalna stanowiły w badanym modelu podstawowe elementy ultrastrukturalne procesu patologicznego. Wtręty śródjądrowe natomiast oraz obrzmienie astrocytów i dendrytów traktowano jako zmiany nieswoiste, ponieważ obserwowano je także u zwierząt kontrolnych.

REFERENCES

1. Agamanolis D, Victor H, Harris JW, Hines JD, Chester EM, Kark J: An ultrastructural study of subacute combined degeneration of the spinal cord in vitamin B12 deficient Rhesus monkeys. J Neuropathol Exp Neurol, 1978, 37 273–299.
2. Beck E, Daniel PM, Matthews WB, Stevens DL, Alpers MP, Asher DM, Gajdusek DC, Gibbs CJ Jr: Creutzfeldt-Jakob disease. The neuropathology of a transmission experiment. Brain, 1969, 92, 699–716.
3. Beck E, Daniel PM, Asher DM, Gajdusek DC, Gibbs CJ Jr: Experimental kuru in chimpanzee: a neuropathological study. Brain, 1973, 96, 441–462.
4. Dustin P, Flament-Durand J: Disturbances of axoplasmic transport in Alzheimer's disease. In: Axoplasmic transport in physiology and pathology. Eds: DG Weiss, A Gorio. Springer, Berlin–Heidelberg–New York, 1982, pp 131–136.
5. Field EJ, Raine CS: An electron microscopic study of scrapie in the mouse. Acta Neuropathol (Berl), 1964, 4, 200–211.
6. Fraser H, Dickinson AG: The sequential development of the brain lesions of scrapie in three strains of mice. J Comp Pathol, 1968, 78, 301–311.
7. Gajdusek DC: Hypothesis: interference with axonal transport of neurofilaments as a common pathogenetic mechanism in certain diseases of the central nervous system. New Engl J Med, 1985, 312, 714–719.
8. Gibson PH, Liberski PP: An electron and light microscopic study of the numbers of dystrophic neurites and vacuoles in the hippocampus of mice infected with scrapie. Acta Neuropathol (Berl), 1987, 73, 379–382.
9. Gonatas NK, Terry RD, Weiss M: Electron microscopic study in two cases of Jakob-Creutzfeldt disease. J Neuropathol Exp Neurol, 1965, 24, 575–598.
10. Griffin JW, Price DL, Engel WK, Drachman DB: The pathogenesis of reactive axonal swellings: role of axonal transport. J Neuropathol Exp Neurol, 1977, 36, 214–227.
11. Hemm DM, Carlton WW: Ultrastructural changes of cuprizone encephalopathy in mice. Toxicol Appl Pharmacol, 1971, 18, 869–882.
12. Jellinger K: Neuroaxonal dystrophy: its natural history and related disorders. In: Progress in Neuropathology. Ed: HM Zimmerman. Grune and Stratton, New York, 1973, pp 129–180.
13. Kao CC, Chang LW, Bloodworth JMB: Electron microscopic observations in the mechanism of terminal club formation in transsected spinal cord axons. J Neuropathol Exp Neurol, 1971, 36, 140.
14. Kim JH, Manuelidis EE : Ultrastructural findings in experimental Creutzfeldt-Jakob disease in guinea pigs. J Neuropathol Exp Neurol, 1983, 42, 29–43.
15. Kim JH, Manuelidis EE: Serial ultrastructural studies of experimental Creutzfeldt-Jakob disease in guinea pigs. Acta Neuropathol (Berl), 1986, 69, 81–90.

16. Kingsbury DT, Smeltzer DA, Amyx HL, Gibbs CJ Jr, Gajdusek DC: Evidence for an unconventional virus in mouse adapted strain of Creutzfeldt-Jakob disease. Infect Immunol, 1982, 37, 1050–1053.
17. Kusaka H, Hirano A, Bornstein MB, Raine CS: Fine structure of astrocytic processes during serum-induced demyelination. J Neurol Sci, 1985, 69, 255–267.
18. Lampert PW: Demyelination and remyelination in experimental allergic encephalitis. J Neuropathol Exp Neurol, 1965, 24, 371–385.
19. Lampert PW: A comparative electron microscopic study of reactive, regenerating, degenerating and dystrophic terminal axons. J Neuropathol Exp Neurol, 1967, 28, 353–370.
20. Lampert PW, Cressman MR: Fine structural changes of myelin sheaths after axonal degeneration in the spinal cord of rats. Am J Pathol, 1966, 49, 1139–1155.
21. Lampert PW, Earle KM, Gibbs CJ Jr, Gajdusek DC: Experimental kuru encephalopathy in chimpanzees and spider monkeys. J Neuropathol Exp Neurol, 1969, 28, 353–370.
22. Lampert PW, Gajdusek DC, Gibbs CJ Jr: Experimental spongiform encephalopathy (Creutzfeldt-Jakob disease) in chimpanzees. J Neuropathol Exp Neurol, 1971, 30, 20–32.
23. Liberski PP: Electron microscopic observations on dystrophic neurites in hamster brains infected with the 263K strain of scrapie. J Comp Pathol, 1987, 97, 35–39.
24. Liberski PP, Yanagihara R, Gibbs CJ Jr, Gajdusek DC: Appearance of tubulovesicular structures in Creutzfeldt-Jakob disease and scrapie precedes the onset of clinical disease. Acta Neuropathol (Berl), 1989a, 79, 349–354.
25. Liberski PP, Yanagihara R, Gibbs CJ Jr, Gajdusek DC: Neuronal dystrophy: an ultrastructural link between subacute spongiform virus encephalopathies and Alzheimer's disease. In: Alzheimer's disease and related disorders. Eds: K Iqbal, HM Wiśniewski, B Winblad. AR Liss, New York, 1989b, pp. 549–558.
26. Liberski PP, Yanagihara R, Gibbs CJ Jr, Gajdusek DC: Scrapie as a model for neuroaxonal dystrophy: ultrastructural studies. Exp Neurol, 1989c, 106, 133–141.
27. Liberski PP, Yanagihara R, Gibbs CJ Jr, Gajdusek DC: White matter ultrastructural pathology of experimental Jakob-Creutzfeldt disease in mice. Acta Neuropathol (Berl), 1989d, 79, 1–9.
28. Manuelidis EE, Manuelidis L: Clinical and morphological aspects of transmissible Creitzfeldt-Jakob disease. In: Progress in Neuropathology. Ed: HM Zimmerman, vol 4, Raven Press, New York, 1979, pp 1–26.
29. Martin O, Vial DJ: Neuropathological and ultrastructural findings in two cases of subacute spongiform encephalopathy. Acta Neuropathol (Berl), 1964, 4, 218–229.
30. Masters CL, Gajdusek DC: The spectrum of Creutzfeldt-Jakob disease and the virus induced subacute spongiform encephalopathies. In: Recent Advances in Neuropathology. Ed: JB Cavanagh. Churchill Livingstone, Edinburgh, 1982, pp 139–163.
31. Masters CL, Richardson EP: Subacute spongiform encephalopathy (Creutzfeldt-Jakob disease). The nature and progression of spongiform change. Brain, 1978, 101, 333–334.
32. Masurovsky EB, Bunge RP: Patterns of myelin degeneration following the rapid death of cells in cultures of peripheral nervous tissue. J Neuropathol Exp Neurol, 1971, 30, 311–324.
33. Pleasure DE, Mishler KC, Engel WK: Axonal transport of proteins in experimental neuropathies. Science, 1969, 166, 524–525.
34. Raine CS: Pathology of demyelination. In: Physiology and pathobiology of axons. Ed: SG Waxman. Raven Press, New York, 1978, pp 283–310.
35. Raine CS: Biology of disease. Analysis of autoimmune demyelination: its impact upon multiple sclerosis. Lab Invest, 1984, 50, 283–310.
36. Robbins DS, Shirazi Y, Drysdake BE, Liberman A, Shin HS, Shin ML: Production of cytotoxic factor for oligodendrocytes by stimulated astrocytes. J Immunol, 1987, 139, 2593–2597.
37. Selmaj KW, Raine CS: Tumor necrosis factor mediates myelin and oligodendrocytes damage *in vitro*. Ann Neurol, 1988, 23, 339–347.
38. Shrenan BJ, Barett PN, Atkins GJ: Demyelination in mice resulting from infection with a mutant form of Semliki virus. Acta Neuropathol (Berl), 1981, 53, 129–136.

39. Tateishi J, Ohta M, Koga M, Sato Y, Kuroiwa J: Transmission of chronic spongiform encephalopathy with kuru plaques from human to small rodents. Ann Neurol, 1978, 5, 581–584.
40. Tellez-Nagel I, Korthals JK, Vlassara HV, Cerami A: An ultrastructural study of chronic sodium cyanate induced neuropathy. J Neuropathol Exp Neurol, 1977, 36, 351–363.
41. Watanabe I, Bingle GJ: Dysmyelination in quaking mouse. Electron microscopic study. J Neuropathol Exp Neurol, 1972, 31, 252–269.
42. Wiśniewski HM, Raine CS: An ultrastructural study of experimental demyelination and remyelination. V. Central and peripheral nervous system lesions caused by diphteria toxin. Lab Invest, 1971, 25, 73–80.

Correspondence address: Dr P. P. Liberski, Dept. of Oncology, School of Medicine, 4 Gagarina Str., 93-509 Łódź, Poland.

NEUROPAT. POL. 1991, 29, 1–2
PL ISSN 0028-3894

ANNA FIDZIAŃSKA, ANNA KAMIŃSKA, ZOFIA GLINKA

MUSCLE CELL DEATH. ULTRASTRUCTURAL DIFFERENCES BETWEEN MUSCLE CELL NECROSIS AND APOPTOSIS*

Department of Neurology, School of Medicine, Warsaw

The morphology and incidence of muscle cell necrosis and apoptosis are presented. Necrosis which occurs as a massive tissue damage is structurally characterized by swelling of the muscle cell and disruption of cellular components. Apoptosis, on the other hand, is a process of active cellular self-destruction. It shows characteristic sequence of muscle cell shrinkage, which is ending in transformation of each muscle cell into compact apoptotic bodies that in turn are phagocytized by adjacent cells or macrophages.

Key words: *apoptosis, muscle cell necrosis.*

Muscle cell death is a stereotyped response *in vivo* to a variety of pathogenetic stimuli and represents final common pathway of degenerative changes in many neuromuscular disorders. A survey of the structural abnormalities displayed by muscle cell dying in a variety of contexts has revealed two commonly occurring pattern of morphological changes. In the first, focal disapearance of sarcolemma is followed by marked swelling of mitochondria and by the appearance of densities in their matrix and subsequently dissolution of overall cell structure. In the second, rapid condensation of sarcoplasm and nuclear chromatin is accompanied by the formation of protuberances on the muscle cell surface which subsequently separate into membrane-bound bodies. The term "muscle necrosis" used in our paper is restricted to the first pattern. The second was orginally described under the name apoptosis (Wyllie et al. 1980). In this paper we will present the morphology and incidence of muscle necrosis and apoptosis. Since the features of muscle necrosis are much more widely known than those of apoptosis we will devote more space to the latter.

---

* The study was partly supported by ICMDiK PAN grant, 06.02.II.5-1.

MUSCLE NECROSIS

Morphology

In light microscopy the necrotic muscle cell appears swollen with indistinct cell boundaries. The contractile substance within such muscle cells loses internal structural details and appears homogenized. Later entire necrotic cells are

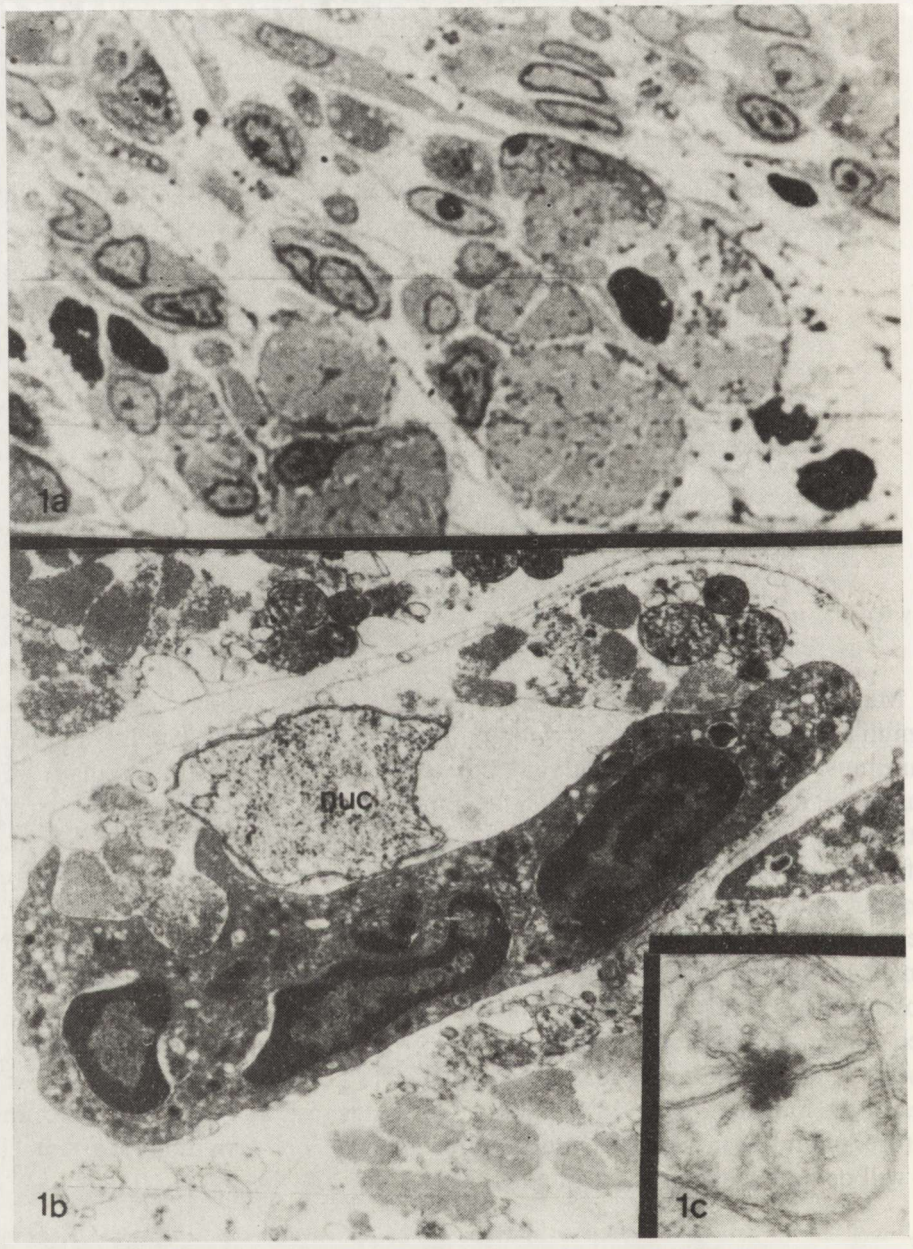

Fig. 1.a. — necrotic muscle cells. Epon. × 1120; *b.* — necrotic muscle cell invaded by neutrophils. Note characteristic ghost-like nucleus (nuc). × 7000; *c.* — mitochondrion with flocculent inclusion. × 33 000

replaced by invading cells (Fig. 1a). Neutrophils and macrophages infiltrate necrotic cells, phagocytize and remove cell debris.

Electron microscopic studies show that the sarcolemma disintegrates and disappears from all or most of the damaged muscle cell surface (Fig. 1b). The basal lamina is preserved and covers the denuded muscle cell surface. Partially lysed myofibrils are separated by irregular spaces that contain swollen mitochondria and distended sarcotubular elements. The presence of flocculent densities (Fig. 1c) in most of the mitochondria of injured cells is generally regarded as being the earliest reliable ultrastructural marker of necrosis (Bodensteiner, Engel 1978). At the latter stage of muscle cell necrosis organelles disintegrate, nuclear chromatin disappears and leaves ghost-like nuclei (Fig. 1b). Even in the necrotic muscle cells, satellite cells are well preserved and no plasma membrane lysis is observed.

Incidence

Muscle cell death with the morphological features of necrosis is observed in muscle subjected to severe ischemia (Karpati et al. 1974; Faber et al. 1981), direct muscle trauma (Walton, Adams 1956) and exposure to membrane-active chemicals and toxins (Pestronk et al. 1982; Nonaka et al. 1983). In myology the necrotic muscle fibers are the characteristic morphological feature of progressive muscular dystrophy (Carpenter, Karpati 1972; Cullen, Fulthorpe 1975; Bodensteiner, Engel 1978), polymyositis (Engel, Arahata 1984; Arahata, Engel 1985) and other complement-mediated cell membrane damage (Engel, Biesecker 1982; Engel, Arahata 1984). Also muscle cell death following severe hyperthermia is known to take the form of necrosis (Harriman et al. 1978).

MUSCLE CELL APOPTOSIS

Morphology

Apoptosis characteristically affects scattered muscle cells in an asynchronous fashion and unlike necrosis is not accompanied by an inflammatory reaction. In light microscopy, muscle cells undergoing apoptosis are very dense and compact (Fig. 2a). Condensation and margination of nuclear chromatin to form sharply circumscribed masses is frequently observed. In addition numerous single sometimes double, well defined, round bodies, centrally or peripherally located are observed in muscle fibers with well preserved architecture (Fig. 2c). In the extracellular space few phagocytic cells, mainly macrophages, with large dense bodies are seen (Fig. 2b).

At higher magnification the morphological changes which identified muscle cell apoptosis are seen in nuclei and sarcoplasm. The nuclear outline is abnormally convoluted, the nuclear chromatin is densely aggregated in large compact granular masses (Fig. 3). Myofibrils are compact and very dense, mitochondria show mild swelling and loss of normal mitochondrial matrix granules. The sarcoplasmic condensation is frequently accompanied by the appearance of clear vacuoles (Fig. 3). With time, many muscle cells display cell surface irregularities.

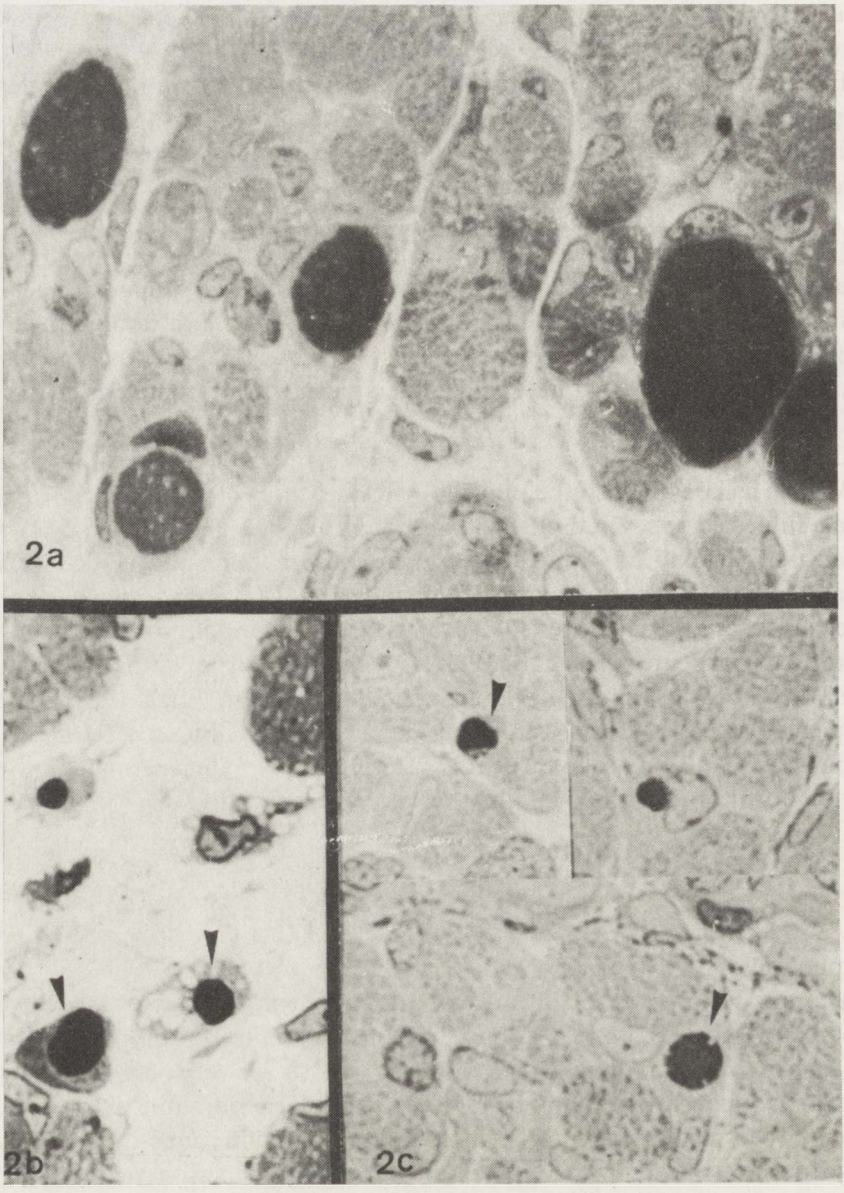

Fig. 2.a — dark stained muscle fibers scattered throughout the normal fibers. Epon. × 1120; *b* — dark bodies within cytoplasm of macrophages (arrows). Epon. 1120; *c* — small, round, dark bodies (arrows) seen within sarcoplasm of intact muscle cells. Epon. × 1120

Multiple small (Fig. 4) or large blebs of sarcoplasm protrude from the surface of apoptotic cells, corresponding to the budding fragments of sarcoplasm. In addition muscle cell fragments are observed within the sarcoplasm of adjacent healthy muscle cells as large round or oval apoptotic bodies. Observation of a number of grids at different magnifications shows that these bodies can be

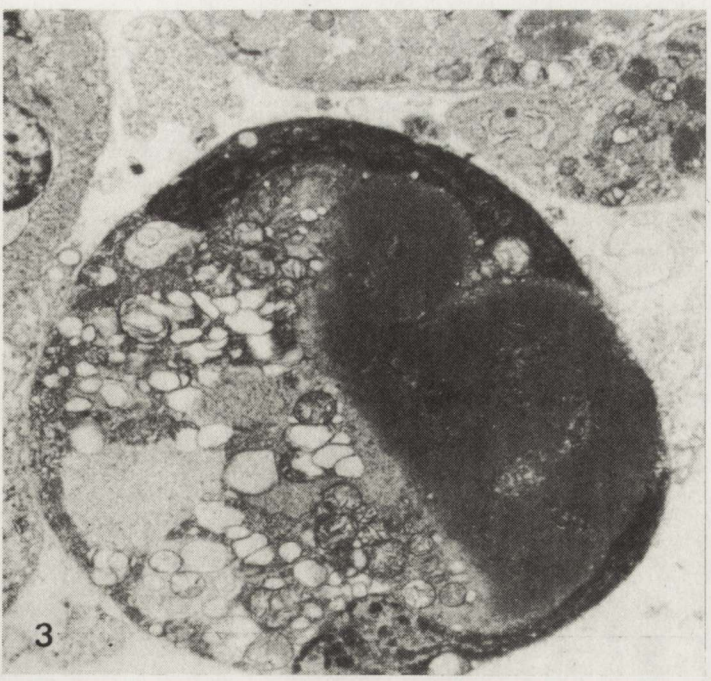

Fig. 3. Muscle cell undergoing apoptosis. ×6800

divided into early and late apoptotic bodies. Early apoptotic bodies, the first products of the process of apoptosis can be recognized as membrane-bound structures containing condensed sarcoplasm with recognizable organelles and sometimes nuclear fragments (Fig. 5).

They are seen within intact muscle cells and sometimes within macrophages. Most of these bodies appear to be broken down to a form in which the organelles are no longer visible. At this stage they are known as late apoptotic or residual bodies. They contain fibrillar or amorphous electron dense material (Fig. 6). and are observed within the sarcoplasm of healthy muscle cells. They are dispersed in extracellular space and are either extruded into the adjacent vascular lumen, or ingested by cells of the mononuclear phagocytic system.

Incidence

A growing number of morphological studies indicate that apoptosis is involved in the programmed focal elimination of muscle cells that accompanies embryonic and fetal development. For example extensive apoptosis has been observed during development of the heart in a number of vertebrates (Pexieder 1975, Hurle et al. 1977; Hurle, Ojeda 1979). Special attention has been given to apoptosis of striated muscle in the tadpole tail during spontaneous metamorphosis (Kerr et al. 1974). The authors claim that deletion of striated muscle during

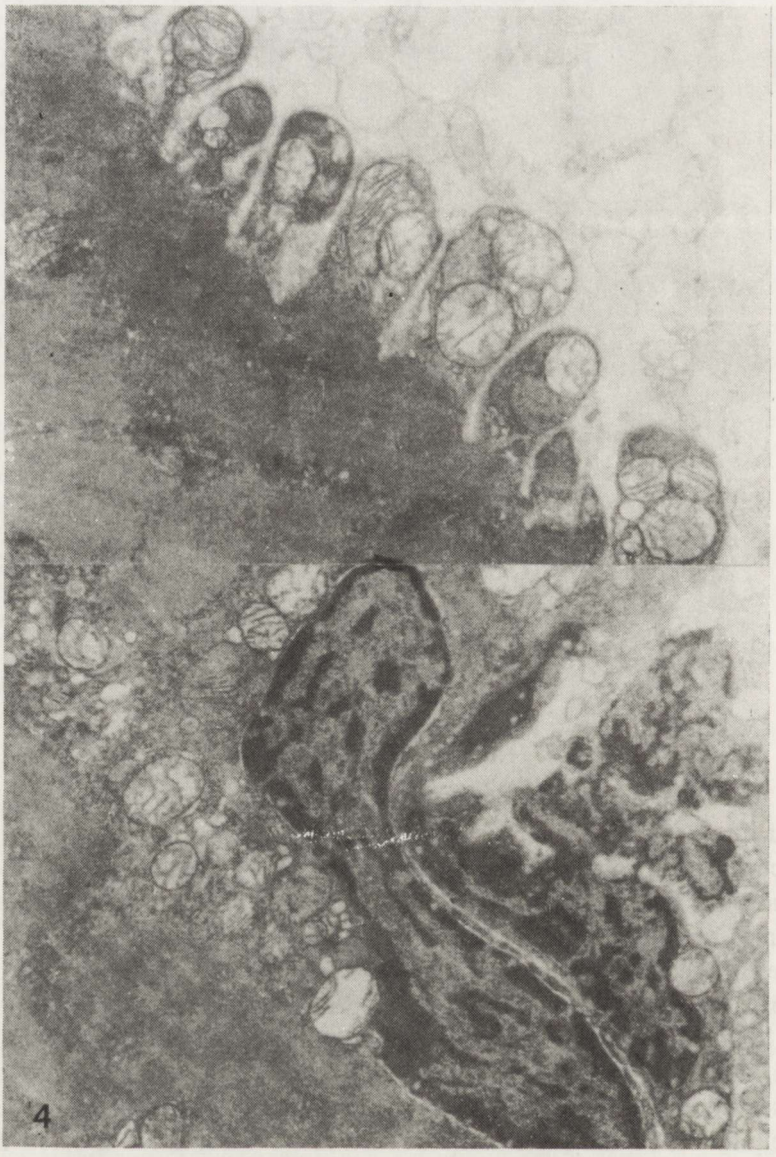

Fig. 4. Condensation of sarcoplasm with irregular blebs formation. × 11 600

metamorphosis is accomplished by a process akin to "classical apoptosis". Dilatation of sarcoplasmic reticulum leads first to internal fragmentation accompanying nuclear pyknosis. This fragmentation is followed by degradation of muscle remnants within neighbouring muscle cells or within macrophages. A similar process has been reported in smooth muscle in the neonatal rat ureter (Hoyes, Barber 1983). Webb (1972, 1977) studying muscle cell death in human embryos, by means of electron microscopy with a series of histochemical tests reported that muscle cell death similar to the process of apoptosis was found in all

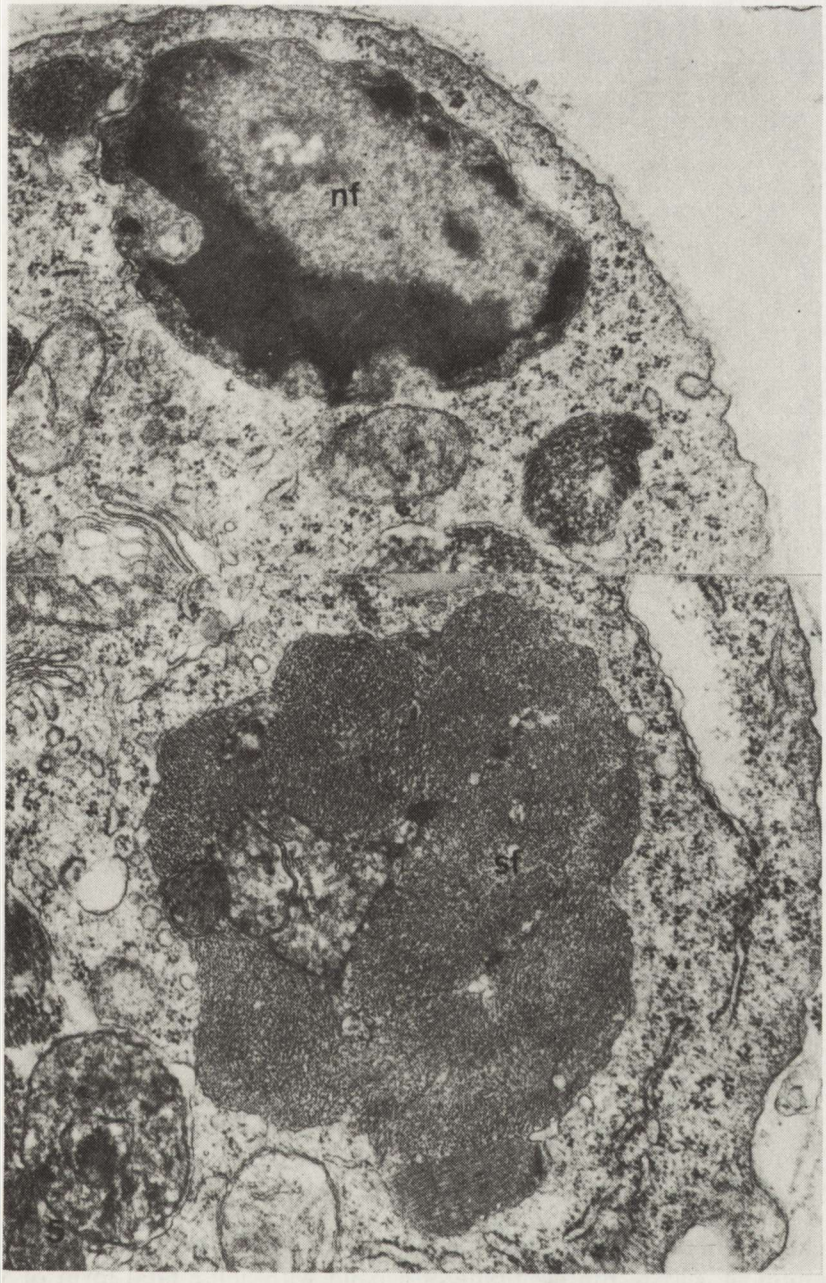

Fig. 5. Immature muscle cell containing nuclear (nf) and sarcoplasmic (sf) fragments identifiable as early apoptotic bodies. × 22 000

fetuses between 10 and 16 weeks of gestation. In experimental conditions, muscle apoptosis has been shown to follow after exposure of neonatal rat cardiac muscle to iodoacetic acid (Buja et al. 1985) and skeletal neonatal muscle to bupivacaine (Fidziańska, Kamińska 1991).

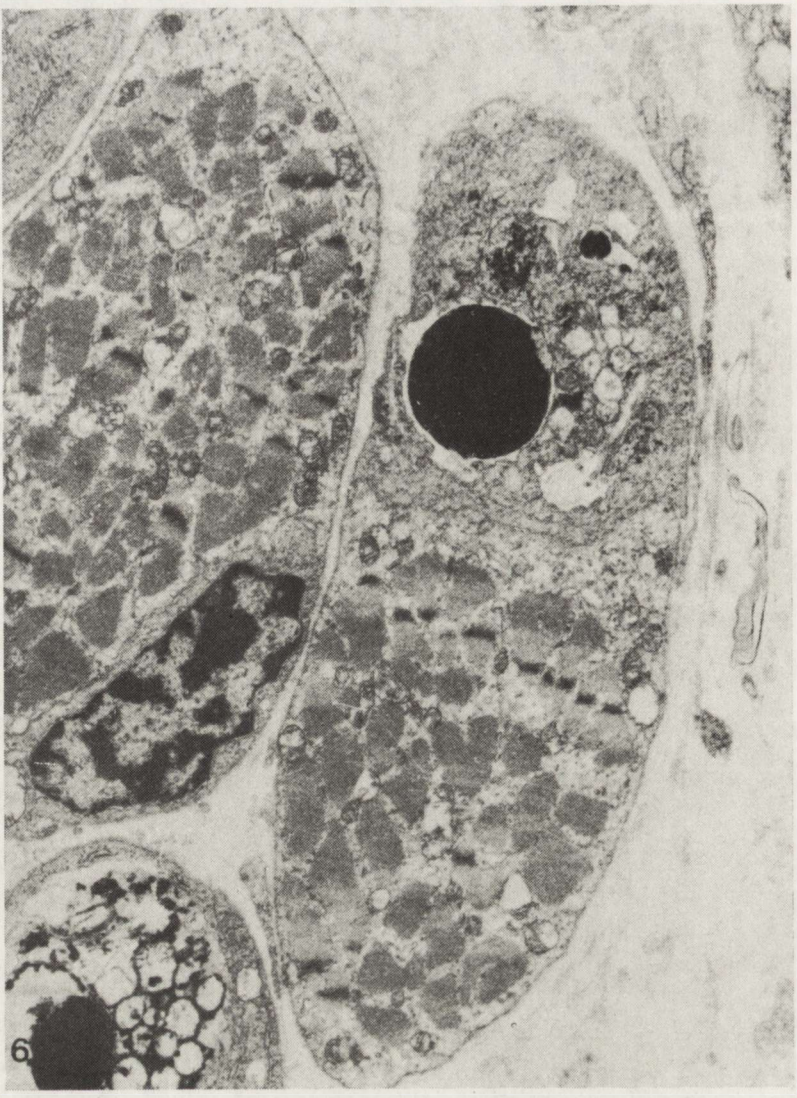

Fig. 6. Late apoptotic body with electron dense, amorphous material. × 11 000

In human neuromuscular disorders apoptosis has been shown to be involved in deletion of cells in muscle tissue of a child with acute fatal form of Werdnig-Hoffman disease (Fidziańska et al. 1990). Morphological analysis of apoptosis occurring in muscle tissue is very difficult. Apoptotic bodies remain visible in tissue for only a few hours (Wyllie et al. 1980) and this, together with the small size of many apoptotic bodies and the absence of inflammatory reaction means that muscle cell deletion by such a mechanism is often unnoticeable.

ŚMIERĆ KOMÓRKI MIĘŚNIOWEJ. ULTRASTRUKTURALNE RÓŻNICE MIĘDZY MARTWICĄ I APOPTOZĄ.

Streszczenie

Przedstawiono różnice morfologiczne i ultrastrukturalne komórki mięśniowej ulegającej martwicy i apoptozie. W odróżnieniu od martwicy cechującej się obrzmieniem komórki i jej organelli, ubytkiem sarkolemmy, pojawieniem się krystalicznych wtrętów w macierzy mitochondriów, obkurczone włókno ulegające apoptozie wykazuje zagęszczenie chromatyny jądrowej i cytoplazmy oraz kolejno rozpad włókna. Fragmenty rozpadłej komórki zwane ciałkami apoptotycznymi wychwytywane przez komórki sąsiadujące ulegają całkowitej dezintegracji. Omówiono takie procesy fizjologiczne i patologiczne, w których opisywano różne typy śmierci komórki mięśniowej.

REFERENCES

1. Arahata K, Engel AG: Immunoelectron microscopic analysis of cell mediated fibre injury in polymyositis and inclusion body myositis. J Neuropathol Exp Neurol, 1985, 44, 361.
2. Bodensteiner J, Engel AG: Intracellular calcium accumulation in Duchenne dystrophy and other myopathies. Neurology, 1978, 28, 439–446.
3. Buja M, Hagler HK, Persons D, Chien K, Reynolds RC, Willerson JT: Alterations of ultrastructure and elemental composition in cultured neonatal rat cardiac myocytes after metabolic inhibition with iodoacetic acid. Lab Invest, 1985, 53, 397–412.
4. Carpenter S, Karpati G: Plasma membrane lysis as the first stage of necrosis in Duchenne muscular dystrophy. Neurology, 1972, 27, 348–349.
5. Cullen MJ, Fulthorpe JJ: Stage in fibre breakdown in Duchenne muscular dystrophy. An electron microscopic study. J Neurol Sci, 1975, 24, 179–200.
6. Engel AG, Arahata K: Monoclonal antibodies analysis of mononuclear cells in myopathies. II Phenotypes of autoinvasive cells in polymyositis and inclusion body myositis. Ann Neurol, 1984, 16, 209–215.
7. Engel AG, Biesecker G: Complement activation in muscle fibre necrosis: demonstration of the membrane attack complex of complement in necrotic fibres. Ann Neurol, 1982, 12, 289–296.
8. Faber JL, Chien KR, Mittnacht SJ: The pathogenesis of reversible cell injury in ischemia. Am J Pathol, 1981, 102, 271–277.
9. Fidziańska A, Kamińska A: Apoptosis: a basic pathological reaction of injured neonatal muscle. Pediat Pathol, 1991 (in press).
10. Fidziańska A, Goebel HH, Warlo I: Acute infantile spinal muscular atrophy. Muscle apoptosis as a proposed pathogenetic mechanism. Brain, 1990, 113, 433–445.
11. Harriman AGF et al.: Malignant hyperthermia myopathy in man. In Second International Symposium on Malignant Hyperthermia. Eds: SA Aldrete, BA Britt, Grune and Stratton, New York, 1978, pp 67–87.
12. Hoyes AD, Barber P: Degeneration and phagocytosis of smooth muscle cells in the neonatal rat ureter. J Anat, 1983, 37, 583–589.
13. Hurle JM, Lafarga M, Ojeda JL: Cytological and cytochemical studies of the necrotic area of the bulbus of the chick embryo heart: phagocytosis by developing myocardial cells. J Embryol Exp Morphol, 1977, 41, 161–170.
14. Hurle JM, Ojeda JL: Cell death during development of the truncus and conus of the chick embryo heart. J Anat, 1979, 129, 427–439.
15. Karpati G, Carpenter S, Melmed C, Eisen AA: Experimental ischemic myopathy. J Neurol Sci, 1974, 23, 29–161.
16. Kerr JFR, Harmon B, Searle J: An elctron microscope study of cell deletion in the anuran tadpole

tail during spontaneous metamorphosi with special reference to apoptosis of striated muscle fibres. J Cell Sci, 1974, 14, 571–585.
17. Nonaka I, Takagi A, Ishiura S, Nakase H, Sugita H: Pathophysiology of muscle fibre necrosis induced by bupivacaine hydrochloride (Marcaine). Acta Neuropathol (Berl), 1983, 60, 167–174.
18. Pestronk A, Parhad JM, Drachman DB, Price DL: Membrane myopathy: morphological similarities tu Duchenne muscular dystrophy. Muscle Nerve, 1982, 5, 209–214.
19. Pexieder T: Cell death in the morphogenesis and teratogenesis of the heart. Adv Anat Embryol Cell Biol, 1975, 51, 6–100.
20. Walton JN, Adams RD: The response of the normal, the denervated and the dystrophic muscle cell to injury. J Pathol Bacteriol, 1956, 72, 273–298.
21. Webb JN: The development of human skeletal muscle with particular reference to muscle cell death. J Pathol, 1972, 106, 221–228.
22. Webb JN: Cell death in developing skeletal muscle: histochemistry and ultrastructure. J Pathol, 1977, 123, 175–180.
23. Wyllie AH, Kerr JFR, Currie AR: Cell death: The significance of apoptosis. Int Rev Cytol, 1980, 68, 251–305.

Address correspondence: Anna Fidziańska MD, PhD, Department of Neurology, School of Medicine, 1A Banacha Street, 02-097 Warsaw, Poland.

NEUROPAT. POL. 1991, 29, 1–2
PL ISSN 0028-3894

EWA SAWICKA

ORIGIN OF THE RING MUSCLE FIBERS IN NEUROMUSCULAR DISEASES*

Department of Neurology, Medicine School of Warsaw, Neuromuscular Unit, Medical Research Centre, Polish Academy of Sciences, Warsaw, Poland

Morphological histochemical and ultrastructural examination of the ring fibers in one case of myotonic dystrophy and one case of mitochondrial myopathy provides evidence that the ring fibers develop in the course of fiber splitting and reinnervation of muscle fiber fragments. The reinnervation may have been due to a neurogenic lesion coexisting in both cases with the myopathic picture. The histologically different type of annular myofibrils observed in one case of cap disease is probably due to delayed embryonic development and abnormal relations between the myofibrils and elements of the cytoskeleton.

Key words: *muscle, ring fibers, splitting, reinnervation.*

The term ring fiber refers to the fiber with subsarcolemmally localized bundles of myofibrils running at right angles to the normal orientation of the myofibrils, known as annular myofibrils (Schotland et al. 1966). It is a rare phenomenon, most often encountered in myotonic dystrophy (Wohlfart 1951, Schröder, Adams 1968, Schotland 1970), though it has been also reported in other muscular dystrophies (Bethlem, Van Wijngaarden 1963, Schotland et al. 1966), and various myopathies, and, occasionally, even in normal human muscle (Engel, Banker 1986). The ring fibers were observed under experimental conditions in muscles undergoing reinnervation (Dubowitz 1967) and in ischemic muscle (Sjöström et al. 1982).

The morphological incidence of ring fibers in association with other histopathological changes observed in muscle biopsy was the aim of this study. The study comprised three cases of three different neuromuscular diseases, in which the ring fibers were seen in great numbers.

* Partly supported by Research Grant 06.02.II.5-1.

MATERIAL AND METHODS

Three muscle biopsies taken from the following clinical cases provided the material. Case 1. Male, aged 42, with mild proximal spinal muscular atrophy progressing over the periody of twenty years. Case 2. Male, aged 42, with coexisting features of myotonic dystrophy and peroneal muscular atrophy. Case 3. Female, aged 15, with mild proximal myopathy and kyphoscoliosis progressing since childhood.

Biceps brachii and quadriceps femoris muscle biopsies were performed under local anesthesia. For light microscopy, the muscle was frozen in liquid nitrogen, cut in a cryostat at $-15°C$, stained with hematoxylin-eosin (HE) and Gomori trichrome, and incubated for NADH dehydrogenase (NADH), succinic dehydrogenase (SDH), lactic dehydrogenase (LDH), myofibrillar adenosine triphosphatase (mATPase) at pH 9.4 and acid-preincubated for myofibrillar ATPase at pH 4.3 and 4.6. For electron microscopy, muscle specimens were fixed in 5% glutaraldehyde with 1 h postfixation in 1% OsO_4, dehydrated in ethanol and acetone series and Epon-embedded for sectioning in an ultramicrotome. Ultrathin sections were stained on grids with uranyl acetate and lead citrate and examined in a JEM 100 S electron microscope.

RESULTS

In all three cases, despite the differences in the histopathological picture, ring fibers were present in great numbers.

Case 1. Biceps brachii muscle

Increased variability in the muscle fiber size, internal nuclei and fiber splitting were observed. The ring fibers were distinctly visible in thick Epon sections as regular rings of myofibrils encircling the periphery of, usually, small fibers (Fig. 1a). The distribution of NADH, SDH and LDH was irregular in many type I fibers. Atrophy of type I fibers and grouping of intermediate and type II C fibers (Fig. 1b) were observed. In the II C fibers the perpendicularly oriented strips of heightened mATPase activity were seen at the periphery (Fig. 1b), most likely produced by the annular myofibrils. Formation of ring fibers in muscle fibers undergoing splitting was observed a few times (Fig. 1c, d). Electron microscopically intramitochondrial crystalline-like inclusions and giant mitochondria with circularly arranged cristae were observed in many muscle fibers; myofibril loss and single lysosomes were usually noted in these fibers. The ring fibers seen in great numbers were formed by annular myofibrils coursing in a plane perpendicular to the long fiber axis and encircling the periphery of the fiber (Fig. 2). The differentiation of the annular myofibrils into actin and myosin filaments was clear, and the organization into bundles and the appearance of sarcomeres were normal. The length of the circularly oriented sarcomeres, although the same in one ring fiber, differed between the ring fibers. Proliferation of T-tubules and the sarcoplasmic reticulum system and numerous polyribosomes and glycogen gra-

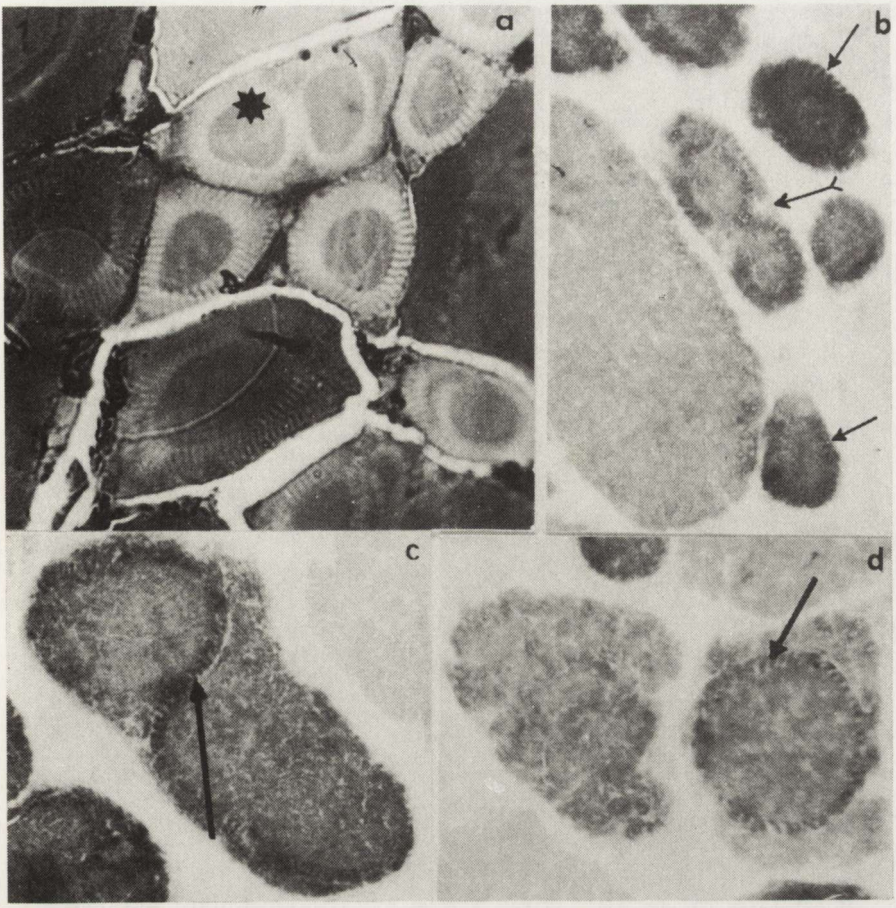

Fig. 1. Mitochondrial myopathy, biceps brachii muscle. *a* — a group of ring fibers A. Annular myofibrils are characterized by their cross-striated appearance. Three rings of annular myofibrils are seen in one muscle fiber (asterisk). Semithin Epon section, toluidin blue. ×440; *b* — grouping of small-size fibers showing high mATPase activity. Most of them have a cross-striated appearance of increased mATPase activity localized subsarcolemmally (arrow). In one of them two rings of increased mATPase activity are visible (double arrow), mATPase. ×440; *c, d* — muscle fiber splitting. Muscle fragments undergoing splitting show a cross-striated appearance of mATPase activity at their periphery (arrows). mATPase. ×800

nules were seen in the vicinity of the annular myofibrils, especially under the sarcolemma and in the perinuclear space, where a prominent Golgi system was often visible. Mitochondria in the ring fibers were sparse within the circularly oriented bundles of myofibrils, and occasionally formed small clusters at various sites between the bundles, most often under the sarcolemma (Fig. 2). Intramitochondrial crystalline-like inclusions within the ring fibers were seldom observed (Fig. 2). Disruption of the filament arrangement and filament loss affecting central parts of the ring fibers were seen only occasionally (Fig. 2). Postsynaptic infoldings of the neuro-muscular junction branching between the bundles of annular myofibrils were observed at times (Fig. 3).

Fig. 2. Mitochondrial myopathy, biceps brachii muscle. Ring fiber A. One bundle of annular myofibrils (amf) seen encircling the periphery of the fiber. Its sarcomere organization is normal, the length of the sarcomeres equal. Mitochondria containing crystalline-like inclusions (m) and concentrically arranged cristae (asterisk) are seen under sarcolemma (sl). Some disruption of myofibrillar arrangement and loss of filaments affecting preexisting myofibrils (mf) of the ring fiber. × 21 500

Case 2. Biceps brachii muscle

There was increased variability in the size of the fibers with many internal nuclei, fiber splitting, some fibers undergoing necrosis, atrophy of type I fibers and a moderate degree of fibrosis. Though the ring fibers were often visible on electron microscopy, only few such fibers were seen in semithin Epon sections.

Fig. 3. Mitochondrial myopathy, biceps brachii muscle. Postsynaptic infoldings (psf) of the neuromuscular junction branching between and under the annular myofibrils (amf) of the ring fiber A. × 21 500

They were formed, as in Case 1, by regular rings of myofibrils running in a plane perpendicular to the long fiber axis and encircling the periphery of the fiber (Fig. 4). Occasionally, some of the peripherally coursing myofibrils turned inwards, transversed deeper regions of the fiber and ran obliquely to the long fiber axis (Fig. 4). The organization of the annular myofibrils into bundles was more regular in deeper parts adjacent to the preexisting myofibrils. Under the sarcolemma shorter sarcomeres and single myofilaments were more often visible. The differen-

Fig. 4. Myotonic dystrophy, biceps brachii muscle. Ring fiber A. Annular myofibrillar alignment of the peripheral part of the muscle fiber. Some annular myofibrils (amf) transverse deeper regions of the fiber. Sarcomere organization of the annular myofibrils better in the deeper parts than under the sarcolemma (sl), where single myofilaments are also present. T-system networks (T) and sarcotubular elements (arrow) visible especially under the sarcolemma. The nucleus (n) localized between the bundles of annular myofibrils. × 6800

tiation of annular myofibrils into actin and myosin filaments was clear (Fig. 4). The length of the annular sarcomeres was a few times shorter than that of the sarcomeres of the preexisting part of the fiber. Proliferation of the T-tubules and the sarcoplasmic reticulum system, numerous polyribosomes and glycogen gra-

nules were seen in the vicinity of the annular myofibrils, especially under the sarcolemma and in the perinuclear space (Fig. 4). Nuclei of the ring fibers, often with prominent nucleoli, were usually localized under the sarcolemma or between the bundles of annular myofibrils (Fig. 4), occasionally only being seen in the central part of the ring fiber. The Golgi system was often present in the vicinity of the nuclei. The mitochondria were sparse between the bundles of annular myofibrils. Degenerative changes were not seen in any of the ring fibers, although different stages of myofibrillar and mitochondrial alterations and a decrease in the number of sarcotubular elements were observed in the other muscle fibers. There were occasionally postsynaptic infoldings of the neuro-muscular junction branching between the bundles of annular myofibrils.

Case 3. Quadriceps femoris muscle

The basic histochemical changes were: focal subsarcolemmal loss or a considerable decrease in SDH, NADH and ATPase activities and lack of differentiation into a mosaic pattern of fiber types (Fig. 5a, b, c). All muscle fibers showed the same moderate activity of oxidoreductive enzymes and ATP-ases. Ultrastructurally, the area of focal alteration, which usually occupied some part of the muscle fiber periphery, consisted of circularly arranged myofibrils (Fig. 6). The differentiation of these myofibrils into myosin and actin filaments was not always clear, their mutual organization and the organization of myofibrils into bundles was irregular, and the length of sarcomeres different (Fig. 6). Proliferation of sarcotubular elements, some polyribosomes and glycogen granules were seen between the bundles of annular myofibrils (Fig. 6). Mitochondria were sparse between them, but occasionally they formed clusters at various sites between the bundles. A prominent Golgi system was often observed in the vicinity of the nuclei, which were usually in their normal subsarcolemmal localization.

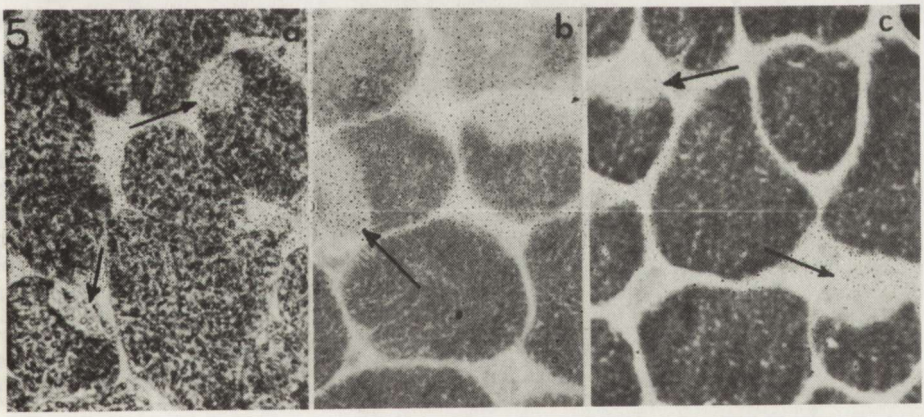

Fig. 5. Cap disease, quadriceps femoris muscle. Lack of differentiation into a mosaic pattern of fiber types, all muscle fibers show the same moderate activity. Focal subsarcolemmal disappearance or considerable decrease in activity is seen in a few fibers (arrows). *a* – SDH. ×440, *b* – mATPase. ×440, *c* – mATPase preincubated at pH 4.3. ×440

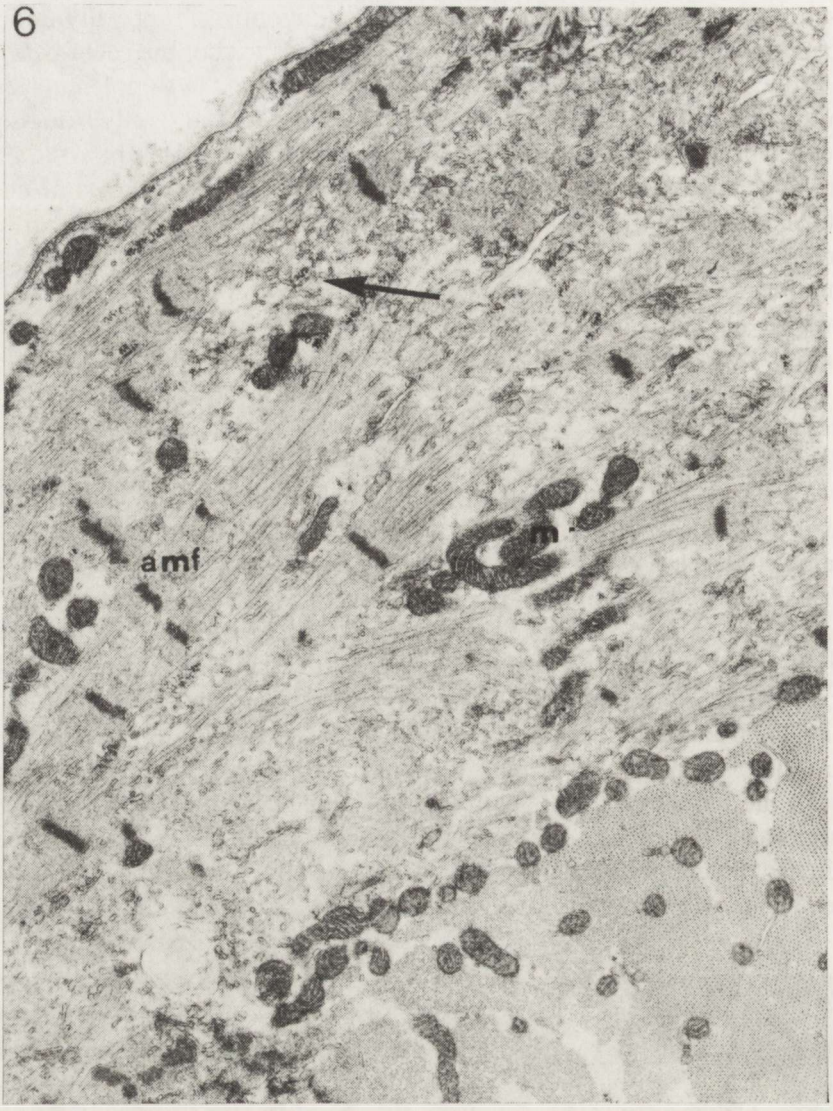

Fig. 6. Cap disease, quadriceps femoris muscle. Ring fiber B. The annular myofibrils (amf) occupy the periphery of the fiber. Differentiation of these myofibrils into actin and myosin filaments is not well discernible, their mutual organization and the organization of myofibrils into bundles are irregular, the length of the sarcomeres is different. Numerous profiles of sarcotubular elements (arrows) and mitochondria (m) in clusters are seen at various sites between the bundles of annular myofibrils. × 21 500

DISCUSSION

On the basis of morphological, histochemical and ultrastructural studies two types of ring fibers, A and B, were distinguished. In type A the annular myofibrils in regular bundles encircle the whole periphery of a muscle fiber, their differen-

tiation into actin and myosin filaments is clear, and the organization of sarcomeres normal. The sarcomeres differ in length between particular ring fibers, although their length in one ring fiber is usually the same. The strong ATPase activity of annular myofibrils seems to indicate their functional activity. In type B the annular myofibrils occupy only a part of the muscle fiber periphery, their differentiation into myosin and actin filaments is not well discernible, and the degree of sarcomere organization and the sarcomere length are different. The annular myofibrils in this type of ring fiber do not show any ATPase activity. The A ring fiber fulfills all the criteria of ring fiber described so far (Schotland et al. 1966; Schröder, Adams 1968), whereas the B ring fiber is consistent with the morphological changes in cap disease (Fidziańska et al. 1981).

Ultrastructural features of ring fibers, A and B type alike, such as nuclei with prominent nucleoli, Golgi networks in the perinuclear space, polyribosomes and the proliferation of sarcotubular and T-system elements, may indicate current formation of annular myofibrils. Differences in the length of annular myofibril sarcomeres between ring fibers A are the evidence of various stages of sarcomerogenesis, and therefore different ages of each ring fiber A. Longitudinal postnatal growth of myofibrils is known to be associated with an increase in the number of sarcomeres in the series, but does not involve a change in the length of the filaments (Williams, Goldspink 1971). The ring fibers of type A were observed in two different clinical entities, i.e. myotonic dystrophy coexisting with peroneal muscular atrophy (Case 2) (Hausmanowa-Petrusewicz et al. 1977) and mitochondrial myopathy showing furthermore electromyographic features of spinal anterior horn cell lesion (Case 1) (Dobkin, Verity 1976; Martin 1981). The overall histopathological picture was similar in the two cases, although the basic character of changes differed (unspecific muscle fiber lesion in myotonic dystrophy and ultrastructural mitochondrial pathology in mitochondrial myopathy). Prominent muscle fiber splitting was observed in both cases. This is a non-specific phenomenon described in denervation and various muscular disorders (Sawicka 1988). Formation of a ring fiber during fiber splitting in the split fragment of a usually large muscle fiber observed in Case 1 seems to suggest an interrelationship between fiber splitting and ring fiber formation.

However, it remains to be answered why the annular myofibrils are formed only in some split muscle fragments. The A ring fibers observed in this study displayed the histochemical pattern characteristic of type 2C fibers and intermediate fibers (Gauthier 1986), and were seen in groups. This probably resulted from reinnervation of split muscle fragments, since type 2C is considered a precursor or an undifferentiated fiber able to develop later into a mature differentiated one (Brooke et al. 1971), and the same type 2C fibers exhibited a localized, high acetylcholinesterase activity suggesting the presence of a heuromuscular junction (Nonaka et al. 1981). The phenomenon of type 2C fiber grouping confirms their reinnervation (Karpati, Engel 1968). Postsynaptic infoldings of the neuromuscular junction branching between the bundles of annular myofibrils found in the two cases with ring fibers A are further convincing evidence of ring fiber

A reinnervation. The reinnervation may have been due to neurogenic lesion coexisting in both cases with the myopathic picture. There is no evidence that a new neuromuscular junction can be formed in a muscle fragment undergoing splitting. Nevertheless, as it is known that the regenerated muscle fiber can have more than one end-plate (Albani, Vrbova 1985), theoretically a contact between the regenerating axon and the muscle fragment undergoing splitting is possible. Formation of a new end-plate on an already split muscle fragment would be more likely, provided the structure of the fragment is well preserved. In our material the structure of the ring fibers A was usually normal in contrast to gross degenerative changes observed in other muscle fibers.

It remains unclear, why the regeneration of reinnervated muscle fragments occurs in the form of annular myofibril formation, though during muscle development as well as regeneration the myofibrils are organized along the long myotube axis. Sarcomerogenesis takes place in close association with the preexisting myofibrillar bundles and depends on normal myofibrillar – cytoskeletal interaction (Długosz et al. 1984). Intermediate filaments, desmin, vimentin and synemin (Granger, Lazarides 1979, 1980) coexisting at the periphery of the myofibrillar Z-discs play an important role in maintenance of the myofibrillar organization. Recently, it has been suggested that on the inner surface of the sarcolemma there is a set of attachment sites, referred to as costameres, for vinculin, spectrin and ankyrin, and this coincides with the electron dense adhesion sites of Z-bands and intermediate filaments with the sarcolemma (Pardo et al. 1983). The appropriate relationship of costameres and the preexisting sarcomeres is a prerequisite for normal alignment of the newly regenerated myofibrils. During muscle fiber splitting, consisting in the division of the fiber by proliferating invaginations of the sarcolemma (Hall-Craggs 1970; Schröder 1970; Sawicka 1988), the failure of relationship between the costameres and the preexisting sarcomeres is likely.

Our observations seem to suggest that the ring fiber A is formed during muscle fiber splitting. Annular myofibrils are a sign of myofibrillar regeneration and are thought to be formed after reinnervation of either a splitting muscle fragment or a newly split muscle fragment. Annular alignment of myofibrils can result from fiber splitting. It is possible that in a muscle fragment split by proliferating sarcolemma there can be no correct relations between the attachment sites of the sarcolemma and the preexisting sarcomeres. This can result in a faulty annular alignment of the myofibrils regenerated from the sarcolemmal side (Długosz et al. 1984) and in a lack of proper contact with the preexisting myofibrils.

Type B of the ring fiber was distinctly different from type A. The annular myofibrils occupied only a part of the fiber periphery, they looked immature because of the poor differentiation between myosin and actin filaments and poor sarcomere organization and did not show any ATPase activity. Type B ring fibers were observed in the case of cap disease (Fidziańska et al. 1981), among muscle fibers lacking differentiation into a mosaic pattern of fiber types, this being another feature of their immaturity (Brooke et al. 1971). The authors of the only

report of cap disease (Fidziańska et al. 1981), demonstrated that impaired myosin synthesis was the main pathological change in this disease. Thus, it seems to us, that the type B ring fiber may result from failure in myofibril development and their faulty interrelationship with the cytoskeleton.

POCHODZENIE OKRĘŻNYCH WŁÓKIEN MIĘŚNIOWYCH W SCHORZENIACH NERWOWO-MIĘŚNIOWYCH

Streszczenie

Na podstawie analizy histochemicznej i ultrastrukturalnej przypadków dystrofii miotonicznej, miopatii mitochondrialnej i tzw. choroby czapeczek wyróżniono dwa typy włókien mięśniowych okrężnych. W dystrofii miotonicznej i miopatii mitochondrialnej okrężne włókno mięśniowe powstaje w procesie rozszczepiania włókien mięśniowych i reinerwacji rozszczepionych fragmentów. Reinerwacja jest zapewne zależna od neurogennego uszkodzenia towarzyszącego w obu przypadkach uszkodzeniu mięśni. Histologicznie różny typ włókien okrężnych obserwowany w tzw. chorobie czapeczek jest raczej wynikiem zaburzenia embrionalnego rozwoju miofibryli i ich powiązania z elementami cytoskeletonu.

REFERENCES

1. Albani M, Vrbova G: Physiological properties and pattern of innervation of regenerated muscles in the rat. Neuroscience, 1985, 15, 489–492.
2. Bethlem J, Van Wijngaarden GK: The incidence of ringed fibers and sarcoplasmic masses in normal and diseased muscle. J Neurol Neurosurg Psychiat, 1963, 26, 326–332.
3. Brooke MH, Williamson E, Kaiser KK: The behavior of four fiber types in developing and reinnervated muscle. Arch Neurol, 1971, 25, 360–366.
4. Dobkin BH, Verity MA: Familial progressive bulbar and spinal muscular atrophy. Juvenile onset and late morbidity with ragged-red fibers. Neurology, 1976, 26, 754–763.
5. Długosz AA, Antin PB, Nachmias VT, Holtzer H: The relationship between stress fiber-like structures and nascent myofibrils in cultured cardiac myocytes. J Cell Biol, 1984, 99, 2268–2278.
6. Dubovitz V: Pathology of experimentally re-innervated skeletal muscle. J Neurol Neurosurg Psychiat, 1967, 30, 99–110.
7. Engel AG, Banker BQ: Ultrastructural changes in diseased muscle. In: Myology. Basic and Clinical. AG Engel, BQ Banker, Eds. Mc Graw-Hill Book Co. New York, 1986, pp 953–957.
8. Fidziańska A, Badurska B, Ryniewicz B, Dembek I: "Cap disease": new congenital myopathy. Neurology, 1981, 31, 1113–1120.
9. Gauthier GF: Skeletal muscle fiber types. In: Myology. Basic and Clinical. AG Engel, BQ Banker, Eds. Mc Graw-Hill Co. New York, 1986, pp 285–307.
10. Granger BL, Lazarides E: Desmin and vimentin coexists at periphery of the myofibril Z-disc. Cell, 1979, 18, 1053–1063.
11. Granger BL, Lazarides E: Synemin: A new high molecular weight protein associated with desmin and vimentin filaments in muscle. Cell, 1980, 22, 727–737.
12. Hall-Craggs ECB: The longitudinal division of fibers in overloaded rat skeletal muscle. J Anat (Lond), 1970, 107, 459–470.
13. Hausmanowa-Petrusewicz I, Jędrzejowska H, Rowińska-Marcińska K, Borkowska J: Coexistence of peroneal muscular atrophy and myotonic dystrophy features. In: Peroneal atrophy and related disorders. G Serratrice, H Roux, Eds. Masson Press, New York, 1977, pp 49–66.
14. Karpati G, Engel WK: "Type grouping" in skeletal muscles after experimental reinnervation. Neurology, 1968, 18, 447–455.

15. Martin JJ, Generalised mitochondrial disturbances and myopathies. Concluding remarks. In: Mitochondria and Muscular diseases. HFM Busch, FGI Jennekens, HR Scholte, Eds. Mefar b.v., Beetsterzwaag, The Netherlands, 1981, pp 219–223.
16. Nonaka I, Takagi A, Sugita H: The significance of type 2C muscle fibers in Duchenne muscular dystrophy. Muscle Nerve, 1981, 4, 326–333.
17. Pardo JV, Siliciano JD, Craig SW: A vinculin-containing cortical lattice in skeletal muscle: Transverse lattice elements ("costameres") mark sites of attachment between myofibrils and sarcolemma. Proc Natl Acad Sci, 1983, 80, 1008–1012.
18. Sawicka E: Ultrastructural analysis of the muscle fiber splitting. Pat Pol, 1988, 39, 153–163.
19. Schotland DL, Spiro D, Carmel P: Ultrastructural studies of ring fibers in human muscle diseases. J Neuropath Exp Neurol, 1966, 25, 431–442.
20. Schotland DL: An electron microscopic investigations of myotonic dystrophy. J Neuropathol Exp Neurol, 1970, 29, 241–253.
21. Schröder JM, Adams RD: The ultrastructural morphology of the muscle fiber in myotonic dystrophy. Acta Neuropath (Berl), 1968, 10, 218–241.
22. Schröder JM: Sarcolemmal identations resembling junctional folds in myotonic dystrophy. In: Muscle Diseases. Eds. JN Walton, N Canal, G Scarlato. Int. Congr. Ser. No 199, Excerpta Medica, Amsterdam, 1970, pp 109–111.
23. Sjöström M, Neglén P, Fridén J, Eklof B: Human skeletal muscle metabolism and morphology after temporary incomplete ischaemia. Eur J Clin Invest, 1982, 12, 69–79.
24. Williams P, Goldspink G: Longitudinal growth of striated muscle fiber. J Cell Sci, 1971, 9, 751–767.
25. Wohlfart G: Dystrophia myotonica and myotonia congenita: histopathological studies with special reference to changes in muscles. J Neuropathol Exp Neurol, 1951, 10, 109–124.

Author's address: Department of Neurology, School of Medicine, 1A Banacha Str., 02-097 Warszawa.

NEUROPAT. POL. 1991, 29, 1–2
PL ISSN 0028-3894

JANINA RAFAŁOWSKA[1], STANISŁAW KRAJEWSKI[2]

DO ASTROGLIAL CELLS PARTICIPATE IN THE PROCESS OF HUMAN SPINAL CORD MYELINATION?

[1]Department of Neurology, School of Medicine, Warsaw, and Neuromuscular Unit, Medical Research Centre, Polish Academy of Sciences, Warsaw, [2]Department of Neuropathology, Medical Research Centre, Polish Academy of Sciences, Warsaw

The material comprised spinal cord segments C_8 or Th_1 of 6 human fetuses aged from 16–17 up to 34 weeks and 6 infants aged from one day to 3 years. On formalin-fixed, paraffin-embedded sections, peroxidase-antiperoxidase Sternberger's et al. (1970) method for visualization of astrocytic proteins (S-100 and GFAP), myelin basic protein (MBP) and neuron specific enolase (NSE), was used. Parallelly to the increasing immunoreactivity to MBP, more S-100 and GFAP-positive cells were observed. Immunoreactivity to S-100 was more distinct in astrocytic perikarya, whereas, in GFAP reaction immunostaining of astrocytic processes was more pronounced. It is very difficult to explain why reactivity of astrocytes appears during myelination.

Key words: *human ontogenesis, spinal cord myelination, astrocytes reactivity.*

In recent years many investigations on astrocytic immunoreactivity during embryonal and early fetal development of the central nervous system (CNS) in some mammals and humans were performed. An important role of radial glia, particularly in the process of migration was noted (Choi et al. 1985, 1987; Choi 1986, 1988). Astroglial cell participation in the process of experimental remyelination within the CNS is also known (Blakemore 1973; Blakemore et al. 1977). Close contact of astroglial processes with myelin sheaths was found in experimental injury of white matter before disintegration of myelin (Goncerzewicz 1988). The present work was undertaken to study the astroglial reactivity during the myelination process in humans.

MATERIAL AND METHODS

The material comprised spinal cord segments C_8 or Th_1, of 6 human fetuses aged from 16–17 up to 34 weeks and 6 infants aged from 1 day to 3 years. In fetal cases autopsy was performed 3 h after interruption of pregnancy (for medical or

social reasons), in infant cases – prior to 24 h after death (diseases not pertaining to the nervous system). On formalin-fixed and paraffin-embedded slices, peroxidase-antiperoxidase Sternberger's et al. (1970) method for visualization of astrocytic proteins (S-100 and glial fibrillary acidic protein, GFAP), myelin basic protein (MBP) and neuron specific enolase (NSE) were used.

The immunocytochemical reactions were run as follows: 5–8 μm thick sections, deparaffinized and pretreated with 0.0125% trypsin for 1 h, were preincubated with 25% normal swine serum diluted with trisma-base (Sigma, USA) at pH 7.6. Thereafter, they were incubated overnight with primary polyclonal antibodies against GFAP (1:3000; Dakopatts, FRG), S-100 (1:1500, Dakopatts), MBP (1:1500, Sigma, USA) and NSE (1:1500, Dakopatts). After rinsing the sections in phosphate buffered solution (PSB) at pH 7.6, 1 h incubation with the following secondary reagents was done: swine antibodies against rabbit IgG (1:50) and rabbit-PAP-complex (1:200) (all antisera from Dakopatts, Denmark). The immune reaction was developed during 15 min incubation at 0.05% concentration of 33-Diaminobenzidine tetrachloride (Sigma, USA) with addition of 0.01% H_2O_2. Then, the sections with hemalum counterstaining were dehydrated and mounted with DePeX (Serva, FRG).

RESULTS

In the 17–18th week of fetal life well differentiated nerve cells of the anterior and posterior spinal cord horn were immunopositive to NSE. In this period immunoreaction to MBP, S-100 and GFAP was negative, although myelination gliosis was evident (Fig. 1). In 18th week a weak immunoreactivity to MBP was observed within phylogenicly old tracts, particularly, in Burdach's tracts (Fig. 2). In those tracts S-100 and GFAP reactions were negative, but numerous activated astrocytic nuclei were seen. In the 20th week an apparent reaction to MBP within the posterior funiculi and less intensive within the remaining old tracts was noted (Fig. 3A). Astrocytic immunoreactivity to S-100 (Fig. 3B) and GFAP (Fig. 3C) was found in a part of the cells. In S-100 reaction, astrocytic perikarya stained

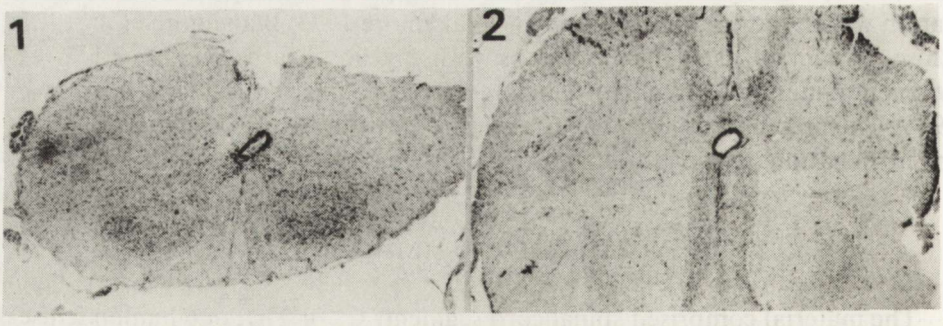

Fig. 1. Fetus 16–17th week. MBP. Negative immunoreactivity. × 45

Fig. 2. Fetus 18th week. MBP. Weak immunoreactivity within phylogenicly old tracts. × 45

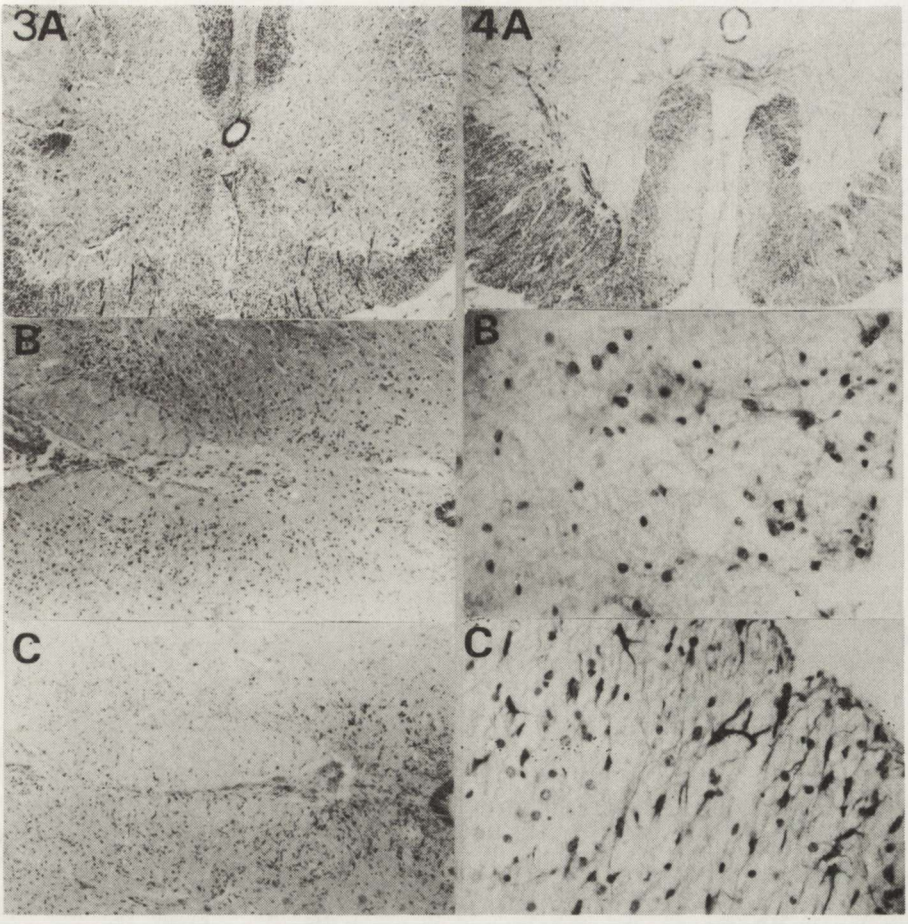

Fig. 3. Fetus 20th week. *A* — MBP. Visible immunoreaction within Burdach's tracts, less intensive within the remaining old tracts. ×45; *B* — anterior pyramidal and old tracts of anterior funiculi. S-100. Clearly visibly astrocytic perikarya. ×102; *C* — anterior pyramidal and old tracts of anterior funiculi. GFAP. More distinctly visible astrocytic processes. ×102

Fig. 4. Fetus 34th week. *A* — anterior funiculi of the spinal cord. Marked reaction within old tracts. ×45; *B* — S-100. n old tracts of anterior funiculus small number of immunopositive astrocytic perikarya. ×448. *C* — GFAP. In old tracts of anterior funiculus evident immunoreactivity perikarya and processes. ×448

rather better than astrocytic processes, which were clearly visible in the GFAP reaction. Parallelly to the increasing immunoreactivity to MBP, more S-100 and GFAP-positive cells were observed (Figs 4 and 5). Immunoreactivity to S-100 was more distinct in astrocytic perikarya (Figs. 4B and 5B), whereas in the GFAP reaction astrocytic processes exhibited more pronounced immunoreactivity (Figs 5C and 6C). Within the anterior horns of the spinal cord, astrocytes located nearby fibers, running to the anterior roots undergoing myelination, were im-

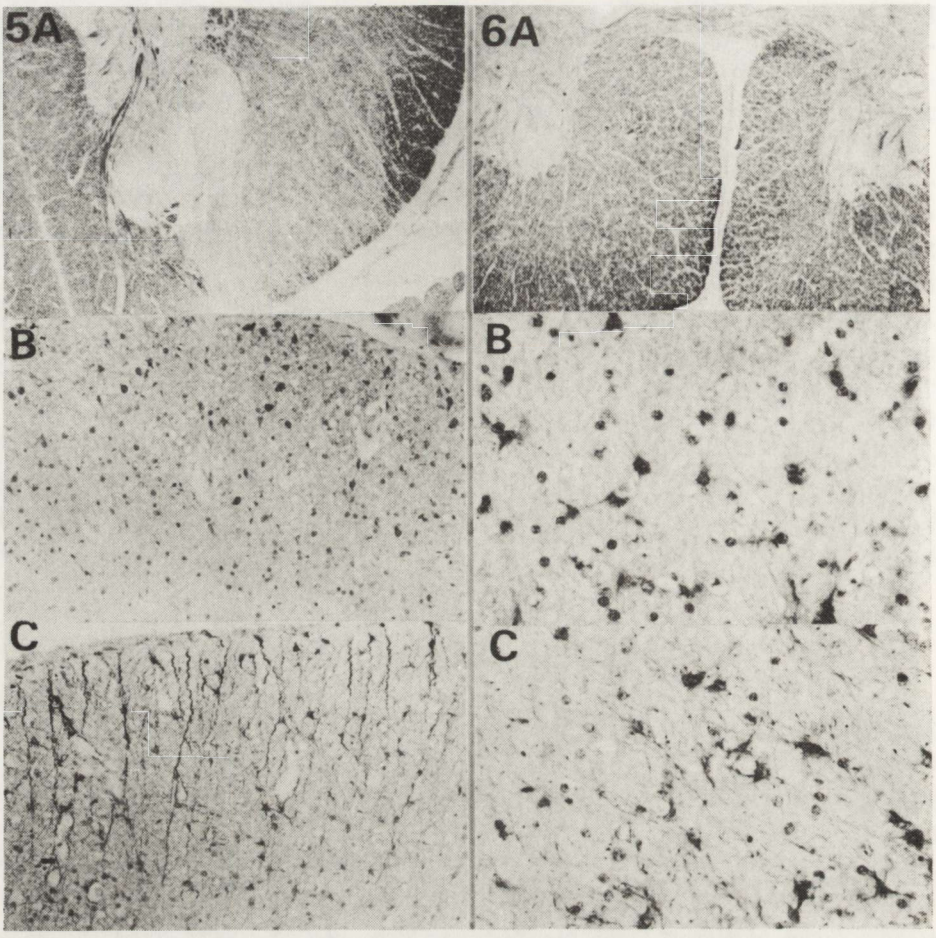

Fig. 5. Newborn, 1 day. *A* — MBP. Posterior-lateral part of the spinal cord. Less pronounced immunoreactivity within lateral pyramidal tract. ×45; *B* — S-100. Old tracts of lateral funiculus and lateral pyramidal tract. Clearly visible astrocytic perikarya within old tracts. ×224; *C* — GFAP. The same localization. Clearly visible astrocytic processes and long radial fibers. ×224

Fig. 6. Infant 3 months. *A* — MBP. Anterior funiculi. Almost the same intensity of myelination of old tracts and anterior pyramidal tract. ×45; *B* — S-100. Anterior funiculus. Small number of immunopositive astrocytic perikarya. ×448; *C* — GFAP. Anterior funiculus. More evident astrocytic processes. ×448

munoreactive both to S-100 as well as to GFAP. As the myelination progressed, the size of immunoreactive astroglial cells increased. In the later period of the myelin development, when light microscopy showed full myelination of the spinal cord (Fig. 7A), reactive astrocytic bodies were not numerous (Fig. 7B). In these stages of myelination, predominance of fibers was observed. Those fibers, radially running to glia limitans, were distinctly stained for GFAP (Fig. 7C). Perivascular astrocytes were immunoreactive both to S-100 and GFAP.

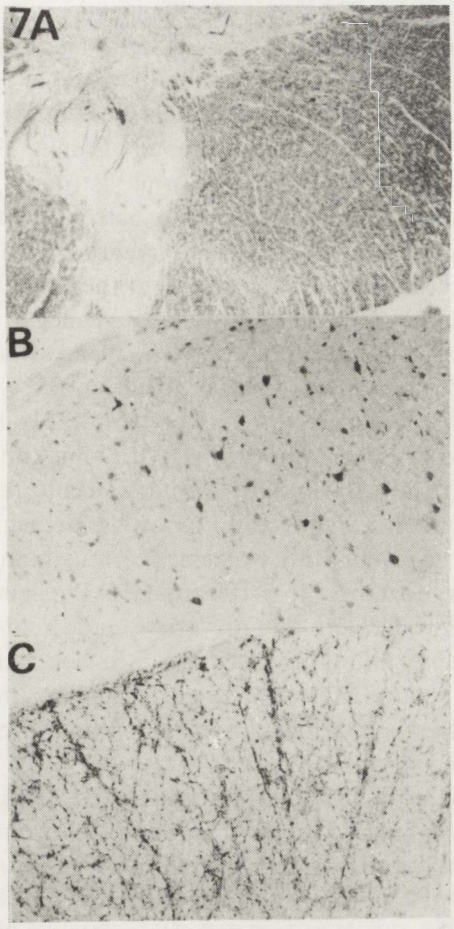

Fig. 7. Infant, 8 months. *A* — MBP. Lateral-posterior part of the spinal cord. Almost full myelination of the lateral pyramidal tract. ×45; *B* — S-100. Small number of reactive astrocytic bodies in old tracts of lateral funiculus and lateral pyramidal tract. ×224; *C* — GFAP. The same localization. Clearly seen radial astroglial fibers. ×224

DISCUSSION

Our results indicated astroglial cell immunoreactivity to S-100 and GFAP within spinal cord tracts undergoing myelination. Immunoreactivity to S-100 was more pronounced in astrocytic perikarya than in processes. This was connected probably with the fact that S-100 is the protein dissolved within the astrocytic cytoplasm, whereas GFAP and vimentin are the principal components of the intermediate filaments of astrocytes (Ciesielski-Treska et al. 1988). Therefore, astrocytic processes were clearly visible in the GFAP reaction.

It is very difficult to explain why the reactivity of astrocytes appears during the myelination process and what is their function. Some data on the latter were

obtained from tissue culture investigations. They indicate that various mitogenic peptides probably play the role of growth factors during myelination. The epidermal growth factor (EGF) causes an increase of glutamine synthetase activity and astrocytic maturation, and the presence of astrocytes facilitates the growth of oligodendrocytes (Honegger, Guentert-Lauber 1983). Type I astrocyte with fibroblast-like morphology (protoplasmic astrocyte *in vivo*) and type II astrocyte with neuron-like structure (fibrous astrocyte *in vivo*) were found in developing rat white matter. Both types of astrocytes were GFAP-positive, however, they did not change from one type to the other in culture (Raff et al. 1983a); whereas, from the A2B5-positive and GFAP-negative precursor of astrocytic cell (in optic nerve culture) both, typ II astrocytes and oligodendrocytes develop depending on the culture medium (Raff et al. 1983b). Some data also indicate that cells phenotypically similar to type I and II astrocytes from tissue cultures exist in humans (Elder, Major 1988). We do not know wether and in what degree it is possible to apply the findings from tissue culture to *in vivo* conditions. It may also be, that under *in vivo* conditions, on the occasion of oligodendroglia proliferation during the myelination process, a certain quantity of astrocytes also develop. Their immunoreactivity to S-100 and GFAP reflects, probably, repeated stages of astrocytes development and maturity. Gaps in our material and use of light microscopy do not allow an accurate estimation of the parallellism of myelination and astrocytes reactivity. However, it seems that immunoreactivity to MBP is more distinct and occurs earlier than immunoreactivity to S-100 and GFAP.

In early periods of myelination numerous reactive astroglial cells were observed. Then, in neonatal spinal cords with advanced morphological myelination, astroglial fibers, radially running to glia limitans were noted. Immunoreactivity to GFAP was also observed after the first postnatal week within rat spinal cord (Joosten, Gribnau 1989), then during myelination. Besides "occasional" proliferation of astrocytes, astroglial cells play, may be a supporting and trophic function. The close morphological and biochemical relationship of astrocytes and blood vessels permit to suppose that astroglial cells influence the metabolism of the young developing myelin sheaths. Difficulties in explanation of numerous findings in our material indicate the necessity of further investigations with the use of other methods including double stainings and, particularly electron microscopy.

CZY KOMÓRKI GLEJU GWIAŹDZISTEGO BIORĄ UDZIAŁ W PROCESIE MIELINIZACJI?

Streszczenie

Na materiale 12 przypadków płodów ludzkich i dzieci zmarłych w wieku 1 dzień – 3 lata za pomocą metod immunocytochemicznych (MBP, S-100, GFAP) stwierdzono obecność odczynowych komórek gleju gwiaździstego w mielinizujących się szlakach rdzenia kręgowego. W reakcji na białko S-100 bardziej były widoczne ciała astrocytów, w odczynie na GFAP natomiast – wypustki astrocytarne. Nie jest jasne, dlaczego w procesie mielinizacji pojawiają się astrocyty odczynowe i jaka jest ich rola.

REFERENCES

1. Blakemore WF: Demyelination of the superior cerebellar peduncle in the mouse induced by cuprisone. J Neurol Sci, 1973, 20, 63–72.
2. Blakemore WF, Eames RA, Smith KJ, McDoland WJ: Remyelination in the spinal cord of the cat following intraspinal injection of lysolecithin. J Neurol Sci, 1977, 33, 31–43.
3. Choi BH: Developmental events in early stages of neocortical plate formation in human brain: immunocytochemical and electron microscopic study. Exp Neurol, 1986, 45, 373 (Abstr).
4. Choi BH: Developmental events during the early stages of cerebral cortical neurogenesis in man. A correlative light, electron microscopic, immunohistochemical and Golgi study. Acta Neuropathol (Berl), 1988, 75, 441–447.
5. Choi BH, Kim RC, Peckham N: Myelin-forming glial cells of developing mouse spinal cord: immunocytochemical and ultrastructural studies. J Neuropathol Exp Neurol, 1985, 44, 345 (Abstr).
6. Choi BH, Kim RC, Peckham N: Ultrastructural and immunocytochemical studies of radial glia and astroglia in the developing mouse forebrain. J Neuropathol Exp Neurol, 1987, 46, 352 (Abstr).
7. Ciesielski-Treska J, Goetschy JF, Ulrich G, Aunis O: Acquisition of vimentin in astrocytes cultured from postnatal rat brain. J Neurocytol, 1988, 17, 79–89.
8. Elder GA, Major EO: Early appearance of type II astrocytes in developing brain. Dev Brain Res, 1988, 42, 146–150.
9. Goncerzewicz A: The role of astroglia in pathological processes characterized by myelin disintegration. II. Electron enzyme and immunocytochemistry of the astroglia in experimental injury to white matter. Neuropatol Pol, 1988, 26, 127–149.
10. Honegger P, Guentert-Lauber B: Epidermal growth factor (EGF) stimulation of cultured brain cells. I. Enhancement of the developmental increase in glial enzymatic activity. Dev Brain Res, 1983, 11, 245–251.
11. Joosten EAJ, Gribnau AAM: Astrocytes and guidance of outgrowth corticospinal tract axons in the rat. An immunocytochemical study using anti-vimentin and antiglial fibrillary acidic protein. Neuroscience, 1989, 31, 439–452.
12. Raff MC, Miller RM, Noble M: A glial progenitor cell that develops in vitro into astrocytes or an oligodendrocyte depending on culture medium. Nature, 1983b, 303, 390–396.
13. Raff MC, Abney ER, Cohon J, Lindsay R, Noble H: Two types of astrocytes in cultures of developing rat white matter: differences in morphology, surface gangliosides, and growth characteristics. J Neurosci, 1983a, 3, 1289–1300.
14. Sternberger LA, Hardy PH Jr, Cuculis FF, Meyer MG: The unlabelled antibody enzyme method of immunohistochemistry: preparation and properties of soluble antigen-antibody complex (horseradish peroxidase anti-peroxidase) and its use in identification of spirochetes. J Histochem Cytochem, 1970, 18, 315–333.

Author's address: Department of Neurology, School of Medicine, 1A Banacha Str., 02-097 Warsaw, Poland.

NEUROPAT. POL. 1991, 29, 1–2
PL ISSN 0028-3894

HANNA DRAC, MAREK BABIUCH, WIESŁAWA WIŚNIEWSKA

MORPHOLOGICAL AND BIOCHEMICAL CHANGES IN PERIPHERAL NERVES WITH AGING*

Department of Neurology, School of Medicine, Warsaw

The ulnar nerve taken at autopsy from 30 subjects aged 24–98 who died without features of clinical involvement of peripheral nerves was examined morphologically. Density of myelinated fibers (m.f) per 0.1 mm^2, frequency distribution of the external diameter of m.f., and teased fiber were estimated. Besides, in 8 nerves some lipids were assessed biochemically. The study showed that the percentage of fibers with morphological changes increases with aging (7–10% in adults and even up to 35% in aged subjects). In older subjects loss of m.f. may be marked. Morphological changes in the nerves of subjects in all groups of age are unspecific (axonal degeneration, and segmental demyelination). Striking feature for the nerve is the preserved ability to repair damage of the fiber independently of the subjects' age. Accidental factors play some role as a cause of morphological changes in the nerve in all groups of age but in the elderly, aging of the neuron seems to be an important factor. Biochemical changes in the nerves with age are not prominent, and much less expressed than morphological changes.

Key words: *peripheral nerves, nerve degeneration, nerve regeneration, lipids, aging.*

The process of aging in latest twenties has attracted attention of many investigators. Much interest concerns the central nervous system, less attention is devoted to the peripheral nervous system, especially to peripheral nerves in man. It is known that paresthesia, diminished sensation, decreased reflexes are not infrequent in aged patients. Such symptoms and signs can reflect the impairment of the lower neuron at various levels including the nerve fiber. A reduction in the number or density of human myelinated fibers with aging in man has been demonstrated in spinal roots and peripheral nerves (Swallow 1966; O'Sulliwan, Swallow 1968; Rafałowska et al. 1976; Toghi et al. 1977; Jacobs, Love 1984).

The present study provides information on morphological changes in aged people as compared with adults, and some correlation with biochemical characteristics viz. lipids in the nerve.

* Work supported by the Institute of Psychiatry and Neurology within agreement No R34.1.

MATERIAL AND METHODS

The ulnar nerve taken at autopsy from 30 subjects aged 24-98 who died without features of clinical involvement of peripheral nerves was examined morphologically, besides, 8 ulnar nerves from subjects aged 33-98 were assessed biochemically. The nerves were taken within 6 up to 24 h after death by excision at elbow level. In the case of cerebral stroke the nerve was removed contralaterally to hemiparesis.

Morphological examination in all cases included: density of myelinated fibers per 0.1 sq mm, frequency distribution of the external diameter of myelinated fibers, qualitative estimation of thick Epon sections, qualitative and quantitative estimation of teased fibers. Internodal length versus diameter for 20-25 fibers in 5 cases was plotted.

After removing the specimen was divided into 4 portions: for routine histological stainings, for thick Epon sections, for teased preparations and for biochemical purposes.

The specimen for routine histology was fixed in Baker's solution and then paraffin sections were stained with hematoxylin and eosin and according to van Gieson method. The second part of the specimen was fixed in 1% osmium tetroxide, dehydrated and embedded in Epon. Thick Epon sections (1-1.5μm) were cut with an LKB ultratome and stained with toluidine blue (modified Pal-Kultschitzky method) or thionine and acridine orange. For histological measurements sections were photographed under a light microscope and magnified up to × 1000 (in cases No. 1, 2, 7, 13, 19-21, 24-26, 29). In remaining cases photographs were magnified × 1600 and measurements were done using the semiautomatic analyzer MINIMOP Opton. The third part of the specimen was fixed in 5% glutaraldehyde, postfixed in 1% osmium tetroxide, washed in buffer and passed through glycerine in increasing concentrations (from 5-40%). Single fibers (30-200) were then isolated without preselection from each available fascicle (as routine we asses 30 fibers consisting of at least 4 internodes). The percentage of demyelinated or remyelinating fibers as well as extention of these processes in the particular fiber and percentage of fibers undergoing axonal degeneration were estimated basing on single fibers. The process of regeneration after axonal degeneration was mainly assessed on thick Epon sections. To compare morphological parameters with the age of the subjects the material was divided into four groups: Group I – subjects aged 20-30 (5 cases), group II – subjects aged 40-59 (7 cases), group III – subjects aged 60-69 (2 cases) and group IV – subjects aged 70-98 (16 cases). Having in mind the not numerous representation of groups I and III statistical correlations have not been established but only regression lines relating some parameters to age of the subjects were plotted.

Biochemical studies. The nerves were weighed, homogenized in a mixture of chloroform and methanol (2:1 v/v) and total lipids were extracted by the method of Folch-Pi et al. (1957). Total lipids were quantitated by the Bio-La-Test (Lacheman, Brno). Total phospholipids were determined by the

method of Bartlett (1959) and total cholesterol by the method of Błaszczyszyn (1970). Neutral lipids were qualitatively tested by thin-layer chromatography on Silica Gel H (Merck) coated glass plates (Muller, Vahar-Matiar 1974). The phospholipids classes were separated similarly, the only difference was the composition of the developing chromatographic mixture (chloroform : methanol : water, 65 : 30 : 5 v/v). The R_f values of the particular separated lipid classes were compared to those of pure Sigma standards. The percentage composition of the lipid fractions after planimetry of the densitometric curves obtained in ERJ-65 densitometer (Zeiss, Jena) was estimated. In statistical analysis of biochemical results the correlation coefficient between the level of the particular lipid classes and the age of the cases was taken into account. Regression lines are presented.

RESULTS

Morphology

In all examined cases on thick Epon sections different in number abnormal fibers were visible. Abnormalities included: loss (not frequently) of myelin sheath (demyelinating fibers), too thin in relation to axonal diameter myelin sheath (remyelinating fibers), complete blurring of fiber structure (Figs 1A, B); splitting of myelin sheath was seen, which in some instances might have been artifactual (excision of the nerves late after death). In most cases were on cross Epon sections groups of small myelinated fibers, numerous not infrequently, observed (Figs 2A, B). A striking feature of some nerves was the lower density of the myelinated fibers. As a rule histograms of diameters of myelinated fibers were bimodal (Figs 3A-C), but two of them were unimodal indicating loss of thick fibers (case No. 3 aged 33, and No. 27 aged 87). For data concerning density of myelinated fibers, range of histograms and percentage of thin and thick fibers see Table 1.

In teased preparations demyelinated, remyelinated, fibers undergoing axonal degeneration and regenerated fibers were seen (Table 2). Remyelination in some older cases was particularly extensive (Tab. 2, Fig. 4). Various stages of axonal degeneration were observed (Figs 5A, B). Internodal length of fibers plotted against their diameter revealed the presence of regenerated and remyelinating thin fibers in most cases (Figs 6A, B). The percentage of abnormal fibers in particular groups is shown in Table 3. For the regression line relating abnormal fibers and density of myelinated fibers per 0.1 sq mm, to age of subjects see Figs 7 and 8.

Summarizing it should be underlined that in groups I, I and IV there were cases with lower density of myelinated fibers, much more numerous in the group of oldest cases (No. 18-20, 24, 29). Degenerative changes of nerve fibers were much pronounced in aged subjects (Tab. 3) and remyelination was in these cases more extensive than in younger cases. In all groups, including old subjects, there were fibers regenerating after axonal degeneration.

Table 1. Density of myelinated fibers (mf) per 0.1 mm^2, range of histogram of mf and percentage of thin and thick fibers

Case no.	age	Density of mf per 0.1 mm^2	Fibers with diameter < 6 μm %	> 6 μm %	Range of histogram (μm)
1	24	984	51.9	48.1	1–14
2	29	752	47.6	42.4	1–16
3	33	773	73.0	52.4	1–10
4	37	753	60.3	39.7	1–13
5	38	649	53.6	46.4	1–15
6	41	532	52.2	47.8	1–15
7	42	1252	58.2	41.8	1–14
8	49	1038	56.0	44.0	1–18
9	51	680	53.0	47.0	1–17
10	53	784	63.3	36.7	1–13
11	56	658	63.6	36.4	1–15
12	59	756	68.6	31.4	1–12
13	60	866	35.3	64.7	1–16
14	66	983	60.4	39.6	1–14
15	72	801	63.7	36.3	1–12
16	72	901	61.8	38.2	1–14
17	76	831	64.9	35.1	1–14
18	78	520	58.6	41.4	1–15
19	80	644	47.2	52.8	1–17
20	81	650	46.4	53.6	1–16
21	83	837	41.0	59.0	1–16
22	84	881	60.0	40.0	1–15
23	84	764	52.2	47.8	1–15
24	86	443	43.9	56.1	1–15
25	87	817	39.6	60.4	1–17
26	88	792	54.1	45.9	1–13
27	89	752	77.2	26.8	1–10
28	91	831	70.6	29.4	1–13
29	93	659	60.2	39.1	1–16
30	98	709	39.8	60.2	1–13

Table 2. Morphological changes in teased fibers

Case		Number of isolated fibers	Segmental de- and remyelination		Axonal degeneration		Regenerated fibers		Total fibers with histological changes
no.	age		number	%	number	%	number	%	%
1	24	100	2	2.0	0	0.0	3	3.0	5.0
2	29	200	5	2.5	4	2.0	4	2.0	6.5
3	33	35	1	2.9	1	2.9	0	0.0	5.8
4	37	35	1	2.9	1	2.9	1	2.9	5.8
5	38	40	3	8.5	2	5.0	0	0.0	13.5
6	41	35	1	2.9	2	5.7	0	0.0	8.6
7	42	200	7	3.5	1	0.5	20	10.0	14.0
8	49	32	1	3.1	1	3.1	0	0.0	6.2
9	51	100	4	4.0	2	2.0	1	1.0	7.0
10	53	30	2	6.6	1	3.3	0	0.0	9.9
11	56	40	2	5.0	1	2.5	1	2.5	10.0
12	59	35	2	5.8	0	0.0	1	2.9	8.7
13	60	200	20	10.0	2	1.0	6	3.0	14.0
14	66	100	3	3.0	3	3.0	3	3.0	9.0
15	72	100	17	17.0	3	3.0	2	2.0	22.0
16	72	30	6	20.0	1	3.3	1	3.3	26.6
17	76	60	2	3.4	1	1.7	0	0.0	5.1
18	78	52	1	1.9	3	5.8	0	0.0	7.7
19	80	100	24	24.0	1	1.0	6	6.0	31.0
20	81	100	55	5.0	0	0.0	2	2.0	7.0
21	83	100	9	9.0	0	0.0	1	1.0	10.0
22	84	100	5	5.0	3	3.0	3	3.3	11.0
23	84	100	10	10.0	6	6.0	1	1.0	17.0
24	86	100	10	10.0	5	5.0	3	3.0	18.0
25	87	100	5	5.0	3	3.0	1	1.0	9.0
26	88	100	12	12.0	1	1.0	0	0.0	13.0
27	89	100	7	7.0	3	3.0	5	5.0	15.0
28	91	30	3	10.0	2	6.3	3	10.0	26.3
29	93	100	25	25.0	3	3.0	3	3.0	31.0
30	98	100	28	28.0	3	3.0	4	4.0	35.0

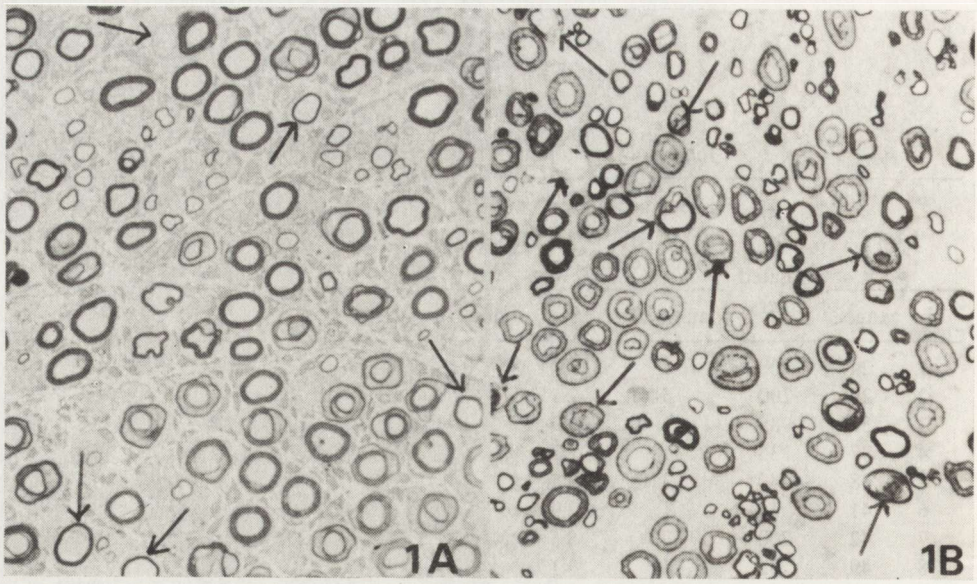

Fig. 1. Transverse section of ulnar nerve. Abnormal fibers (arrows). *A* — Case No. 7, M 42 yrs old; *B* — Case No. 25, F 78 yrs old. Thick Epon sections, Pal-Kultschicky method. ×440

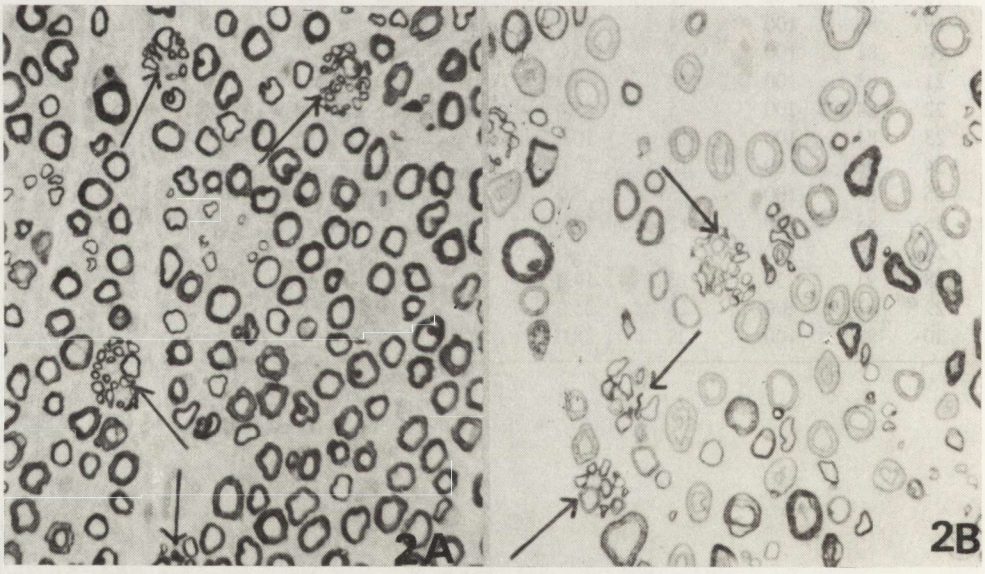

Fig. 2. Transverse sections of ulnar nerve. Fibers with blurred structure (arrows). *A* — Case No. 1. F 24 yrs old; *B* — Case No. 19. M 80 yrs old. Method and magn. as in Fig. 1

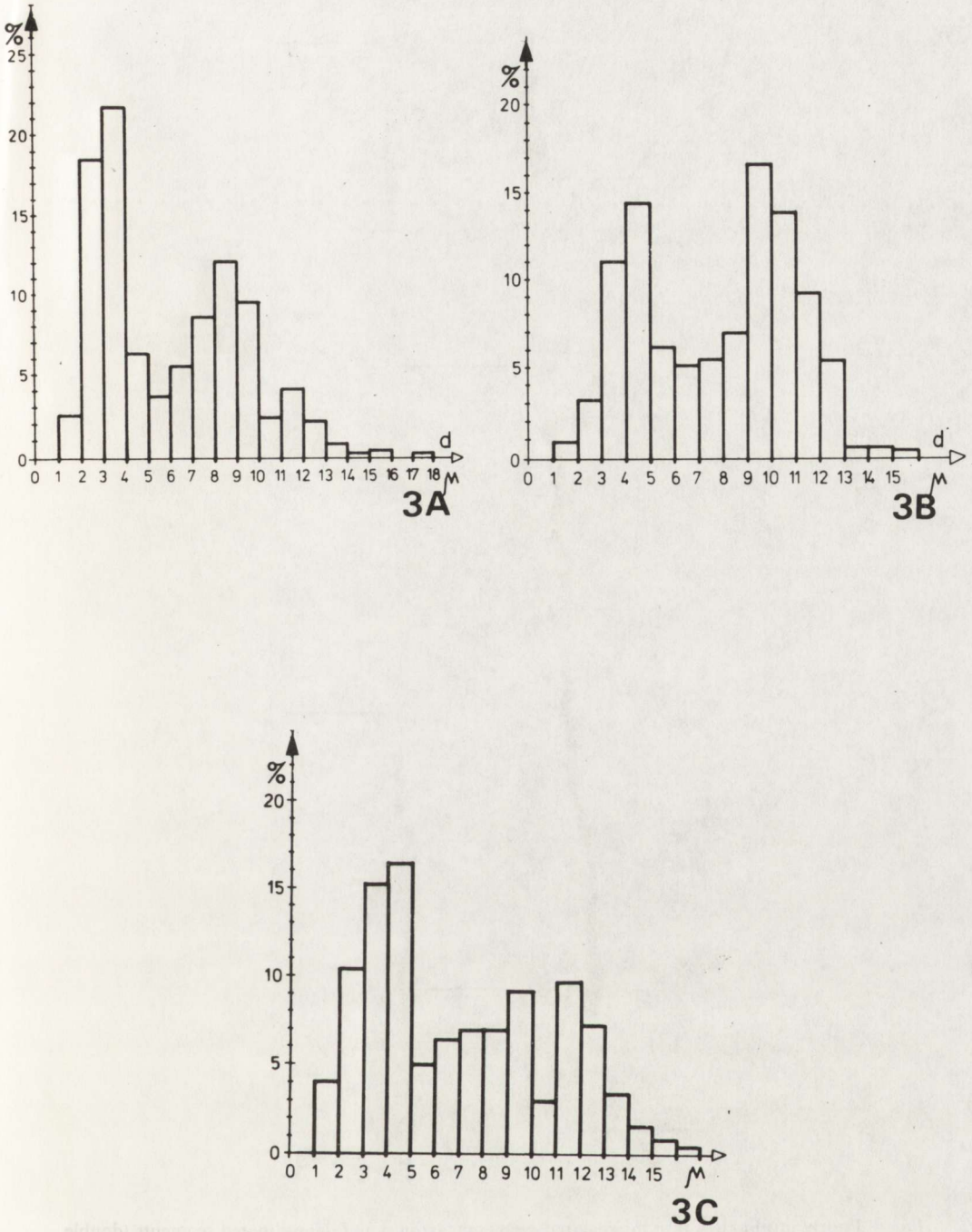

Fig. 3. Histograms of diameters of myelinated fibers. *A* – Case No. 2. M 29 yrs old, 752 mf/0.1 mm^2; *B* – Case No. 13. M 60 yrs old, 860 mf/0.1 mm^2; *C* – Case No. 19. M 80 yrs old, 644 mf/0.1 mm^2

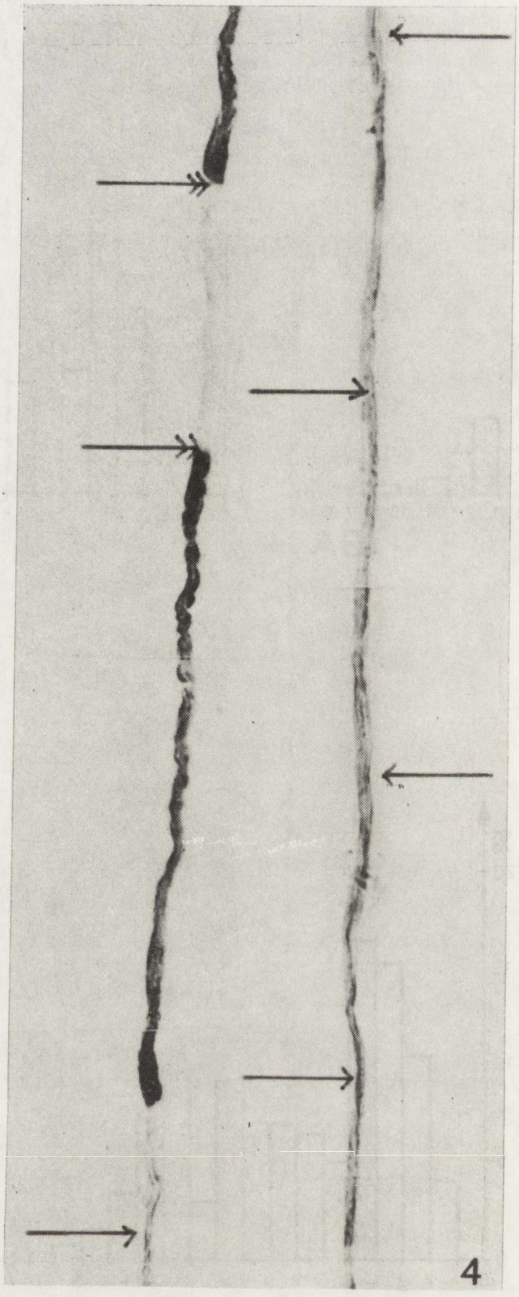

Fig. 4. Poorly myelinated, thin intercalated segments (arrows) and demyelinated segments (double arrows). Teased fiber. × 110

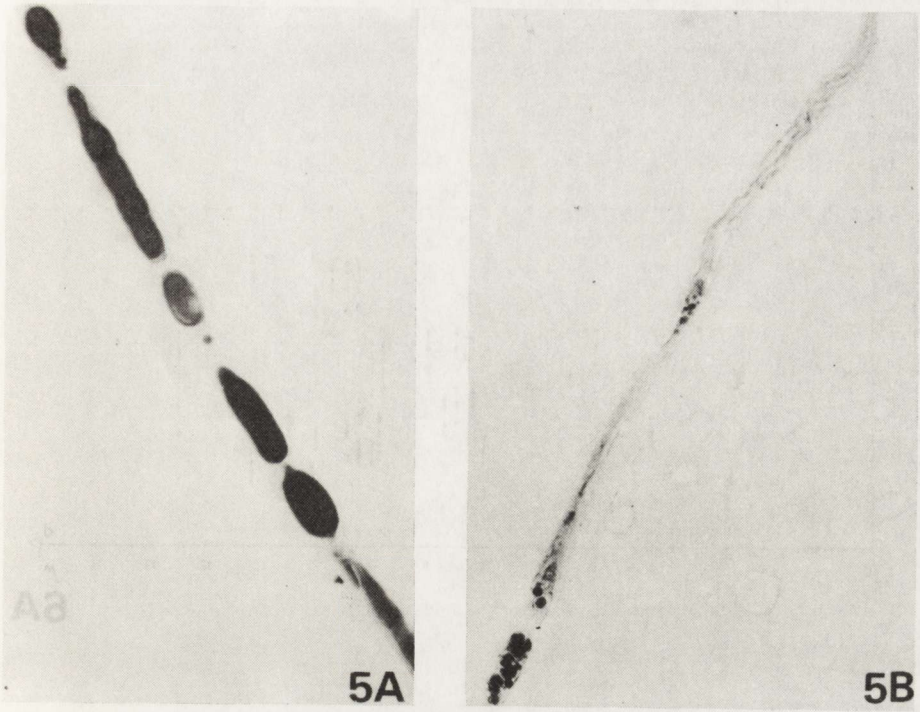

Fig. 5A, B. Various stages of axonal degeneration. Teased fibers. × 220

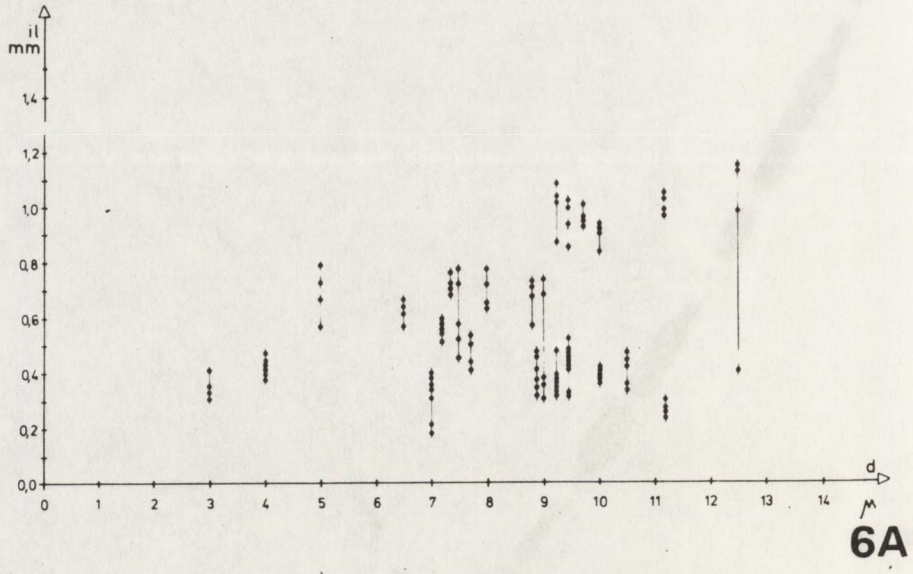

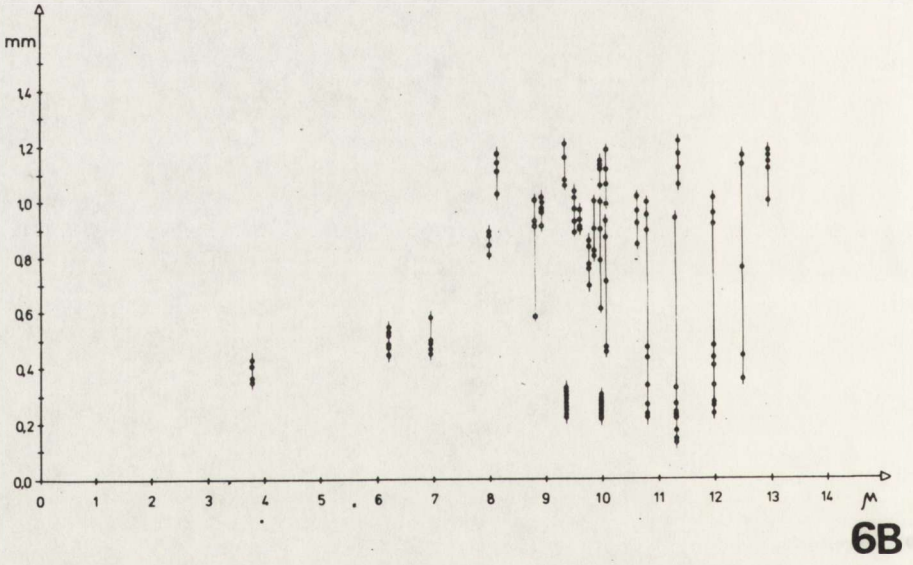

Fig. 6. Inernodal length (il) of fibers plotted against their diameter. Note remyelinating and regenerating fibers. *A* — Case No. 7. M 42 yrs old; *B* — Case No. 13. M 60 yrs old

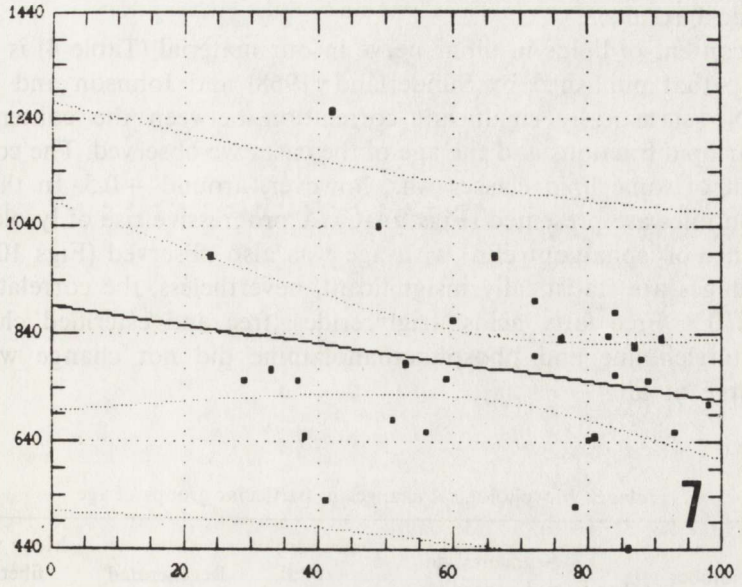

Fig. 7. Regression line relating abnormal fibers to age of subjects

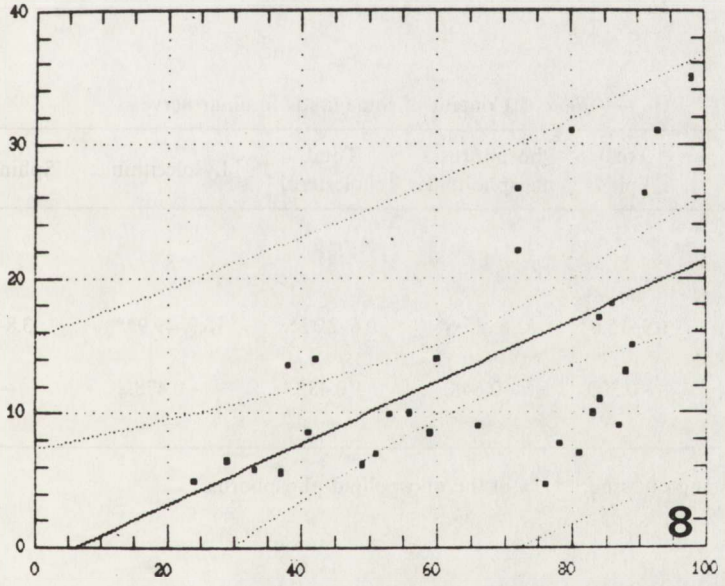

Fig. 8. Regression line relating density of myelinated fiber per 0.1 mm^2 tu age of subjects

Biochemical results

The content of lipids in ulnar nerve in our material (Table 4) is generally similar to that published by Sunderland (1968) and Johnson and McNabb (1948). No statistically significant correlation between the content of the particular lipid fractions and the age of the cases we observed. The correlation coefficient of some lipid classes was, however, around +0.5. In these cases regression lines are presented (Figs 9A-C). A progressive rise of lysolecithin at the expence of sphingomyelin with age was also observed (Figs 10A,B). All these changes are statistically insignificant, nevertheless, the correlation coefficient is 0.5. Free fatty acids, triglycerides, free and esterified cholesterol, phosphatidylcholine and phosphoethanolamine did not change within the ulnar nerve at all.

Table 3. Morphological changes in particular groups of age

Group	Number of cases	Age	Segmental de- and remyelination	Axonal degeneration	Regenerated fibers	Mean values of fibers with morphological changes (%)
I	5	20–29	~ 3.7	~ 2.7	1.0	~ 7.38
II	17	40–59	4.4	2.3	2.3	~ 9.7
III	12	60–69	6.5	2.0	3.0	11.5
IV	16	70–90	~ 11.9	~ 3.1	2.7	17.7

Table 4. Content of some lipids in ulnar nerve

	Total lipids	Phosphorus a. phospholipids	Total cholesterol	Lysolecithin	Sphingomyelin
Number of cases	8	8	8	8	8
Range of value	6.9–15.6*	52.8–25.6*	0.6–2.32*	16.9–49.9**	3.8–11.0**
Correlation coefficient	+0.300	+0.648	+0.433	+0.478	−0.312
Significance	–	–	–	–	–

* µg/100 mg of tissue; ** % of the phospolipid phosphorus.

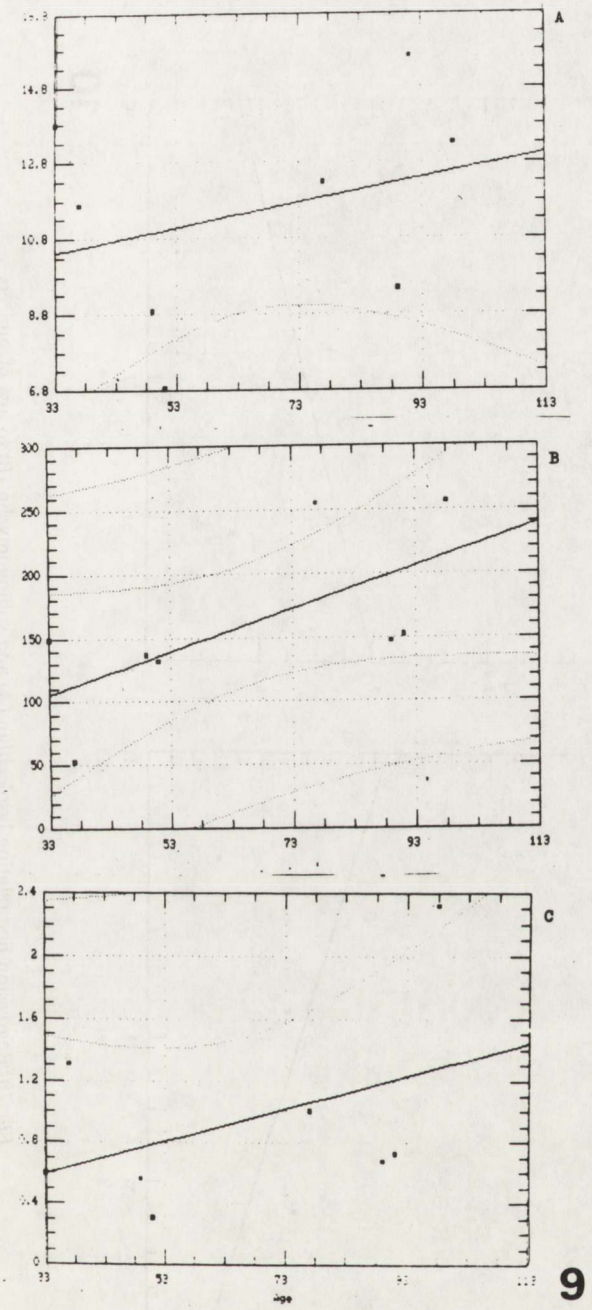

Fig. 9. Regression line relating total lipids (4) total phospholipids, (*B*) cholesterol, (*C*) to age of subjects

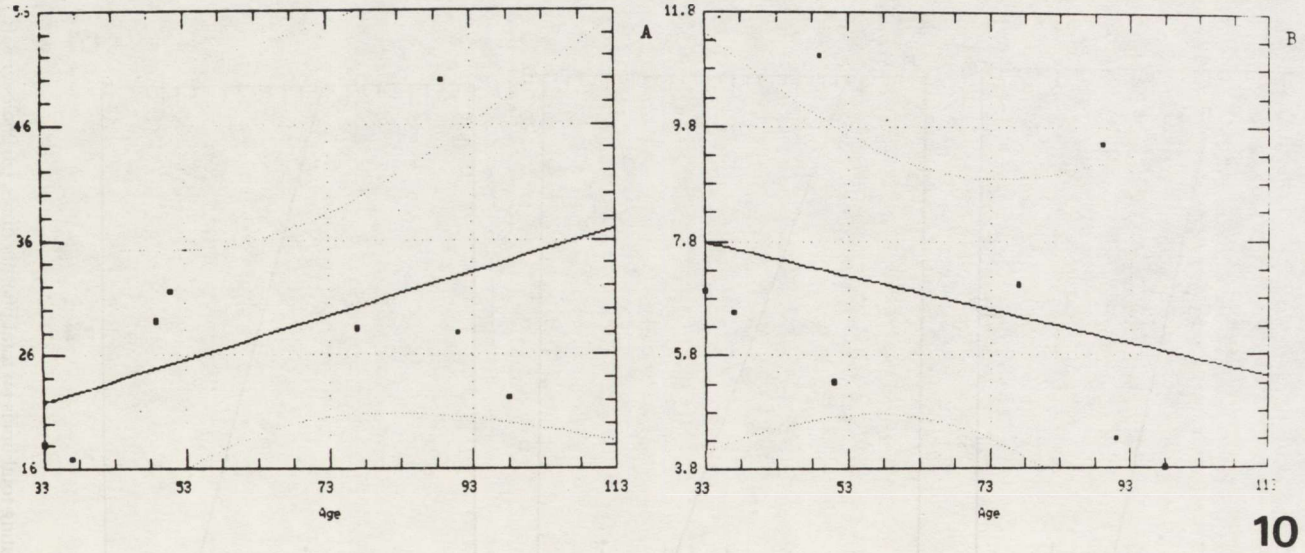

Fig. 10. Regression line relating lysolecithin (*A*) and sphingomyelin (*B*) to age of subjects

DISCUSSION

The presented results revealed morphological differences in the peripheral nerves related to the age of the subjects as well some differences in the nerves of subjects belonging to the same group of age. It is justified to assume that common features of the nerves of subjects from a given group are an exponent of general biological events such as development, maturation and aging. The differences within the same group may reflect individual variability, accidental changes and subclinical involvement of peripheral nerve in the course of some unknown general disorder.

Differences in density of myelinated fibers in the nerves of particular subjects are in agreement with the data presented by other authors (Sunderland, Bedbrook 1949; Buchtal, Rosenfalck 1966; O'Sullivan, Swallow 1966; Dyck et al. 1968, 1971; Chopra, Hurwitz 1969; Ochoa, Mair 1969; Toghi 1972). As the degree of damage to the particular nerves is similar it seems, that different density of myelinated fibers in the younger and less advanced groups of age may reflect the individual variability of subjects. In some cases the high density of fibers is connected with the presence of thin regenerated and remyelinating fibers. These fibers are thinner than their maternal fibers (Thomas 1971). The regeneration and remyelination processes are manifested as disturbance of normal proportions between internodal length and diameter of fiber (Vizoso 1950; Lascelles, Thomas 1966; Arnold, Harriman 1970; Drac 1976), what is especially observed in old age.

Degenerative changes in the nerves of aged subjects are more pronounced than in younger ones. The percentage of remyelinating, regenerating and fibers undergoing breakdown is similar. The presence of a few fibers with segmental demyelination in comparison with the high percentage of remyelinating fibers can probably be explained by the ability to reparation in healthy subjects. Our results concerning the percentage of fibers with morphological changes in aged people are in agreement with the observation of Arnold and Harriman (1971). These authors basing upon median, musculocutaneous and sural nerve examination affirmed that the destructive process can involve 12% of fibers. This is not in full accordance with Dyck et al. (1971), who found 1% of fibers with morphological changes in the sural nerve of subjects above 30 years. If one excludes subclinical involvement of the nerve in the course of some unknown general disorder, it seems that degenerative changes in fibers of adult subjects may be connected with repeated microtrauma, trauma, or pressure on the nerve. The anatomical localization of the ulnar nerve exposes it to mechanical trauma (Gairns et al. 1960; Garren et al. 1962; Thomas, Fullerton 1963; Nearry et al. 1975). It is not possible to decide whether the direct cause of changes in the fiber is mechanical pressure on it or ischemia due to pressure of its nutritional vessels. It seems that morphological changes in the nerves of adults are mostly accidental. However, it is also possible that some of them are a result of aging of the neuron because individual differences in the onset of aging process.

Degenerative changes of nerve fibers are a striking feature of the aged nerves

and are probably the cause of lower density of myelinated fibers in this group of age in comparison with adults. This fact was also noted by others authors (Lascelles, Thomas 1966, Ochoa, Mair 1969a, b). In our material a lower density of fibers was found in single cases (No. 18–20, 24, 29), which could be an exponent of individual expression of the aging. Our results do not confirm that with age thick fibers degenerate first of all (Rexed 1944; Lascelles, Thomas 1966; O'Sullivan, Swallow 1966; Swallow 1966). Decrease of thick fibers was found only in one case. The high percentage of regenerating fibers in the nerves of subjects from the adult group can influence the lack of essential differences between the mean value of the percentage of thin fibers in the adult and senile groups. The high density of fibers in some nerves in the aged group may be connected with the presence of thin remyelinating and regenerating fibers. It seems that the protraction and mildness of the aging process do not impede the ability of neurons to repair impairment of their processes. It is difficult to determine whether in case of axonal degeneration renewal of fibers takes place with participation of the maternal neuron or by axonal sprouting from undestroyed fibers.

The high percentage of fibers with extensive remyelination and axonal degeneration in old age is in keeping with the observations of other authors (Visozo 1950; Arnold, Harriman 1970; Lascelles, Thomas 1966; Jacobs, Love 1985). We agree with Arnold and Harriman (1970) that above 60 years of life the percentage of such fibers is up to 24 (in one of our cases even 35). Morphological changes in the nerve with aging are probably connected with aging of the organism as a whole, however, the role of accidental factors remains unchanged. So, if one thinks of degenerative changes in the nerves in the elderly, one should take into consideration aging of neuron, vascular and in the surrounding tissue abnormalities and accidental factors. Impaired blood supply to peripheral nerves as a factor resulting in damage of the nerve fibers in the elderly, have been stressed by some authors (Swallow 1966; Lascelles, Thomas 1966; Toghi et al. 1977; Jacobson, Love 1985). Examination of vessels in some nerves from the presented material (Rafałowska et al. 1976) did not reveal any abnormality so it would seem that vascular and surrounding tissue changes only contribute to the damage of the peripheral nerves in the elderly.

Extensive remyelination in aged subjects prevail over axonal degeneration. Such a picture is characteristic of demyelination secondary to axonal damage. Loss of motor cells in the ulnar nerve nucleus and atrophy of motor cells in the senile group as compared with that in control (Rafałowska et al. 1976) suggest neuronal atrophy as an expression of aging of the peripheral motor neuron. Besides, some neurons undergo with age different morphological and metabolic changes. Accumulation of lipofuscin in the anterior horn cells is connected with a decrease of RNA in the cell (Mann, Yates 1974). Decrease of protein synthesis results in death of cells and their processes. Axonal transport, especially proteins of microtubuli and microfilaments, is slowed down with age this can result in difficulties in saving of the cytoskeleton network and contribute to atrophy of the axon and loss of fibers (Ochs 1973). On the other hand, segmental demyelination

could also indicate Schwann cell aging. It is impossible to estimate to what extent and which of the above mentioned factors or mechanisms contributed to the segmental demyelination and axonal degeneration, but aging of neurons seems to play an important role.

The lipid pattern of peripheral nerves has been already tested (Johnson, Nabb 1949; Horrocks 1967; Sunderland 1968; Nowicka 1973; Spritz et al. 1973; Norton 1977). Mostly, different animals were, however, the subject of examination. Nevertheless, the lipid composition of peripheral nerves in humans as compared with that of animals does not differ significantly (Nowicka 1973; Spritz et al. 1973). There are no qualitative, but only quantitative differences. The age of the subjects has no evident influence on the lipid composition of peripheral nerves (Nowicka 1973; Spritz et al. 1973). It was so in our material. The lipid pattern even in the 98-yrs-old case did not differ significantly from that of the younger ones. An insignificant increase of total lipids, phospholipids and total cholesterol, and lysolecithin at the expense of sphingomyelin with age is, however, noted. This tendency may be the consequence of some changes of the ratio of lipid to non-lipid components. It could be also the result of regeneration processes appearing in older age. A high lipid level in peripheral nerves is often observed in early stages of regeneration. The regeneration processes would be in older cases more advanced than the concomitantly proceeding demyelination (see the high amount of lysolecithin). The fact that no drastic lipid changes with age are observed is possibly the consequence of some slowness of overall metabolic processes. The latter in peripheral nerves is visible as, e.g. a progressive decrease of oxygen and high-energy compounds consumption (Low et al. 1986). The presented material gives evidence that small differences in lipid composition in the nerve appear with age. They point at a process of demyelination, remyelination and breakdown of fiber. This is in keeping with similar morphological processes in the nerve. It should be underlined that morphological changes are more conspicuous than biochemical ones.

CONCLUSIONS

1. The percentage of fibers with morphological changes in adults is about 7–10 and increases with aging ranging sometime to 35. In older subjects in comparison to adults loss of fibers per 0.1 mm^2 may be marked.

2. The morphological changes in the nerves of subjects in all groups of age are unspecific (axonal degeneration and segmental demyelination). The striking feature of the nerve is the preserved ability to repair damage of the fiber independently of the subjects age.

3. Accidental factors play some role as a cause of morphological changes in the nerve in all groups of age, but in the elderly aging of the neuron seems to be an important factor.

4. Biochemical changes in the nerves with age are not prominent, and much less expressed than morphological changes.

ZMIANY MORFOLOGICZNE I BIOCHEMICZNE NERWU OBWODOWEGO W PROCESIE STARZENIA

Streszczenie

Badano nerw łokciowy pobrany na sekcji od 30 osobników w wieku 24–98 lat, zmarłych bez klinicznych cech uszkodzenia neuronu obwodowego. Oceniano gęstość włókien mielinowych na 0,1 mm^2, zewnętrzną średnicę włókien mielinowych i włókna czesane. Ponadto w 8 nerwach oceniono biochemicznie zawartość niektórych lipidów.

Badanie wykazało, że procent włókien ze zmianami morfologicznymi wzrasta z wiekiem (7–10% u dorosłych i niekiedy do 35% u starych osobników). W miarę starzenia się obserwuje się niekiedy dość znaczny ubytek włókien mielinowych. Zmiany morfologiczne, stwierdzane we wszystkich grupach wieku, są nieswoiste (zwyrodnienie aksonalne i odcinkowa demielinizacja). W nerwach tzw. zdrowych osobników, niezależnie od ich wieku, zasługuje na uwagę zdolność do odnowy uszkodzenia (remielinizacja, regeneracja). W powstawaniu zmian we włóknach czynniki przypadkowe odgrywają rolę w każdym wieku. W wieku starczym istotne znaczenie w powstawaniu zmian wydaje się mieć proces starzenia się neuronu. Zmiany biochemiczne w nerwie obwodowym wraz z wiekiem są nikłe, znacznie mniej wyrażone niż zmiany morfologiczne.

REFERENCES

1. Arnold M, Harriman DGF: The incidence of abnormality in control human peripheral nerves studied by single axon dissection. J Neurol Neurosurg Psychiatry, 1970, 33, 55–61.
2. Bartlett GR: Phosphorus assay in column chromatography. J Biol Chem, 1959, 234, 466–468.
3. Błaszczyszyn M: Oznaczanie cholesterolu. Probl Lek, 1970, 9, 219–221.
4. Buchtal F, Rosenfalck A: Number and diameter of myelinated fibers in the median nerve. Brain Res, 1966, 3, 85–94.
5. Chopra JS, Hurwitz LJ: Sural nerve myelinated fibre density and size in diabetics. J Neurol Neurosurg Psychiatry, 1969, 32, 149–154.
6. Drac H: Zmiany w nerwach obwodowych osobników w różnym wieku bez cech uszkodzenia neuronu obwodowego. Ph.D. thesis, School of Medicine, Warsaw, 1976.
7. Dyck PJ, Gutrecht JA, Bastron JA, Karnes WE, Dale AJD: Histologic and teased fiber measurements of sural nerve in disorders of lower motor and primary sensory neurons. Mayo Clin Proc, 1968, 43, 81–123.
8. Dyck PJ, Lambert EH, Nicholas PC: Quantitative measurements of sensation related to compound action potential and number and size of unmyelinated fibers of sural nerve in health, Friedraich's ataxia, hereditary sensory neuropathy and tabes dorsalis. In: Handbook of electroencephalography and clinical neurophysiology, Elsevier, Amsterdam, 1971, vol 9, pp 93 and 118.
9. Folch-Pi J, Lees M, Sloane-Stanley GH: A simple method for the isolation and purification of total lipids from animal tissues. J Biol Chem, 1957, 226, 487–509.
10. Gairns FW, Garven HSD, Smith G: The nerve fibre populations of the leg in chronic occlusive arterial disease in man. Scott Med J, 1962, 7, 250–265.
11. Garren HSD, Gairns FW, Smith G: The digital nerve and the nerve endings in progressive obliterative arterial disease of the leg. Scott Med J, 1962, 7, 260–280.
12. Horrocks LA: Composition of myelin from peripheral and central nervous system of the squirrel monkey. J Lipid Res, 1967, 8, 569–576.
13. Jacobs JM, Love S: Qualitative and quantitative morphology of human sural nerve at different ages. Brain, 1985, 108, 897–924.
14. Johnson AC, McNabb RA: Lipids in Wallerian degeneration. Biochem J, 1948, 44, 494–498.
15. Lascelles RG, Thomas PK: Changes due to age in internodal lenght in the sural nerve in man. J Neurol Neurosurg Psychiatry, 1966, 29, 40–44.

16. Low PA, Schmelzer JD, Ward KK: The effect of age on energy metabolism and resistance to ischaemic conduction failure in rat peripheral nerve. J Physiol, 1986, 374, 263–271.
17. Mann DMA, Yates PO: Lipoprotein pigments – their relationship to aging in the human nervous system. X. The lipofuscin content of nerve cells. Brain, 1974, 97, 481–488.
18. Muller J, Vahar-Matiar H: Eine chromatographische Micromethode zur Bestimmung der Lipide cerebrospinalis. Z Neurol, 1974, 206, 333–334.
19. Nearry D, Ochoa J, Gilliat RN: Subclinical entrapment neuropathy in man. J Neurol Sci, 1975, 24, 283–298.
20. Norton WT: Isolation and characterization of myelin. In: Myelin. Ed.: P Morell, Plenum Press, New York–London, 1977, pp 161–199.
21. Nowicka K: Skład lipidów w nerwie łydkowym w polineuropatiach i niektórych genetycznie uwarunkowanych chorobach ośrodkowego układu nerwowego. Ph D thesis. School of Medicine, Warsaw, 1973.
22. Ochoa J, Mair WGP: The normal sural nerve in man. Ultrastructure and numbers of fibers and cells. Acta Neuropathol (Berl), 1969a, 13, 197–216.
23. Ochoa J, Mair WGP: The normal sural nerve in man. II. Changes in the axons and Schwann cells due to ageing. Acta Neuropathol (Berl), 1969b, 13, 217–239.
24. Ochs S: Effect of maturation and aging on the rate of fast axoplasmic transport in mammalian nerve. Prog Brain Res, 1973, 40, 349–362.
25. O'Sullivan DJ, Swallow M: The fibre size and content of the radial and sural nerves. J Neurol Neurosurg Psychiatry, 1968, 31, 464–470.
26. Rafałowska J, Drac H, Rowińska H: Histological and electrophysiological changes of the lower motor neurone with aging. Pol Med Sci Histol Bull, 1976, 15, 271–280.
27. Rexed B: Contribution to the knowledge of postnatal development of the peripheral nervous system in man. Acta Psychiatr Scand (suppl), 1944, 33.
28. Spritz N, Singh H, Coyer B: Myelin from human peripheral nerves. Quantitative and qualitative studies in two age groups. J Clin Invest, 1973, 52, 520–523.
29. Sunderland S: Nerves and nerves injuries. Livingstone, Edinburgh–London, 1986.
30. Sunderland S, Bedbrook AM: The cross sectional area of peripheral nerve trunks occupied by the fibres representing individual muscular cutaneous branches. Brain, 1949, 72, 613–624.
31. Swallow M: Fibre size and content of anterior tibial nerve of the foot. J Neurol Neurosurg Psychiatry, 1966, 29, 205–213.
32. Thomas PK: The morphological basis for alteration in nerve conduction in peripheral neuropathy. Proc Roy Soc Med, 1971, 64, 295–298.
33. Toghi H: Quantitative variation with age in normal sural nerve. Clin Neurol (Tokyo), 1972, 12, 484–494.
34. Toghi H, Tsukagoshi H, Toyokura Y: Quantitative changes with age in normal sural nerves. Acta Neuropathol (Berl), 1977, 38, 213–220.
35. Thomas PK, Fullerton PM: Nerve size in the carpal tunnel system. J Neurol Neurosurg Psychiatry, 1963, 26, 520–528.
36. Vizoso AD: The relationship between internodal lenght and growth in human nerves. J Anat, 1950, 84, 342–353.

Authors' address: Department of Neurology, School of Medicine, 1A Banacha Str., 02-097 Warsaw, Poland.

NEUROPAT. POL. 1991, 29, 1–2
PL ISSN 0028-3894

EWA MATYJA, ELŻBIETA KIDA

PROTECTIVE EFFECT OF NIMODIPINE AGAINST QUINOLINIC ACID-INDUCED DAMAGE OF RAT HIPPOCAMPUS *IN VITRO*

Department of Neuropathology, Medical Research Centre, Polish Academy of Sciences, Warsaw, Poland

The study was undertaken to examine the effect of nimodipine, calcium channels blocker, on the morphological alterations induced by quinolinic acid (QUIN). The experiment was performed on 21-day-old organotypic rat hippocampal cultures. Nimodipine was applied to the nutrient medium simultaneously with QUIN (both at 100 μM). Ultrastructural changes were evaluated 24 h, 5 and 7 days after the exposure to tested agent. It was shown that nimodipine induced distinct cytoprotective effect, especially considering the development of late neurotoxic injury produced by QUIN. However, the protection was not complete, indicating the participation of the other factors in the pathomechanism underlying structural damage produced by QUIN.

Key words: *quinolinic acid, calcium channels blocker-nimodipine, tissue culture.*

The neurotoxic properties of excitatory acidic amino acids have been widely studied, but so far the exact mechanisms of neuronal injury are not convincingly enough explained. The suggestion that more than one factor may be responsible for the neurotoxicity of these compounds, including the well-known effect of sustained depolarization (Olney 1978), has been proposed. More recently, an excessive calcium influx from the extracellular space triggered by amino acids has been suggested as one of the toxic mechanisms (Coyle et al. 1981; Berdichevsky et al. 1983; Griffiths et al. 1983; Retz, Coyle 1984; Mayer, Westbrook 1987).

Quinolinic acid (QUIN), an endogenous excitatory amino acid, has been considered as a possible etiological factor in several neurodegenerative disorders (Schwarcz et al. 1984) and the prevention of its neurotoxicity is of important therapeutic value. Since it has been indicated that changes in Ca^{2+} could be potent modulators of neuronal excitability (Choi 1985; Garthwaite et al. 1986; Kohr, Heinemann 1988), it seems interesting to study the protective effect of calcium entry blockers.

The present study was undertaken to examine the effect of one of the calcium entry blockers – nimodipine on the development of QUIN-induced neuronal damage in organotypic cultures of the hippocampal formation.

MATERIAL AND METHODS

The experiments were performed on 21-day *in vitro* (DIV) organotypic cultures of rat hippocampus, well differentiated and sensitive to QUIN action (Kida, Matyja 1988). The cultures prepared from 2–3-day-old Wistar rats were kept in Maximow assemblies et 36.5°C and fed twice weekly. The nutrient medium consisted of 20% fetal bovine serum and 80% Minimal Essential Medium (MEM) supplemented with glucose to a final concentration of 600 mg% without any antibiotics. On the 21st day *in vitro* selected cultures were divided into four groups. One group of cultures was exposed to a medium supplemented with 100 μM of QUIN (Sigma, Ch.Co). The second was maintained in medium containing both QUIN and nimodipine 100 μM each. Sister cultures were exposed to medium supplemented with 100 μM nimodipine alone. The control cultures were grown under standard conditions in nutrient medium. The cultures were regularly observed in living state by light microscopy. They were fixed for electron microscopy 24 hours, 3 and 7 days post exposure to the agents. Briefly, they were fixed in 1.5% cold glutaraldehyde for 1 h, washed in cacodylate buffer pH 7.2–7.6, postfixed in 2% osmium tetroxide, dehydrated in graded alcohols and embedded in Epon 812. Ultrathin sections were counterstained with lead citrate and uranyl acetate and examined in a JEM 1500 XB electron microscope.

RESULTS

The hippocampal cultures exposed to nimodipine displayed normally appearing neurons and densely packed neuropil rich in synapses, identical with control cultures grown in standard conditions.

The cultures exposed to QUIN alone showed a typical for this neurotoxin morphological pattern of tissue injury, involving damage of both large pyramidal neurons and postsynaptic dendrites. After a lapse of 24 h post QUIN exposure, severely damaged neurons exhibited clumping of nuclear chromatin and destruction of cytoplasmic organelles. The great majority of damaged neurons displayed electron-lucent cytoplasm containing few degenerating organelles such as severely enlarged channels of granular endoplasmic reticulum and damaged mitochondria accompanied by vacuoles and vesicles of various size (Fig. 1). This kind of neuronal changes predominated in the later periods of observation, after 5 and 7 days of QUIN treatment. The postsynaptic abnormalities were characterized by swelling of dendritic processes containing damaged mitochondria and/or various amounts of vacuoles (Fig. 2). The axonal endings remained intact.

The culture exposed simultanously to QUIN and nimodipine showed markedly less pronounced ultrastructural changes in comparison with the cultures exposed to QUIN alone. At an early time of observation, 24 h post QUIN and nimodipine application, some pyramidal neurons revealed morphological alterations consisting mainly of the presence of vacuoles and vesicles of various size and multilaminar bodies (Fig. 3). Nevertheless, the mitochondria of these affected neurons remained quite well preserved and the nucleus was intact. Only a few

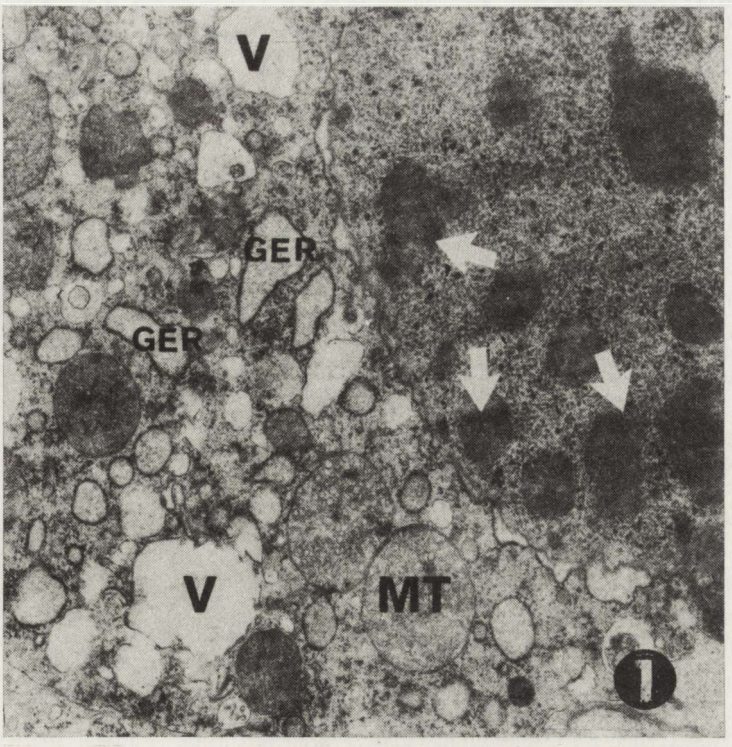

Fig. 1. Hippocampal culture, 24 h post QUIN exposure. Neurons exhibiting clumping of nuclear chromatine (arrows), damaged mitochondria (MT), enlarged channels of granular endoplasmic reticulum (GER) and vacuoles (v). × 16 650

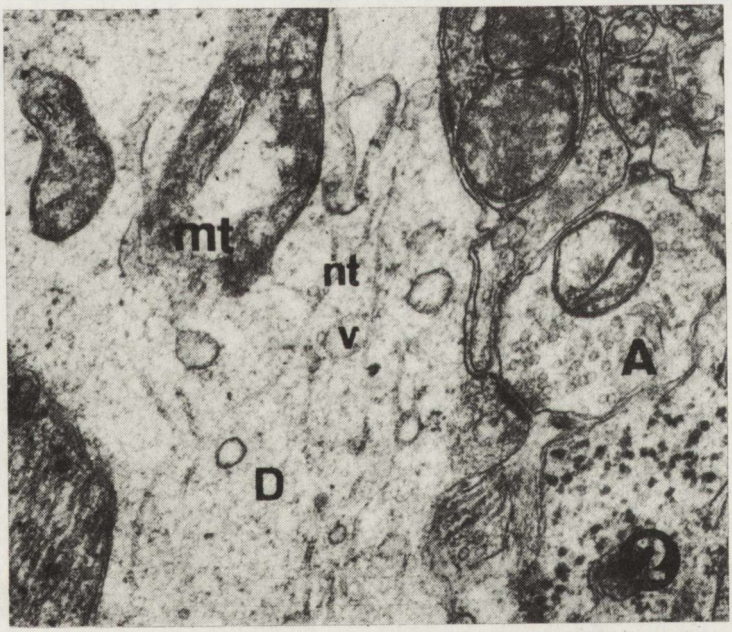

Fig. 2. The same culture. Swollen dendrite (D) containing damaged mitochondria (MT), small vacuoles (v) and neurotubules (nt). Normally appearing axonal bouton (A). × 20 000

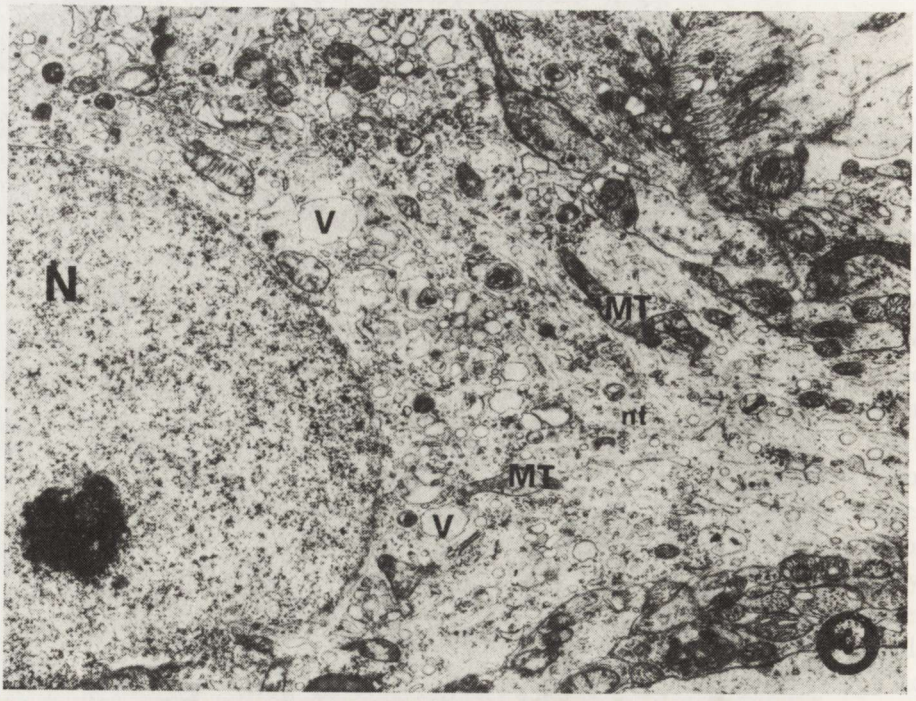

Fig. 3. 24 h post QUIN and nimodipine treatment. Pyramidal neurons exhibiting numerous vacuoles (v) and vesicles, quite well-preserved mitochondria (MT) and unchanged nucleus (N). Numerous neurotubules (nt) between organelles. × 12 500

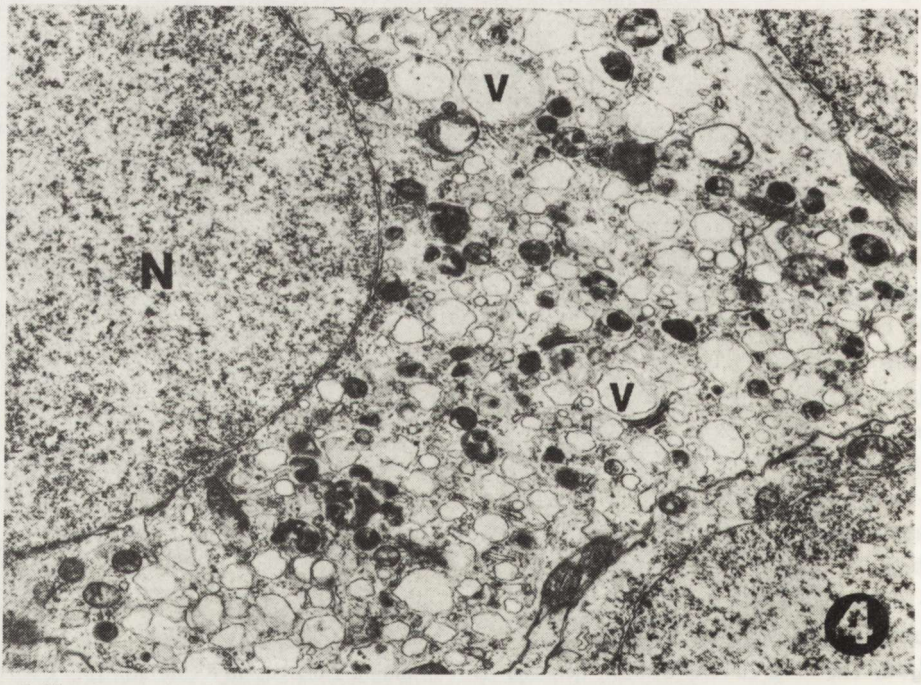

Fig. 4. The same culture. Neuron with advanced vacuolization of the cytoplasm (v). Intact nucleus (N). × 10 000

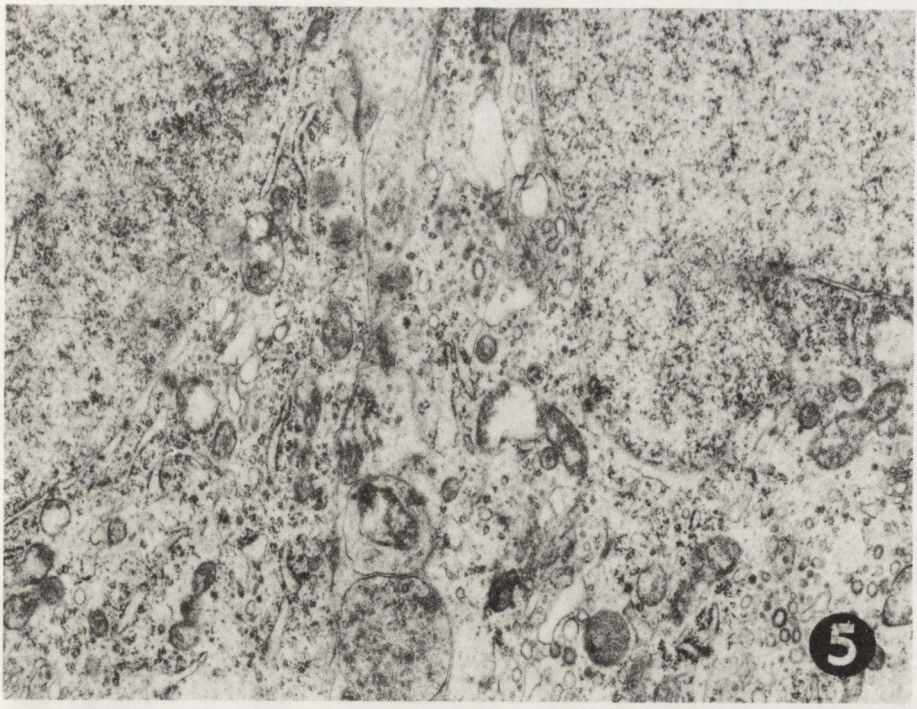

Fig. 5. 7 days post QUIN and nimodipine application. Quite well preserved neurons. × 15 000

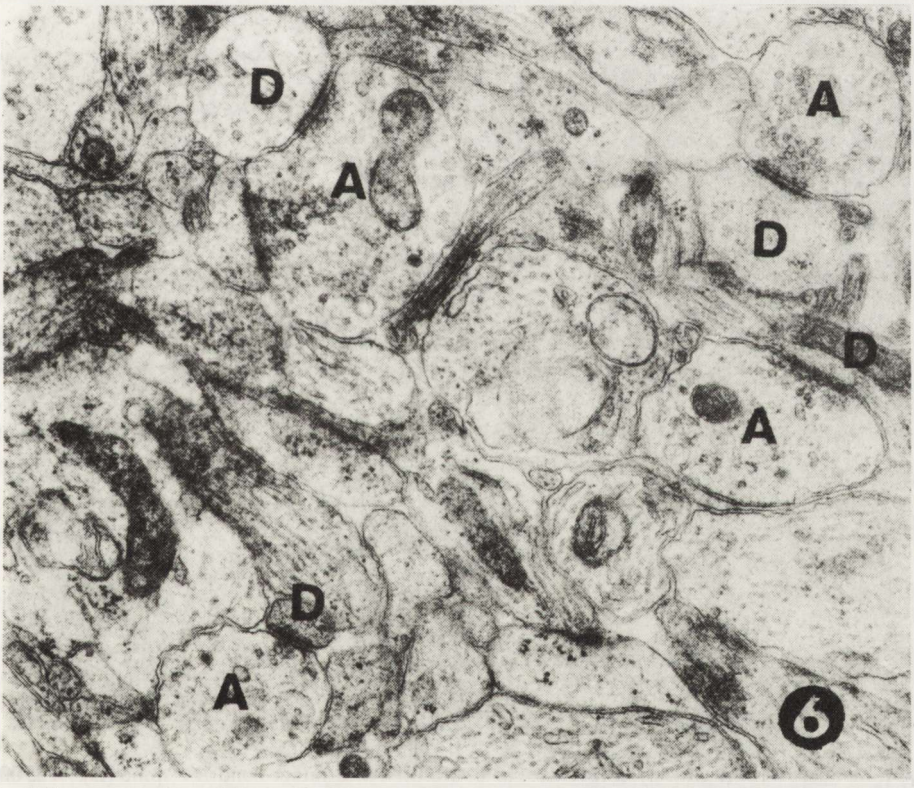

Fig. 6. The same culture. Neuropil with normally appearing both axonal boutons (A) ans dendritic processes (D). × 25 000

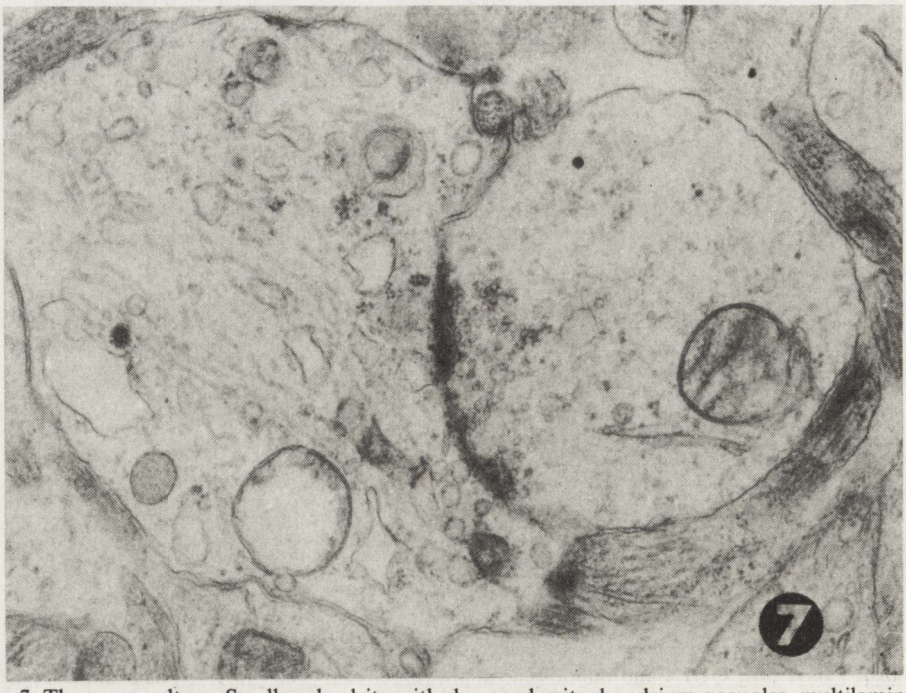

Fig. 7. The same culture. Swollen dendrite with damaged mitochondrium vacuoles, multilaminar bodies and dense core vesicles. ×25000

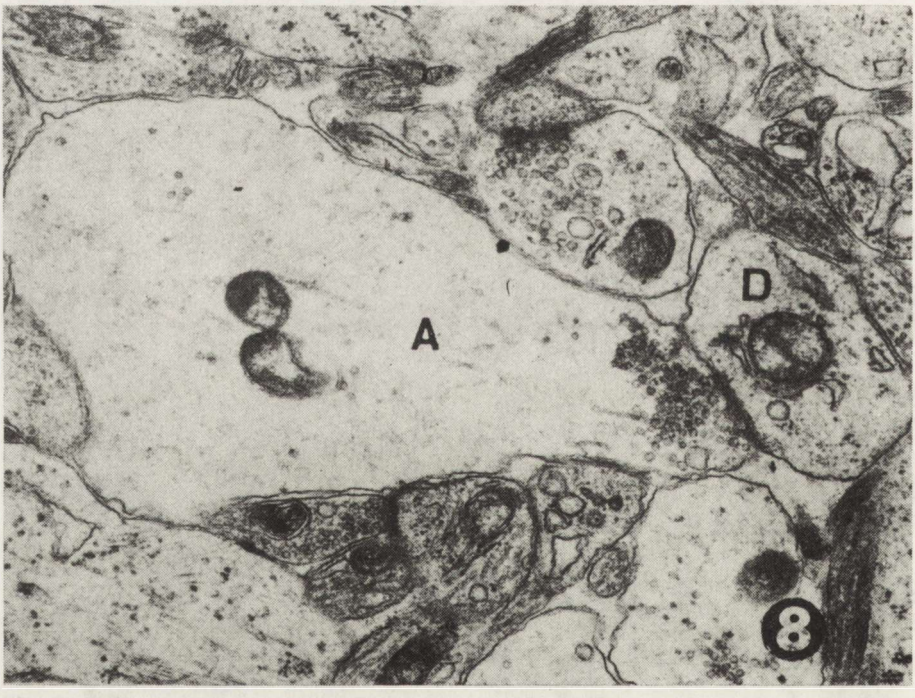

Fig. 8. Swollen, almost entirely empty axonal bouton (A) and intact dendritic spine (D). ×25000

neurons exhibited more advanced vacuolar degenerative changes but even in these severely damaged neurons, nucleus only sporadically reveal clumping of nuclear chromatin (Fig. 4). After 5 and 7 days of experiment, the great majority of neurons displayed normally appearing ultrastructural features (Fig. 5). Both pre- and post-synaptic endings did not reveal distinct morphological abnormalities (Fig. 6). A few moderately swollen dendritic processes containing damaged mitochondria, vacuoles or vesicles and multilaminar bodies could be seen only occasionally (Fig. 7). Beside the sporadically observed postsynaptic changes some presynaptic endings seemed to be more or less enlarged and revealed a small number of synaptic vesicles (Fig. 8). Some of these swollen axonal boutons were almost entirely empty and contained only a few synaptic vesicles close to the synaptic cleft. Some glial cells and their processes were markedly swollen.

DISCUSSION

The present study demonstrated that the neurotoxic effect of QUIN on hippocampal cultures diminished in the presence of nimodipine. The majority of nerve cells did not reveal advanced morphological abnormalities and exhibited an unchanged nucleus and mitochondria, damage to which usually represents morphological features of irreversible cell injury. The typical QUIN-induced post-synaptic changes were also detected only sporadically.

The exact mechanism of nerve cell injury in different pathological states is complicated, including depolarization, calcium entry, chloride and potassium influx, and possibly contribution of second messenger. There was increasing evidence that the brain damages associated with anoxia, stroke, epilepsy and neurodegenerative disorders may be at least partially caused by excessive activation of N-methyl-D-aspartate receptors (Rothman, Olney 1987). The neurotoxic effect of QUIN via activation of NMDA subtype receptors has been widely documented (Perkins, Stone 1983; Stone, Connick 1985). More recently the possibility that Ca entry could be associated with cell injury and that voltage-sensitive calcium channels are involved in the neurotoxic mechanism of amino acidic compounds has been suggested (Coyle 1983; Choi 1987; Murphy et al. 1988a, b). It was found that nimodipine could prevent both glutamate neurotoxicity and glutamate-induced dendritic regression (Mattson et al. 1988). These results indicate that activation of glutamate receptors leads to the opening of voltage-dependent calcium channels and induces calcium influx causing alteration in dendritic outgrowth and neuronal survival.

Our findings demonstrating the protective effect of nimodipine, which is expected to block voltage-dependent calcium channels support these recent suggestions. However, in the present experiments, the protective effect of the calcium entry blocker was not efficient in elimination the whole cytotoxic effect of QUIN, what suggests that calcium influx is not the only mechanism responsible for acidic amino acids toxicity. Some recent reports disclosed that acute neurotoxicity of excitatory amino acids is mediated by a calcium-independent mecha-

nism, i.e. passive chloride influx (Rothman 1985), while a calcium-dependent mechanism is involved in more chronic toxicity (Choi et al. 1987). This is in agreement with the present study demonstrating more severe damage in the early period of experiment than in later stages of observation. Neverthelles, these results support the hypothesis that Ca^{2+} plays an important role in the neurotoxic consequences of acidic amino acids receptor activation.

CYTOPROTEKCYJNY WPŁYW NIMODIPINY NA DZIAŁANIE NEUROTOKSYCZNE KWASU CHINOLINOWEGO W HODOWLI HIPOKAMPA

Streszczenie

Celem pracy była ocena wpływu nimodipiny, jednego z blokerów kanałów wapniowych, na zmiany morfologiczne wywoływane przez kwas chinolinowy. Badania przeprowadzono na dobrze zróżnicowanych, 21-dniowych organotypowych hodowlach hipokampa szczura. Nimodipinę podawano jednocześnie z kwasem chinolinowym (po 100 μM) do środowiska odżywczego hodowli. Zmiany ultrastrukturalne oceniano po 24 godz., 5 i 7 dniach. Stwierdzono wyraźne cytoprotekcyjne działanie nimodipiny dotyczące zwłaszcza rozwoju uszkodzeń późnych. Uzyskany efekt nie był jednak całkowity, co wskazuje na udział jeszcze innych czynników patogennych aniżeli tylko nadmiernego napływu jonów wapniowych, w mechanizmie uszkodzeń strukturalnych wywoływanych przez kwas chinolinowy.

REFERENCES

1. Berdichevsky E, Riveros N, Sanchez-Armass S, Orrego F: Kainate, N-methylaspartate and other excitatory amino acids increase calcium influx into rat brain cortex cells *in vitro*. Neurosci Lett, 1983, 36, 75–80.
2. Choi DW: Glutamate neurotoxicity in cortical cell culture is calcium dependent. Neurosci Lett, 1985, 58, 293–297.
3. Choi DW: Ionic dependence of glutamate neurotoxicity. J Neurosci, 1987, 7, 369–379.
4. Choi DW, Maulucci-Gedde M, Kriegstein AR: Glutamate neurotoxicity in cortical cell culture. J Neurosci, 1987, 7, 357–368.
5. Coyle JT, Bird SJ, Evans RH, Gulley RL, Nadler JV, Nicklas WJ, Olney JW: Excitatory amino acid neurotoxins: selectivity, specificity and mechanism of action. Neurosci Res Prog Bull, 1981, 19, 331–427.
6. Coyle JT: Neurotoxic action of kainic acid. J Neurochem, 1983, 41, 1–11.
7. Garthwaite G, Hajos F, Garthwaite J: Ionic requirements for neurotoxic effects of excitatory amino acid analogues in rat cerebellar slices. Neuroscience, 1986, 18, 437–447.
8. Griffiths T, Evans MC, Meldrum BS: Temporal lobe epilepsy, excitotoxin and the mechanism of selective neuronal loss. In: Excitotoxins. Eds. K Fuxe, P Roberts, R Schwarcz. McMillan, London, 1983, pp. 331–342.
9. Kida E, Matyja E: Ultrastructural alterations induced by quinolinic acid in organotypic cultures of rat hippocampus. Clin Neuropathol, 1988, 7, 176.
10. Kohr G, Heinemann U: Differences in magnesium and calcium effect on N-methyl-D-aspartate and quisqualate-induced decreases in extracerebellar sodium concentration in rat hippocampal slices. Exp Brain Res, 1988, 71, 425–430.
11. Mattson MP, Dou P, Kater SB: Outgrowth-regulating actions of glutamate in isolated hippocampal pyramidal neurons. J Neurosci, 1988, 8, 2087–2100.

12. Mayer ML, Westbrook GL: Cellular mechanisms underlying excitotoxicity. Trends Neurosci, 1987, 10, 59–61.
13. Murphy TH, Malouf AT, Sastre A, Schnaar RL, Coyle JT: Calcium-dependent glutamate cytotoxicity in a neuronal cell line. Brain Res, 1988a, 444, 325–332.
14. Murphy TH, Schnaar RL, Coyle JT, Sastre A: Glutamate cytotoxicity in a neuronal cell line is blocked by membrane depolarization. Brain Res, 1988b, 460, 155–160.
15. Olney JW: Neurotoxicity of excitatory amino acids. In: Kainic acid as a tool in neurobiology. Eds. E McGeer, JW Olney, PL McGeer. Raven Press, New York, 1978, pp 95–121.
16. Perkins MN, Stone TW: Quinolinic acid: regional variations in neuronal sensitivity. Brain Res, 1983, 259, 172–176.
17. Retz KC, Coyle JT: The differential effects of excitatory amino acids on uptake of $CaCl_2$ by slices from mouse striatum. Neuropharmacology, 1984, 23, 89–94.
18. Rothman SM: The neurotoxicity of excitatory amino acids is produced by passive chloride influx. J Neurosci, 1985, 5, 1483–1489.
19. Rothman SM, Olney JW: Excitotoxicity and the NMDA receptor. Trends Neurosci, 1987, 10, 299–302.
20. Schwarcz R, Foster AC, French ED, Whetsell Jr WO, Kohler C: Excitotoxic models for neurodegenerative disorders. Life Sci, 1984, 35, 19–32.
21. Stone TW, Connick JH: Quinolinic acid and other kynurenines in the central nervous system. Neuroscience, 1985, 15, 597–617.

Authors' address: Department of Neuropathology, Medical Research Centre, Polish Academy of Sciences, 3 Dworkowa Str., 00-784 Warsaw, Poland.

NEUROPAT. POL. 1991, 29, 1–2
PL ISSN 0028-3894

JOLANTA WAŚKIEWICZ, ELŻBIETA WAŁAJTYS-RODE, URSZULA RAFAŁOWSKA

EFFECT OF HYPEROXIA ON HISTAMINE METABOLISM IN RAT BRAIN SYNAPTOSOMES: PRELIMINARY OBSERVATIONS

Department of Neurochemistry, Medical Research Centre, Polish Academy of Sciences, Warsaw, and Clinic of Pneumonology, School of Medicine, Warsaw, Poland

Adult male Wistar rats were submitted to normobaric hyperoxygenation for 1 and 4 hours, then brain synaptosomes were isolated and uptake and release of the histamine precursor – histidine (His), histamine (HA) level and His metabolizing enzymes activities were measured. This uptake in hyperoxic synaptosomes was inhibited by about 20%. After 1-hour hyperoxia, a tendency towards an increase of the HA level, but a significant increase histidine decarboxylase (HD) and histamine methyltransferase (HMT) activities were observed. Four-hour hyperoxia caused a decrease of both the HA level and the activities of both enzymes, especially HMT. The changes were reversed in 1-hour posthyperoxic recovery, except for histidine uptake which remained inhibited.

Key words: *hyperoxia, histamine, synaptosomes.*

Histamine (HA) function as a neurotransmitter and the presence of histaminergic pathways and specific receptors to HA in the brain have been confirmed by biochemical, histochemical and electrophysiological evidence (Schwartz et al. 1981; Wilcox, Seybold 1982; Lakoshi, Aghajanian 1983; Hough, Green 1984; Watanabe et al. 1984). HA localization in at least two different cell types: neurons and mast cells is at present well established (Garbarg et al. 1976). The neuronal pool of HA is characterized by fast turnover and the presence of both the HA synthesizing enzymes, histidine decarboxylase (HD) (E.C. 4.1.1.22) and the HA catabolizing enzyme, histamine N-methyltransferase (HMT) (E.C. 2.1.1.8) (Kuhar et al. 1971; Baudry et al. 1973; Garbarg et al. 1980; Nishibori et al. 1984).

Recently many investigators have focused on histamine metabolism in pathophysiologically or pharmacologically altered brain (Green et al. 1978; Hough, Green 1984). The sensitivity of the central nervous system to oxygen is well known. In particular, the decrease of oxygen supply causes changes in brain energy metabolism as well as disturbances of the neurotransmitter transport (Siesjö 1978; Fahn et al. 1979; Rafałowska et al. 1980; Pastuszko et al. 1982). No

information, however, is available on the effect of hyperoxia on HA brain metabolism.

The aim of this study was to investigate the effect of experimental hyperoxia on a) the uptake and release of HA precursor – histidine (His) and b) the level of HA and the activities of HD and HMT in highly purified synaptosomes from rat brain. The reversibility of the observed changes was also studied.

MATERIAL AND METHODS

Adult male Wistar rats (approx. 200 g of body weight) fed a standard diet were used in all experiments.

The animals were exposed to 100% oxygen in normobaric conditions for 1 and 4 h. Oxygen was passed at a rate of 3 l/min through an 8.4–1 chamber. The animals were decapitated immediately after hyperoxia or after 1 hour of post-hyperoxic recovery. The synaptosomes were isolated from fore- and midbrains by centrifugation in discontinuous Ficoll gradient as described previously (Booth, Clark 1978; Deutsch et al. 1981). The synaptosomes were suspended in a modified Krebs-Henseleit medium containing 140 mM NaCl, 5 mM KCl, 1.3 mM $MgSO_4$, 1 mM Pi, 10 mM Hepes, pH 7.4.

Uptake and release of His (histidine) and HA (histamine) was measured as described by Troeger et al. (1984). Synaptosomes were suspended in Krebs-Henseleit medium containing 2.5 mM $CaCl_2$ and 10 mM glucose at concentration of 5 mg protein/ml. Measurements started with addition of [U-^{14}C] histidine (spec. act. 8.88 GBq/mmol), Amersham U.K., at 1 μM concentration. Samples (300 μl) were withdrawn at the indicated time intervals and rapidly centrifuged (Beckman microcentrifuge) through a layer of silicone oil (spec. gravity 1.03, General Electric Water, Ford, N.Y.). For determination of histidine/histamine release, after 20 min of incubation 75 mM KCl was added and samples for centrifugation were collected 5 min later. Radioactivity of the pellets was measured in a Beckman LS 9000 liquid scintillation spectrometer using the Bray scintillation fluid.

HD and HMT activities were assayed using the radioenzymatic microassay as described by Taylor and Snyder (1972). S-adenosylmethionine used for HMT assay was purified from S-adenosylhomocysteine by chromatography on a Dowex 1 (Cl^-) column. HA was measured by the single isotope-enzymatic method of Shaff and Beaven (1979) with minor modifications using S-adenosyl-[^{3}Hmethyl] methionine (spec. act. 5.55 GBq/mmol, Amersham U.K.) and HMT obtained from guinea pig brain (Brown et al. 1959). HA was assayed after the samples had been boiled for 5 min.

Protein was determined by the method of Lowry et al. (1951) using bovine serum albumin as standard.

RESULTS AND DISCUSSION

No statistically significant changes in the HA level and HD and HMT activities were observed after 1 hour of hyperoxia (Fig. 1). A 4 h exposure to O_2 caused a slight, nonsignificant decrease of the HA level, a 30% decrease of HD activity and a decrease of HMT activity to about 54% of control value (Fig. 1).

The most likely cause of the decrease of both enzyme activities is accumulation of products of free radical oxidation in brain synaptosomes, as the result of peroxidative processes, especially concerning membrane integrity and function (Baudry et al. 1973; Booth, Clark 1978; Pastuszko et al. 1983; Braughler 1985). On the other hand, the adaptive mechanism protecting the histaminergic system might be involved.

The reversibility of observed changes was conformed by the fact, that after 1 h of posthyperoxic recovery the HA level and HD and HMT activities were similar as in the control group (Fig. 1). Peroxidative decomposition of membrane lipids may be also responsible for the significant inhibition of ^{14}C-histidine uptake by synaptosomes which was observed after 1 hr of hyperoxia and persisted until 4 h of hyperoxygenation (Fig. 2).

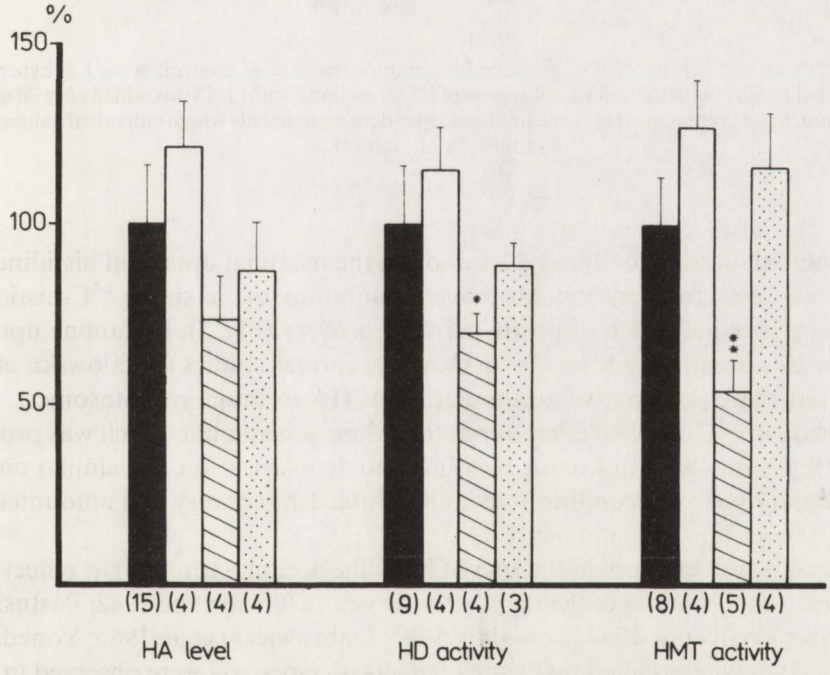

Fig. 1. Levels of histamine and activities of histidine decarboxylase and histamine methyltransferase in synaptosomes under different experimental condition. The results are presented as percent of control which were for: histamine level = 3.1 ± 0.5 pmoles/mg protein, HD activity = 11.9 ± 2 pmoles/mg protein/h, HMT activity = 330 ± 50 pmoles/mg protein/h. ■ – control, □ – 1 h hyperoxia, ▨ – 4 h hyperoxia, ⊡ – 1 h recovery from 4 h hyperoxia. Numbers of experiments are shown in parentheses. Statistical significances according to Student's t test were *$p < 0.05$, **$p < 0.001$

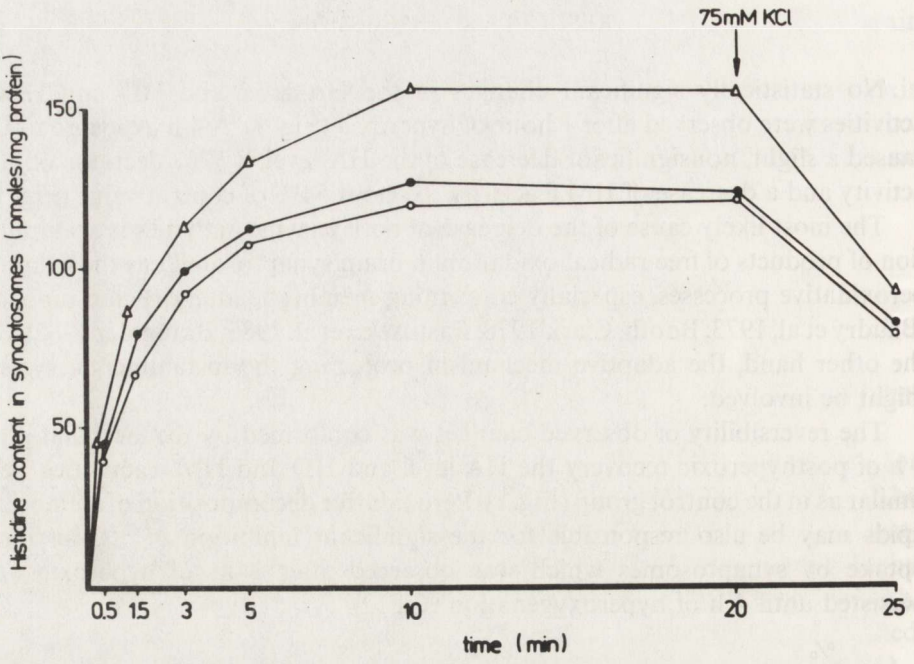

Fig. 2. Uptake and release of ^{14}C histidine by synaptosomes: △ — control, ● — 1 h hyperoxic, ○ — 4 h hyperoxic; for determination of release of ^{14}C-histidine 75 mM KCl was added after 20 min of incubation. Each point represents a mean of 3 independent experiments where individual values were within 5% of each other

Hyperoxia lasting for 1 and 4 h inhibited the maximal uptake of histidine by 19% and 23%, respectively. Moreover, inhibition of maximal ^{14}C-histidine uptake persisted after 1 h of posthyperoxic recovery (Fig. 3). Histamine uptake was not measured since it has been shown in former studies (Rafałowska et al. 1987) that there is no active accumulation of HA in brain synaptosomes.

Release of ^{14}C-labelled compounds (histidine + histamine which was produced during incubation) due to the KCl-induced depolarization, was similar under control and hyperoxic conditions as well as after 1 h recovery and amounted to about 30% of maximal uptake (Figs 2 and 3).

The observed changes in the rate of histidine accumulation might reflect the conformational changes of the membrane structure (Chan et al. 1982; Pastuszko et al. 1983; Chan et al. 1984; Braughler 1985; Dąbrowiecki et al. 1985; Yoneda et al. 1985). It may be recalled that similar effects of hyperoxia were observed in the case of GABA transport (Gordon-Majszak et al. 1987; Rafałowska, Floyd 1988).

The results taken together indicate that the mechanism of histamine uptake as well as activities of histamine metabolizing enzymes in brain synaptosomal fraction are highly sensitive to free radical formation under condition of normobaric hyperoxia of rats.

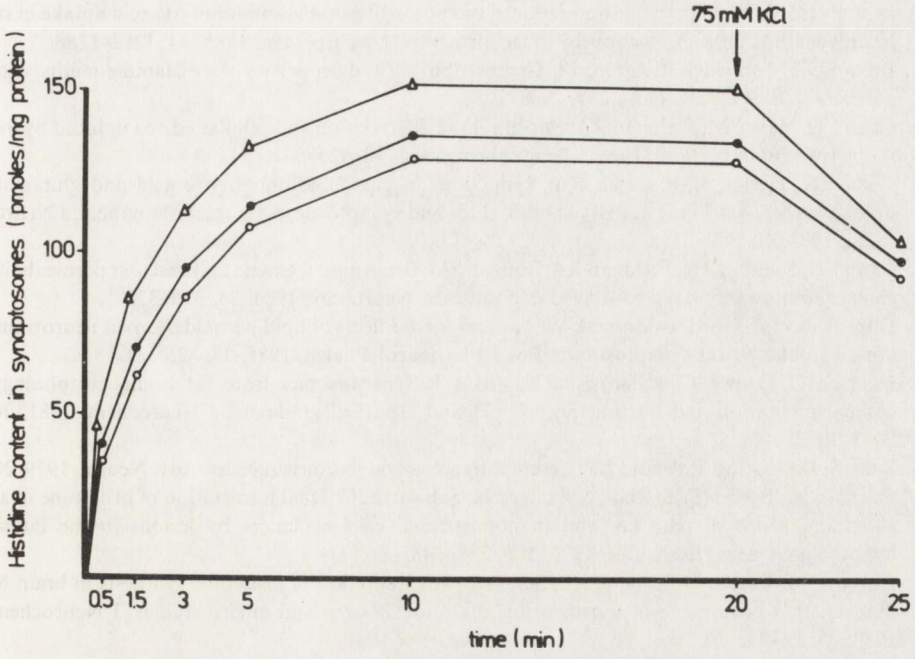

Fig. 3. Uptake and release of ^{14}C-histidine by control and posthyperoxic recovery synaptosomes: △ — control, 1 h recovery from: ● — 1 h hyperoxia and ○ — 4 h hyperoxia. Each point represents a mean of 3 independent experiments where individual values were within 5% of each other

WPŁYW HIPEROKSJI NA METABOLIZM HISTAMINY W SYNAPTOSOMACH Z MÓZGU SZCZURA

Streszczenie

Dorosłe szczury, samce rasy Wistar poddano 1- i 4-godzinnej hiperoksji. W wyizolowanej z mózgu frakcji synaptosomalnej badano pobieranie i uwalnianie prekursora histaminy (HA) — histydyny (His). Ponadto oznaczano poziom histaminy oraz aktywność enzymów metabolizujących. Pobieranie His do synaptosomów po hiperoksji zostało zahamowane o 20% w stosunku do wartości kontrolnych. Po jednogodzinnej hiperoksji obserwowano tendencję do wzrostu poziomu HA oraz znaczący wzrost aktywności dekarboksylazy histydynowej (HD) i metylotransferazy histaminowej (HMT). Czterogodzinna hiperoksja powodowała spadek poziomu HA, jak również aktywności enzymów, zwłaszcza HMT. Zmiany te były odwracalne i ulegały normalizacji u zwierząt z jednogodzinnym przeżyciem po hiperoksji, z wyjątkiem pobierania His do synaptosomów, które pozostawało zahamowane.

REFERENCES

1. Baudry M, Martres MP, Schwartz JC: The subcellular locatization of histidine decarboxylase in various regions of rat brain. J Neurochem, 1973, 21, 1301–1309.
2. Booth PF, Clark JB: A rapid method for the preparation of relatively pure, metabolically compatent synaptosomes from rat brain. Biochem J, 1978, 176, 365–370.

3. Braughler JM: Lipid peroxidation-induced inhibition of gamma-aminobutyric acid uptake in rat brain synaptosomes: protection by glucocorticoids. J Neurochem, 1985, 44, 1282–1288.
4. Brown DD, Tomchich R, Axelrod J: The distribution and properties of a histamine-methylating enzymes. J Biol Chem, 1959, 234, 2948–2950.
5. Chan PH, Yurko M, Fishman RA: Phospholipid degradation and cellular edema induced by free radicals in brain cortical slices. J Neurochem, 1982, 38, 525–531.
6. Chan PH, Kerlan R, Fishman RA: Reductions of gamma-aminobutyric acid and glutamate uptake Na^+-K^+-ATPase activity in brain slices and synaptosomes by arachidonic acid. J Neurochem, 1983, 40, 309–316.
7. Chan PH, Schidley JW, Fishman RA, Longan SM: Brain injury, edema and vascular permeability changes induced by oxygen-derived free radicals. Neurology, 1984, 34, 315–320.
8. Dąbrowiecki Z, Gordon-Majszak W, Łazarewicz J: Effects of lipid peroxidation on neurotransmitter uptake by rat synaptosomes. Pol J Pharmacol Pharm, 1985, 37, 325-331.
9. Deutsch C, Drown C, Rafałowska U, Silver J: Synaptosomes from rat brain, morphology, compartmentation and transmembrane pH and electrical gradients. J Neurochem, 1981, 36, 2063–2072.
10. Fahn S, Davies JM, Rawland LP: Cerebral hypoxia and its consequences. Adv. Neurol, 1979, 26.
11. Garbarg M, Barbin C, Bischoff S, Pollard H, Schwartz JC: Dual localization of histamine in an ascending neuronal pathway and in nonneuronal cells evidences by lesions in the lateral hypothalamic area. Brain Res, 1976, 106, 338–348.
12. Garbarg M, Barbin G, Rodergas E, Schwartz JC: Inhibition of histamine synthesis in brain by fluoromethyl histidine, a new irreversible inhibitor: *in vitro* and *in vivo* studies. J Neurochem, 1980, 35, 1045–1052.
13. Green JP, Johnson CL, Weinstein H: Histamine as a neurotransmitter. In: Psychopharmacology: A generation and progress. Eds: MA Lipton, A DiMascio, KF Killan. Raven Press, New York, 1978, pp 319–332.
14. Gordon-Majszak W, Rafałowska U, Łazarewicz JW: Metabolic changes in rat brain synaptosomes after exposure to normobaric hyperoxia *in vivo*. Bull Pol Acad Sci, Biol Sci, 1987, 35, 97–104.
15. Hough LB, Green JP: Histamine and its receptors in the nervous system. In: Handbook of neurochemistry. Ed: A Lajtha. Plenum Press, New York, London, 1984, v 6.
16. Kuhar MJ, Taylor KM, Snyder SH: The subcellular localization of histamine and histamine methyltransferase in rat brain. J Neurochem, 1971, 18, 1515–1527.
17. Lakoshi JM, Aghajanian GK: Effects of histamine H_1 and H_2 receptor antagonists on the activity of serotonergic neurons in the dorsal raphae nucleus. J Pharmacol Exp Ther, 1983, 227, 517–523.
18. Lowry OH, Rosebrough NJ, Farr AL, Randall RJ: Protein measurements with the Folin phenol reagent. J Biol Chem, 1951, 193, 265–275.
19. Nishibori M, Oishi R, Saeki K: Histamine turnover in the brain of different mammalian species: implication for neuronal histamine half-life. J Neurochem, 1984, 43, 1544–1549.
20. Pastuszko A, Wilson D, Erecińska M: Neurotransmitter metabolism in rat brain synaptosomes: Effect of anoxia and pH. J Neurochem, 1982, 1657–1667.
21. Pastuszko A, Gordon-Majszak W, Dąbrowiecki Z: Dopamine uptake in striatal synaptosomes exposed to peroxidation *in vitro*. Biochem Pharmacol, 1983, 32, 141–146.
22. Rafałowska U, Erecińska M, Wilson D: The effect of acute hypoxia on synaptosomes from rat brain. J Neurochem, 1980, 34, 1160–1163.
23. Rafałowska U, Floyd RA: Peroxidative induced changes in synaptosomal-aminobutyric acid and dopamine transport. FASEB J, 1988, 2, 1374.
24. Rafałowska U, Waśkiewicz J, Albrecht J: Is neurotransmitter histamine predominantly inactivated in astrocytes? Neurosci Lett, 1987, 80, 106, 110.
25. Schwartz JC, Barbin TT, Duchemin AM, Garbard M, Pollard H, Quach TT: Functional role of histamine in the brain. In: Neuro-Pharmacology of central nervous system and behavioral disorders. Ed: GC Palmer. Academic Press, New York – London – Toronto – Sydney – San Francisco, 1981.

26. Shaff RE, Beaven MA: Increased sensitivity of the enzymatic isotopic assay of histamine: Measurement of histamine in plasma and serum. Anal Biochem, 1979, 94, 425–430.
27. Siesjö BK: Brain energy metabolism. J Wiley and Sons, Chichester, New York – Brisbane – Toronto, 1978.
28. Taylor KM, Snyder SH: Isotopic microassay of histamine, histidine decarboxylase and histamine methyltransferase in brain tissue. J Neurochem, 1972, 19, 1343–1358.
29. Troeger MB, Rafałowska U, Erecińska M: Effect of oleate on neurotransmitter transport and other plasma membrane functions in rat brain synaptosomes. J Neurochem, 1984, 42, 1735–1742.
30. Watanabe T, Taguchi Y, Shiosaka S, Tanaka Y, Kubota H, Terano Y, Tohyama M, Wada H: Distribution of the histaminergic neuron system in the central nervous system of rats: a fluorescent immunohistochemical analysis with histidine decarboxylase as a marker. Brain Res, 1984, 295, 13–25.
31. Wilcox BJ, Seybold VS: Localization of neuronal histamine in rat brain. Neurosci Lett, 1982, 29, 105–110.
32. Yoneda Y, Kuriyama K, Takahashi M: Modulation of synaptic GABA receptor. Binding by membrane phospholipids: possible role of active oxigen radicals. Brain Res, 1985, 333, 111–112.

Authors' address: Department of Neurochemistry, Medical Research Centre, Polish Academy of Sciences, 3 Dworkowa Str., 00-784 Warsaw, Poland.

NEUROPAT. POL. 1991, 29, 1–2
PL ISSN 0028-3894

MIECZYSŁAW WENDER, ZOFIA ADAMCZEWSKA-GONCERZEWICZ,
JOLANTA DORSZEWSKA, JÓZEF SZCZECH, ANTONI GODLEWSKI,
JADWIGA PANKRAC, DANUTA TALKOWSKA

MYELIN LIPIDS IN ISCHEMIC STROKE

Department of Neurology, School of Medicine, Poznań

Slices of ischemic focus (infarct area) and of the contralateral frontal lobe were submitted to histological and biochemical studies. The obtained results indicate that in stroke cases the necrotic focus as well as contralateral brain hemisphere are characterized by a marked decrease of cholesterol and cerebrosides content and an increase of lysophosphatidylcholine and cholesterol esters in the myelin fraction. We conclude that ischemia as well as the degenerative aging process are both responsible for the abnormal lipid pattern in the myelin of the white matter in stroke cases. The long lasting hypoxia resulting from cerebral vessel atheromatosis contributes to biochemical changes in the myelin of the apparently healthy white matter of the contralateral hemisphere in brain infarction.

Key words: *myelin lipids, ischemic stroke, white matter.*

The aging process in the central nervous system involves two principal pathological events: degenerative changes in the vascular system: atheromatosis, arteriosclerosis or amyloid angiopathy and local amyloidosis of the nervous tissue, known under the term senile atrophy of Alzheimer type. Both processes may lead to alterations of membraneous structures of all morphological components of the nervous tissue in the cerebral grey and white matters. The essential part of the latter are changes in the myelin sheaths, the basic component of the white matter. In our previous studies (Wender et al. 1988), concerning myelin lipids in aging human brain, we compared chemical alterations in patients with vascular pathology in the brain and in those with senile atrophy of Alzheimer type. Chemical alterations included an increase in lysophosphatidylcholine content and a marked decrease in myelin yield. Additionally, in the cerebellum a decrease of sulfatide content was observed. The chemical results were almost identical in each subgroup of patients. The above described changes do not seem to be primarily related to atrophy of Alzheimer type, but to result from secondary changes provoked by vascular degeneration.

In continuation of our studies we have focused our attention on the pattern of myelin lipids in cases of stroke, studying it in the infarct area and in the

contralateral brain hemisphere. A similar problem, i.e. the chemistry of cerebral myelin in senile patients with brain infarction, was studied by Niebrój-Dobosz et al. (1986). The authors emphasized that changes in the biochemical composition of myelin in the course of brain infarction depend on the age of the patient and upon survival time after it.

MATERIAL AND METHODS

The studies were performed on autopsy material of 16 patients deceased between 62 and 86 years of age with diagnosis of acute cerebral stroke. Slices of ischemic focus (infarct area) and of the contralateral frontal lobe were submitted to histological and biochemical studies. The results were compared with those obtained in 5 patients who died between 23 and 44 years of age of diseases not involving the central nervous system.

The material was grouped according to the age at which stroke occurred (60–70 years or 70–90 years) and according to survival time after stroke (1–6 days or 10–20 days).

The white matter, isolated from the brain slices according to macroscopic morphological criteria, provided a source of the myelin fraction. Isolation of myelin was performed using the method of Norton and Poduslo (1973), by means of differential centrifugation of the homogenate in a discontinuous surcrose gradient (0.32 and 0.85 M, pH 7.0) using a swing-out rotor at 75 000 × g for 30 min. The isolated myelin fraction was washed 3 times with distilled water, each washing procedure being followed by centrifugation at 75 000 × g for 20 min. The final sediment was lyophilized. Total lipids of the myelin fraction were extracted by the procedure described by Folch-Pi et al. (1957) with 20 vol. of chloroform/methanol (2:1, v/v) and partitioned with 0.2 vol. of 0.05 M KCl. Total lipids of the lower phase were separated by means of column and thin-layer chromatography (TLC). Cholesterol was determined by the Sperry and Webb method (1950), cerebrosides and sulfatides by the method of Radin et al. (1955) and phosphorus content of the individual phospholipid fractions by the method described by Bartlett (1959).

RESULTS

In cases of clinical stroke, neuropathological studies revealed morphological signs of brain infarct.

Results of chemical studies on myelin lipids are presented in Tables 1 and 2. The characteristic changes observed in the ischemic necrotic focus as well as in the contralateral brain hemisphere included a marked decrease in cholesterol and cerebroside content and an increase of lysophosphatidylcholine and cholesterol esters. The latter change was noticed only in absolute values. The obtained results were almost identical in all studied parts of the brain in stroke cases. Tables 3 and 4 demonstrate the results of studies in the material, grouped according to the age of patients, in whom the stroke occurred. Cholesterol and sphingomyelin con-

tents were significantly lower, in relative values, in the ischemic necrotic focus in the younger age class. Results of the material grouped according to the survival time are presented in Tables 5 and 6. In patients who died a few days after stroke higher values of cholesterol, lysophosphatidylcholine and phosphatidylethanoloamine were noticed.

Table 1. Pattern of myelin lipids of the cerebral white matter in ischemic stroke (Results in percent of total lipids)

	Control cases n = 5	Stroke cases n = 16		
		Ischemic focus	Contralateral brain hemisphere	Contralateral frontal lobe
Cholesterol	40.1±1.3	28.2±2.8*	29.9±2.4*	29.7±1.9*
Cholesterol esters	0.2±0.05	0.3±0.04	0.7±0.3	0.4±0.1
Sulfatides	4.9±0.4	4.9±0.5	4.7±0.5	5.2±0.6
Cerebrosides	21.7±1.0	18.7±0.9*	19.0±0.9*	16.8±0.7*
Total galactolipids	26.6±1.3	23.6±1.3*	23.7±1.1*	22.0±1.0*
Sphingomyelins	5.7±0.5	7.7±0.9	6.9±0.6	7.7±0.9
Phosphatidylcholine	8.9±0.5	11.9±0.6*	12.5±0.6*	12.5±0.5*
Lysophosphatidylcholine	0.3±0.2	4.1±1.0*	2.7±0.4*	5.0±1.4*
Phosphatidylserine +Phosphatidylinositide	4.2±0.9	6.9±1.6	4.5±0.8	5.5±0.6
Phosphatidylethanolamine	2.9±0.4	6.2±0.9*	8.0±2.1*	6.0±0.9*
Plasmalogens	11.1±0.7	11.7±1.2	11.1±0.8	11.6±1.5
Total phospholipids	33.1±2.3	48.5±3.4*	45.7±2.2*	48.3±2.1*

Mean ± SEM; * differences significant.

Table 2. Pattern of myelin lipids of the cerebral white matter in ischemic stroke (in mmol/100 g of dry tissue)

	Control cases n = 5	Stroke cases n = 16		
		Ischemic focus	Contralateral brain hemisphere	Contralateral frontal lobe
Cholesterol	23.5±1.6	21.8±2.1	23.4±2.0	20.1±2.1
Cholesterol esters	0.1±0.03	0.3±0.04*	0.5±0.2*	0.3±0.05*
Sulfatides	2.9±0.1	2.1±0.2	2.1±0.2	1.9±0.2
Cerebrosides	13.3±1.0	8.4±0.6*	9.2±0.9*	7.4±0.8*
Total galactolipids	16.2±1.2	10.5±0.7*	11.3±1.0*	9.3±0.9*
Sphingomyelins	3.4±0.5	4.6±1.0	3.6±0.4	3.6±0.7
Phosphatidylcholine	5.2±0.8	6.5±1.0	6.3±0.4	5.8±0.5
Lysophosphatidylcholine	0.2±0.05	3.1±1.2*	1.7±0.2*	1.8±0.3*
Phosphatidylserine +Phosphatidylinositide	2.5±0.6	3.8±1.1	2.2±0.4	2.8±0.5
Phosphatidylethanolamine	1.7±0.2	4.0±1.2	4.0±0.9	2.5±0.3
Plasmalogens	6.7±0.8	6.9±1.2	6.0±0.5	5.7±0.9
Total phospholipids	19.7±5.4	28.9±6.2	23.8±1.5	22.2±2.0

Mean ± SEM; * differences significant.

Table 3. Pattern of myelin lipids of the cerebral white matter in ischemic stroke in material divided according to the age of patients (results in percent of total lipids)

	Ischemic focus Age of patients		Contralateral brain hemisphere Age of patients		Contralateral frontal lobe Age of patients	
	60–67 yrs n = 7	71–86 yrs n = 9	60–67 yrs n = 7	71–86 yrs n = 9	60–67 yrs n = 7	71–86 yrs n = 9
Cholesterol	24.3±3.8	31.2±3.9*	27.8±4.4	31.5±2.7	27.6±3.4	31.3±2.3
Cholesterol esters	0.4±0.07	0.3±0.05	1.0±0.6	0.5±0.08	0.6±0.1	0.3±0.06
Sulfatides	5.4±0.9	4.6±0.6	3.6±0.3	5.6±0.5	5.5±1.3	5.0±0.4
Cerebrosides	21.5±2.9	16.5±2.5	18.2±3.5	19.6±2.2	17.2±3.2	17.7±1.9
Total galactolipids	26.9±3.6	21.1±2.8	21.8±3.6	25.2±2.6	22.7±4.0	22.7±2.0
Sphingomyelins	6.5±1.0	8.5±1.2*	7.9±1.1	6.1±0.7	8.7±2.0	6.9±0.6
Phosphatidylcholine	12.3±1.3	11.7±0.6	12.9±0.7	12.2±0.9	12.5±0.8	12.6±0.7
Lysophosphatidylcholine	3.1±1.0	3.7±1.3	2.9±0.6	2.6±0.5	4.7±1.2	3.2±1.4
Phosphatidylserine + Phosphatidylinositide	8.3±3.4	5.8±1.0	4.4±1.0	4.6±1.3	5.0±0.8	6.0±0.8
Phosphatidylethanolamine	6.1±1.5	6.3±1.3	9.8±5.6	6.6±1.5	5.9±1.1	6.0±1.5
Plasmalogens	12.1±2.6	11.4±1.2	11.5±1.4	10.8±1.2	12.8±2.8	10.9±1.7
Total phospholipids	48.4±5.1	47.4±4.8	49.4±4.7	42.9±1.4	49.6±4.3	45.6±1.8

Mean ± SEM; * differences significant.

Table 4. Pattern of myelin lipids of the cerebral white matter in ischemic stroke in material divided according to the age of patients (results in mmol/100 g of dry tissue)

	Ischemic focus Age of patients		Contralateral brain hemisphere Age of patients		Contralateral frontal lobe Age of patients	
	60–67 yrs n = 7	71–86 yrs n = 9	60–67 yrs n = 7	71–86 yrs n = 9	60–67 yrs n = 7	71–86 yrs n = 9
Cholesterol	18.9±3.6	24.2±2.0	22.6±2.2	24.1±3.2	16.3±2.7	23.1±3.0
Cholesterol esters	0.3±0.02	0.3±0.07	0.7±0.4	0.3±0.05	0.3±0.07	0.3±0.07
Sulfatides	1.9±0.3	2.3±0.4	1.7±0.3	2.5±0.2*	1.7±1.5	2.0±0.2
Cerebrosides	8.5±0.7	8.4±1.0	9.0±1.8	9.4±1.0	6.5±1.3	8.0±1.1
Total galactolipids	10.4±0.4	10.7±1.1	10.7±1.8	11.9±1.1	8.2±1.5	10.0±1.0
Sphingomyelins	3.0±0.5	5.9±1.9	4.0±0.6	3.0±1.6	4.0±1.5	3.3±1.3
Phosphatidylcholine	5.5±1.0	7.7±1.7	6.5±0.3	6.0±0.5	5.1±0.9	6.1±0.7
Lysophosphatidylcholine	2.0±0.7	4.0±2.1	1.9±0.4	1.5±0.2	2.0±0.5	1.6±0.3
Phosphatidylserine + Phosphatidylnositide	3.6±1.8	4.0±1.4	2.1±0.4	2.3±0.7	2.0±0.5	3.4±0.8
Phosphatidylethanolamine	3.1±1.0	4.2±2.0	4.7±1.8	3.5±0.8	2.2±0.4	2.8±0.5
Plasmalogens	5.8±1.4	7.7±1.6	6.2±0.6	5.7±0.8	5.7±1.6	5.9±1.2
Total phospholipids	23.0±4.0	33.5±10.7	25.4±0.8	22.0±1.9	21.0±4.7	23.1±3.0

Mean ± SEM; * differences significant.

Table 5. Pattern of myelin lipids of the cerebral white matter in ischemic stroke in material divided according to survival time after stroke (results in percent of total lipids)

	Ischemic focus Survival time Days		Contralateral brain hemisphere Survival time Days		Contralateral frontal lobe Survival time Days	
	1–6 n = 8	10–20 n = 8	1–6 n = 8	10–20 n = 8	1–6 n = 8	10–20 n = 8
Cholesterol	30.7±1.4	25.7±1.5*	33.6±1.0	26.2±2.1*	32.7±2.5	26.6±2.8
Cholesterol esters	0.4±0.1	0.3±0.03	1.0±0.5	0.4±0.05	0.5±0.1	0.4±0.1
Sulfatides	5.1±0.8	6.0±1.2	4.6±0.8	4.7±0.4	5.5±1.0	4.9±0.5
Cerebrosides	17.4±3.2	20.0±2.3	15.8±2.9	22.3±2.0	15.4±2.3	19.5±2.4
Total galactolipids	22.5±3.9	26.0±2.5	20.4±3.5	27.0±1.9	20.9±3.0	24.4±2.8
Sphingomyelins	6.5±0.9	8.8±1.3	5.8±1.0	8.0±0.7	6.3±1.0	9.1±1.5
Phosphatidylcholine	11.8±1.2	12.1±0.6	12.5±0.7	12.5±1.0	11.3±0.6	13.7±0.6
Lysophosphatidylcholine	4.4±1.6	2.5±0.3	3.0±0.7	2.4±0.3	5.6±1.1	2.0±0.4
Phosphatidylserine + Phosphatidylinositide	5.1±1.0	8.7±2.9	3.0±0.6	6.0±1.4	5.4±1.0	5.6±0.4
Phosphatidylethanolamine	7.6±1.6	4.8±0.9	11.3±4.0	4.8±0.8	7.3±1.5	4.8±1.0
Plasmalogens	11.0±2.1	11.2±1.3	9.5±1.3	12.6±0.8	10.0±1.7	13.3±3.0
Total phospholipids	46.4±4.2	48.1±4.1	45.1±4.2	46.3±2.0	45.9±1.9	48.5±3.9

Mean ± SEM; * differences significant.

Table 6. Pattern of myelin lipids of the cerebral white matter in ischemic stroke in material divided according to survival time after stroke (results in mmol/100 g of dry tissue)

	Ischemic focus Survival time Days		Contralateral brain hemisphere Survival time Days		Contralateral frontal lobe Survival time Days	
	1–6 n = 8	10–20 n = 8	1–6 n = 8	10–20 n = 8	1–6 n = 8	10–20 n = 8
Cholesterol	24.1±2.7	19.6±2.9	26.3±3.4	20.6±1.7	25.1±2.6	15.2±2.5*
Cholesterol esters	0.3±0.06	0.3±0.04	0.4±0.05	0.6±0.3	0.4±0.04	0.2±0.02
Sulfatides	2.1±0.3	2.2±0.3	2.1±0.6	2.1±0.3	2.1±0.2	1.7±0.3
Cerebrosides	9.6±0.9	7.2±0.6	11.0±1.0	7.4±1.3	9.2±0.8	5.5±0.9*
Total galactolipids	11.7±1.0	9.4±0.8	13.2±1.0	9.4±1.5	11.3±0.9	7.2±1.1*
Sphingomyelins	5.0±1.5	4.2±1.7	4.1±0.8	2.8±0.6	4.8±1.1	2.5±0.5
Phosphatidylcholine	6.3±0.9	6.7±1.9	6.5±0.7	5.9±0.4	7.0±0.7	4.3±0.6
Lysophosphatidylcholine	2.9±1.1	3.9±2.2	1.8±0.3	1.6±0.3	1.6±0.5	2.1±0.3
Phosphatidylserine + Phosphatidylinositide	4.5±1.6	3.2±1.5	2.9±4.4	1.5±0.3	3.3±0.8	2.2±0.7
Phosphatidylethanolamine	2.8±0.8	5.2±2.2	2.8±0.6	5.3±1.6	2.6±0.6	2.5±0.4
Plasmalogens	7.1±1.2	6.6±2.2	7.2±0.7	4.8±0.7	7.3±1.3	4.3±1.1
Total phospholipids	28.6±6.0	29.8±11.4	25.3±2.2	21.9±1.9	26.6±3.6	17.9±2.8

Mean ± SEM; * differences significant.

DISCUSSION

Hypoxia as well as ischemia, acting on the brain, provoke several biochemical alterations in the main component of the cerebral white matter: the oligodendroglia-myelin complex. However, the pronounced diffuse demyelination, known as delayed hypoxic encephalopathy (Plum, Posner 1972), occurs only rarely in cerebral atheromatosis and only as a casuistic event after cardiac arrest, carbon monoxide intoxication or deep hypoglycemia (Wender et al. 1964; Traugott, Raine 1984).

Brain infarction, being the result of a drastic shortage in blood supply to the brain, provokes very profound metabolic alterations (Raichle 1983). Niebrój-Dobosz et al. (1986) emphasized the decrease of myelin yield, drop of phospholipids and increase of cholesterol esters in the brain hemisphere affected by infarction. In our material the ischemic focus exhibited a mild decrease of cerebrosides and some elevation of cholesterol esters and lysophosphatidylocholine content. The changes cannot be regarded to represent biochemical signs of myelin decomposition, characteristic for primary or secondary demyelination.

The observation of a similar pattern of changes in myelin lipids in the region of the infarct and in the contralateral hemisphere, established in our studies, is of interest. Elucidation of the problem would require comparison of our findings with the lipid pattern of the myelin observed in aging and hypoxia. White matter in senile and presenile dementia of Alzheimer type is characterized by reduction of the cerebroside and sulfatide content but only when dementia occurs concomitantly with the lesion of the grey and white matter (England, Brun 1986). The authors expressed the opinion that the above mentioned changes are an independent pathological process and are not related to secondary demyelination. In our previous studies (Wender et al. 1988), three main types of changes have been disclosed in the aging brain: marked fall in myelin yield, increased content of lysophosphatidylcholine and decrease of sulfatides in some parts of the brain. Most pronounced changes of cerebral myelin lipids in hypoxia involved a marked increase of cholesterol esters and lysophosphatidylcholine content in the myelin fraction (Wender, Adamczewska-Goncerzewicz 1989).

Confrontation of our results in stroke cases: decrease of cerebrosides and elevation of cholesterol esters and lysophosphatidyl content, with those in aging and in hypoxia leads to the suggestion that both factors, i.e. ischemia as well as the degenerative aging process, are responsible for the abnormal lipid pattern in the myelin of the white matter in stroke cases.

The next question arises, how to explain the striking similarity between the myelin lipid pattern in the necrotic focus and in the contralateral brain hemisphere. First of all it should be taken into consideration that the degradation of myelin lipids and their removal from the necrotic field is a slow process, which may not be completed in cases of short survival time after stroke.

In our previous studies (Wender et al. 1989) we have observed a long lasting increase in the fatty acid pool in the white matter after exposure of rats to

hypoxia. We speculated that the degradation process of several lipid-rich membranes in the brain starts immediately after hypoxia and goes on for months. This may explain not only progression of the clinical pattern observed in some cases of stroke, but also contributes to the biochemical deviations in the myelin of apparently healthy white matter of the contralateral hemisphere in brain infarction. It may also be added that our findings represent another indication that brain infarction is only the terminal event in long lasting ischemic lesions of the white matter in cerebral vascular disease.

CONCLUSIONS

1. In stroke cases, the ischemic necrotic focus in the white matter as well as contralateral brain hemisphere are characterized by a marked decrease of cholesterol and cerebrosides content and an increase of lysophosphatidylcholine and cholesterol esters in the myelin fraction.
2. Cholesterol and sphingomyelin contents in the myelin are significantly lower in the ischemic necrotic focus in the younger age class (below 70 years of life).
3. The ischemic changes in the white matter in stroke cases are different from the pattern of myelin decomposition characteristic for primary or secondary demyelination.
4. Ischemia as well as the degenerative aging process are both responsible for the abnormal lipid pattern in the myelin of the white matter in stroke cases.
5. Long lasting hypoxia resulting from cerebral vessel atheromatosis contributes to biochemical changes in the myelin of the apparently healthy white matter of the contralateral hemisphere in brain infarction.
6. Brain infarction represents only the terminal event in long lasting ischemic lesions of the white matter in cerebral vascular disease.

LIPIDY MIELINY W UDARZE NIEDOKRWIENNYM

Streszczenie

Badania przeprowadzono na materiale autopsyjnym 16 chorych w wieku od 62 do 86 lat, którzy zmarli z rozpoznaniem niedokrwiennego udaru mózgu. Wyniki porównano z materiałem pochodzącym od 5 pacjentów w wieku 23 do 44 lat, którzy zmarli z powodu chorób nie dotykających ośrodkowego układu nerwowego. Wyniki badań doprowadziły do następujących wniosków:

1. W przypadkach udarów mózgu niedokrwienne ogniska martwicze w istocie białej, a także przeciwstawną półkulę mózgu charakteryzuje wyraźny spadek zawartości cholesterolu i cerebrozydów oraz wzrost poziomu lysofosfatydylocholiny i estrów cholesterolu we frakcji mielinowej.
2. Zawartość cholesterolu i sfingomielin w mielinie są istotnie niższe w niedokrwiennym ognisku martwiczym w młodszej grupie wieku (poniżej 70 roku życia).
3. Zmiany niedokrwienne w istocie białej w przypadkach udaru różnią się od obrazu rozpadu mieliny charakterystycznego dla pierwotnej lub wtórnej demielinizacji.

4. Zarówno niedokrwienie, jak i zwyrodnieniowy proces starczy są odpowiedzialne za nieprawidłowy obraz lipidów mieliny istoty białej mózgu w przypadkach udaru.

5. Długo trwające niedotlenienie, będące wynikiem miażdżycy naczyń mózgu, przyczynia się do zmian biochemicznych w mielinie w pozornie zdrowej istocie białej przeciwstawnej półkuli w zawale mózgu.

6. Zawał mózgu jest tylko ostatnim zjawiskiem w długo trwających zmianach niedokrwiennych istoty białej w chorobie naczyniowej mózgu.

REFERENCES

1. Barcikowska-Litwin M: Obraz morfologiczny ogniska rozmiękania mózgowego w wieku starczym. Neuropatol Pol, 1984, 22, 563–582.
2. Bartlett G: Phosphorus assays in column chromatography. J Biol Chem, 1959, 234, 466–468.
3. England E, Brun A: The white matter changes in senile dementia of Alzheimer type: neuropathological and biochemical correlates. X Intern Congr Neuropathol Stockholm, 1986, Abstracts, p 291.
4. Folch-Pi J, Lees M, Sloane-Stanley G: A simple method for the isolation and purification of total lipid from animal tissues. J Biol Chem, 1957, 226, 497–511.
5. Niebrój-Dobosz I, Rafałowska J, Barcikowska-Litwin M: Brain myelin in senile patients with brain infarction. Neuropatol Pol, 1986, 24, 351–364.
6. Norton N, Poduslo S: Myelination in rat brains. Method of myelin isolation. J Neurochem, 1973, 21, 749–758.
7. Plum F, Posner J: Stupor and Coma. Ed. FA Davis, New York, 1972.
8. Radin N, Lavin F, Brown J: Determination of cerebrosides. J Biol Chem, 1955, 217, 789–796.
9. Raichle M: The pathophysiology of brain ischemic. Ann Neurol, 1983, 13, 2–9.
10. Sperry W, Webb M: A revision of the Schoenheimer-Sperry method for cholesterol determination. J Biol Chem, 1950, 187, 97–106.
11. Traugott U, Raine C: The neurology of myelin disease. In: Myelin. Ed: P Morell. Plenum Press, New York, London, 1984, pp 311–335.
12. Wender M, Adamczewska-Goncerzewicz Z: Cerebral white matter in hypoxia. Neurology India, 1989, 37, 514.
13. Wender M, Adamczewska-Goncerzewicz Z, Szczech J, Godlewski A: Myelin lipids in aging human brain. Neurochem Pathol, 1988, 8, 121–130.
14. Wender M, Adamczewska-Goncerzewicz Z, Żórawski A, Sroczyński E, Grochowalska A: Influence of experimental hypoxia on content and composition of free fatty acids in cerebral white matter. Exp Pathol, 1989, 36, 123–127.
15. Wender M, Jurczyk W, Stengert K: Cerebral lipids in myelinopathy caused by cardiac arrest. Acta Neuropathol (Berl), 1964, 4, 238–244.

Authors' address: Department of Neurology, School of Medicine, 49 Przybyszewskiego Str., 60-355 Poznań, Poland.

NEUROPAT. POL. 1991, 29, 1–2
PL ISSN 0028-3894

ANDRZEJ KAPUŚCIŃSKI

CHANGES OF CONCENTRATION OF CYCLIC AMP IN RAT BRAIN AND PLASMA IN THE CLINICAL DEATH MODEL

Department of Neuropathology, Medical Research Centre, Polish Academy of Sciences, Warsaw

In the experimental model of clinical death in rats (Korpachev et al. 1982) cyclic AMP concentrations were evaluated in the brain and plasma at the end of 5-min clinical death, and 5, 15, 30, 60 and 120 min after resuscitation. The cAMP ^{125}I assay system has been used. At the end of clinical death the cAMP level decreased in the brain with normalization 15 min after resuscitation; the second decrease of the cAMP level was observed 30 min post resuscitation with normalization in later periods. In the plasma cAMP concentration did not change at the end of clinical death, followed by a significant increase 5 min after resuscitation. Later the level of plasma cAMP decreased being still above the control value after 2 hours. The possible role of endogenous catecholamines stimulation on adenylate cyclase activity is discussed.

Key words: *clinical death, cAMP, brain, plasma.*

Interruption of cerebral blood flow produces immediate biochemical alterations progressing in time, which after a longer period of ischemia lead to irreversible damage and brain death. If cerebral circulation is reestablished promptly, cerebral damage due to global ischemia may be mild or absent. No aspect of metabolism is spared in severe hypoxia or ischemic injury, therefore, the key biochemical determinants of irreversible cell damage are not completely known. However, the interrelated factors of energy failure, lactic acidosis, and Ca^{2+} imbalance are presently viewed as critical steps leading to ischemic cell damage or death.

Progression of events at the molecular level may be presented in the sequence of time and divided into early, intermediate and late changes (Flynn et al. 1989). The early changes (seconds – minutes) consist in abolition of EEG, Ca^{2+} influx, activation of lipolytic enzymes, mitochondrial swelling and increased NADH. The intermediate changes (less than 10 min) are increased glycolysis, decreased glucose and glycogen, increased lactate, decreased energy charge, failure of Na, K-ATPase, development of edema, neurotransmitter release and increased cAMP. Late changes (more than 10 min) are decreased protein sythesis, increased proteolysis and activation of lysosomal enzymes.

Among many molecular disorders alteration of cyclic nucleotides regulation play an important role, in particular the intracellular second messenger, adenosine-3'5'monophosphate (cAMP) which mediates neurotransmission and neuromodulation by biogenic amines (Kaczmarek, Levitan 1987). Intracellular levels of cAMP are determined by the rates of cAMP synthesis from ATP by hormone-sensitive adenylate cyclase and metabolism to 5'-AMP by any of several cyclic nucleotide phosphodiesterases.

Several laboratories have described the effect of hypoxia and ischemia on the time course of changes of adenine nucleotides metabolism, in particular cAMP in the brain (Kleihues et al. 1974; Mrsulja et al. 1976, 1986; Kobayashi et al. 1977; Lust et al. 1977; Sikorska 1978; Taylor et al. 1984; Onodera et al. 1986; Pylova 1988). In this report, the concentration of cAMP was measured in rat brain and plasma at the end of clinical death and after resuscitation.

MATERIAL AND METHODS

Under ether anesthesia 5-min clinical death was induced in 35 adult female Wistar rats, weighing 170–180 g, by intrathoracic compression of the cardiac vessels bundle at the base of the heart with a hook-like device without major surgery (Korpachev et al. 1982). Cardio-pulmonary resuscitation was performed by external cardiac massage and artificial ventilation with air. The animals were sacrificed in groups of five at the end of ischemia and 5, 15, 30, 60 and 120 min after resuscitation. Five animals served as a control group in which under ether anesthesia the sham-operation was performed.

In the above periods of time 1.5 ml of blood was drawn from the right cardiac ventricle and the brain was removed from the skull. Blood was placed in cooled polyethylene tubes containing 7.5 mM EDTA and the plasma immediately separated by centrifugation at 4°C (7000 g, 5 min). Plasma was frozen in liquid nitrogen and stored at −20°C until analysed. Brains were removed from the skulls in less than 30 sec, and forebrain samples were cut-off at 4°C, weighed (approx. 80 mg), immediately frozen in liquid nitrogen and stored at −20°C until analysed.

cAMP was measured in the brain and plasma by means of the radioimmunologic competition method with anigen labelled ^{125}I and dual antiserum: rabbit anti-succinyl cAMP serum and donkey anti-rabbit serum (cAMP ^{125}I assay system, dual range, Amersham).

Frozen brain samples were homogenized in cold 6% TCA (1 ml), centrifuged at 2000 g for 15 min at 4°C, and the supernatant washed four times with 5 volumes of water-saturated diethyl ether. The remaining aqueous extract was dried under a stream of nitrogen at 60°C, and the dried extract dissolved to 1:5000 in a suitable volume of 0.05 M acetate assay buffer, pH 5.8 with 0.01% thimerosal. Plasma was assayed in 1:20 dilution. All samples including standards, antigen and antiserum were incubated for 3 h at 4°C. After 10 min incubation with Amerlex-M second antibody at room temperature, the antibody-bound fraction

was separated by centrifugation (10 min, 1500 g). The radioactivity was determined in an automatic gamma scintillation counter (Beckman). All samples were assayed in duplicate including standards to construct the standard curve for calculations of results. Results were expressed as mean ± SD and were analysed by Student's t test.

RESULTS

The dynamics of changes of cAMP concentration in the rat brain and plasma in the control group, at the end of 5-min clinical death and after resuscitation is presented in Table 1.

In the control sham-operated group the mean level of cAMP in the brain was 1.27 ± 0.30 nmol/g of wet tissue. At the end of the 5-min clinical death cAMP level significantly decreased. In the early period after resuscitation (5 and 15 min) cAMP concentration quickly increased reaching in 15 min the control values. In 30 min after resuscitation cAMP concentration once again significantly decreased. In the later period (60 and 120 min) the level of cAMP increased to the values which did not differ from control ones.

Table 1. cAMP concentration in the rat brain (nmol/g wet tissue) and plasma (pmol/ml) during clinical death and after resuscitation

	Control	End of clinical death	Period after resuscitation				
			5 min	15 min	30 min	60 min	120 min
Brain	1.27 ± 0.30 (100%)	0.78 ± 0.13* (61%)	0.97 ± 0.13 (76%)	1.30 ± 0.58 (102%)	0.66 ± 0.10** (52%)	1.17 ± 0.23 (92%)	1.04 ± 0.26 (82%)
Plasma	20.4 ± 5.2 (100%)	22.8 ± 21.3** (112%)	148.0 ± 21.3** (725%)	68.9 ± 22.2** (338%)	65.9 ± 12.8** (323%)	42.5 ± 12.8** (208%)	38.4 ± 5.9** (188%)

Values represent means ± SD from 5 animals. Significant in reference to control: *$p < 0.05$; **$p < 0.01$.

In the control sham-operated group, the cAMP level in the plasma was on the average 20.4 ± 5.2 pmol/ml. At the end of clinical death, concentration of cAMP did not differ significantly from the control. Five minutes after resuscitation the level of cAMP in the plasma significantly increased, later (15–120 min) gradually decreased, being still significantly elevated after 120 min.

DISCUSSION

The obtained results indicated that the character of changes of cAMP concentration in the brain and plasma differ from each other, and changes in plasma should not inflence the brain level, because cAMP content in the plasma is of one order lower. The level of cAMP in the brain of control rats was similar to the values obtained by other authors (Onodera et al. 1986) and lower as com-

pared with the results obtained in decapitated rats, after ether anesthesia or sham-operation related to exposure of common carotid arteries in ether anesthesia, evaluated 2 min after operation (Sikorska 1978). The level of cAMP in the plasma of control rats did not differ significantly from the values quoted by Amersham.

Authors analysing changes of brain cAMP level under the influence of ischemia or hypoxia in different experimental models and different species, indicate an increase of cAMP concentration already during ischemia (Mrsulja et al. 1976, 1986; Kobayashi et al. 1977; Sikorska 1978; Pylova 1988) with subsequent reversible increase in the postischemic period and a decrease to the control level or even below it. Mrsulja et al. (1986) in gerbils subjected to 5-min bilateral common carotid artery occlusion, showed elevation of the cAMP level in the brain (cortex, striatum, hippocampus) as early as after 40 s of ischemia with the peak concentration in 60 s. During the further 4 min of ischemia cAMP level did not change significantly. In more recent investigations, Mrsulja et al. (1989) using the same experimental model with extension of ischemia to 15 min, observed a fourfold decrease of the cAMP level in the hippocampus as compared with the maximal concentration at 5 min. One hour recirculation produced even a deeper decrease of cAMP concentration, reaching the control level. Sikorska (1978) employing several experimental models of brain hypoxia and ischemia in rats, found a transient increase of cAMP level and adenylate cyclase in the brain. She claimed that this phenomenon could be unspecific because a comparable effect occurred after ether anesthesia and in sham-operated animals. Pylova (1988) observed an increase of cAMP concentration and activity of adenylate cyclase in the brain cortex and striatum in the second minute of 15-min clinical death induced in dogs by electric shock. Two and three days after resuscitation cAMP concentration was significantly lower, particularly in the animals with neurological disorders.

The results of brain cAMP content in the 5th min of clinical death in rats are in contradiction to the majority of results obtained in other experimental models. Instead of a rise of cAMP concentration, a significant decrease was observed. Neither did Onodera et al. (1986) when studying mononucleotide metabolism in a rat which survived 10 min of forebrain ischemia, employing Pulsinelli and Brierley's model (1979), observe elevation of cAMP concentration in the brain at the end of the ischemic period, but even a decrease, however, not statistically significant. In the early period of recirculation (3 and 5 min) they observed a transient increase of cAMP content with later normalization. Lust et al. (1977) employing bilateral common carotid artery occlusion in gerbils, found no increase of cAMP level in the cerebellum during 5 min ischemia, and a decrease of its concentration during 20 min ischemia and after recirculation, as well as a significant drop of cAMP level in the spinal cord during ischemia and after recirculation. The above mentioned authors emphasize that it is probably the first case of a significant decrease of the cAMP level in nerve tissue during ischemia and recirculation.

In our studies 5 and 15 min after resuscitation, the increase of cAMP content in the brain was observed, as compared with the level at the end of ischemia, however, the peak content did not differ from the control level. In 30 min after resuscitation once again a decrease of cAMP concentration was observed with later normalization.

The results of our studies and data from literature seem to indicate differences in the molecular mechanisms acting in different experimental models. The so-called occlusive models (bilateral ligation of carotid artery in gerbil and rat) produce a prompt and considerable rise of peripheral blood pressure as result of catecholamine release into the peripheral blood (Kapuściński, Mossakowski 1983). The similars mechanism occurs in animals exposed to hypoxic hypoxia, at the beginning of CO intoxication (Sikorska 1978) and in clinical death produced by electroshocks (Pylova 1988). An extreme example of this mechanism is the model of complete cerebral ischemia in rabbits produced by increase of intracranial pressure or occlusion of all arteries supplying the brain (Kapuściński et al. 1981).

Catecholamines are listed as known factors stimulating adenylate cyclase (Sutherland et al. 1962; Robinson et al. 1967; Spatz et al. 1983; Pylova 1988; Northup 1989). The stimulating effect of adrenaline, noradrenaline and dopamine on adenylate cyclase in the endothelium of cerebral vessels was shown by Spatz et al. (1983), and the same effect of dopamine and noradrenaline on adenylate cyclase in the cortex and striatum during 15 min clinical death in dogs was observed by Pylova (1988).

The specificity of the experimental model employed in this study characterized by immediate arrest of blood inflow and outflow from the heart, resulted in no increase of arterial blood pressure. On the contrary, the peripheral blood pressure drops to zero after several second of heart bundle compression (Kapuściński 1987). The level of total catecholamines (noradrenaline + adrenaline), assayed in the same experimental model, in brain and plasma did not show any increase at the end of 5-min clinical death (Kapuściński 1991). In the brain- at the end of clinical death, as well as up to 120 min after resuscitation, a significant decrease of total catecholamines concentration was observed. In the plasma, however, in 5th min after resuscitation a significant increase of catecholamines content appeared with peak level after 15 min, and tendency toward later normalization. This could explain among other factors the lack of cAMP increase in the plasma at the end of clinical death and the considerable rise of its concentration in the early period after resuscitation with later progressing decrease of its level. At 120 min after resuscitation its level was still significantly elevated as compared with control level.

In the accessible literature we found no papers dealing with changes of catecholamines and cAMP concentrations in the brain and plasma in vivo in the same ischemic model. Spatz et al. (1983) reported an increase of blood-brain barrier permeability for monoamines in gerbils with common carotid arteries occlusion. However, their stimulating effect on adenylate cyclase in the endo-

thelium of cerebral vessels was proved only *in vitro*. In the recent paper on gerbils Mrsulja et al. (1989) suggested that changes in monoamines level in the brain are independent of energy metabolism. However, the problem of influence of endogenous catecholamines concentration changes in the plasma on adenylate cyclase activity in the brain in ischemic conditions still seems to be an open question.

ZMIANY STĘŻENIA CYKLICZNEGO AMP W MÓZGU I OSOCZU SZCZURA W MODELU ŚMIERCI KLINICZNEJ

Streszczenie

W doświadczalnym modelu śmierci klinicznej u szczura oceniono stężenie cAMP w mózgu i osoczu w kontroli, w 5 min śmierci klinicznej oraz w 5, 15, 30, 60 i 120 min po resuscytacji. Zastosowano cAMP ^{125}J metodę radioimmunologiczną. Na końcu okresu śmierci klinicznej poziom cAMP w mózgu obniżył się normalizując się w 15 min po resuscytacji. Obniżenie poziomu cAMP obserwowano również 30 min po resuscytacji z normalizacją w późniejszym okresie. W osoczu stężenie cAMP nie zmieniało się na końcu okresu śmierci klinicznej i znamiennie wzrosło 5 min po resuscytacji. W późniejszym okresie stężenie cAMP w osoczu stopniowo zmniejszało się, jednakże po 2 godz. było nadal powyżej wartości kontrolnych. Przedyskutowano możliwą rolę endogennych katecholamin w stymulacji aktywności cyklazy adenylowej.

REFERENCES

1. Flynn CJ, Farooqui AA, Harrocks LA: Ischemia and hypoxia. In: Basic neurochemistry. Molecular, cellular and medical aspects. Eds. GJ Siegel, BW Agranoff, RW Albers, PB Molinoff. Raven Press, New York, 1989, pp 783–795.
2. Kaczmarek LK, Levitan JB: Neuromodulation. The biochemical control of neuronal excitability. Oxford Univ Press, Oxford, 1987.
3. Kapuściński A, Pluta R, Mossakowski MJ: Is acute failure of adrenals an important factor limiting recovery from cerebral ischemia? In: Cerebral microcirculation and metabolism. Eds. J Cervos-Navarro, E Fritschka, Raven Press, New York. 1981, pp 293–302.
4. Kapuściński A, Mossakowski MJ: Pathophysiological and morphological observations after 30 min bilateral occlusion of the common carotid artery in gerbils. In: Stroke: Animal models. Ed. V Stefanovich. Adv Biosci, 1983, 43, 63–82.
5. Kapuściński A: Cerebral blood flow in the experimental model of clinical death in rat. In Polish, summary in English. Neuropatol Pol, 1987, 25, 287–298.
6. Kapuściński A: Dynamics of changes of catecholamines concentration in rat brain and plasma in the clinical death model. Neuropatol Pol, 1991 (in press).
7. Kleihues P, Kobayashi K, Hossmann K-A: Purine nucleotide metabolism in the cat brain after one hour of complete ischemia. J Neurochem, 1974, 23, 417–425.
8. Kobayashi M, Lust WD, Passonneau JV: Concentration of energy and cyclic nucleotides during and after bilateral ischemia in the gerbil cortex. J Neurochem, 1977, 29, 53–59.
9. Korpachev VG, Łysenkov SP, Tiel LZ: Modelirowanije kliniczeskoj smierti i postreanimacjonnoj bolezni u krys. Patol Fizjol Eks Ter, 1982, 3, 78–80.
10. Lust WD, Kobayashi M, Mrsulja BB, Wheaton A, Passonneau JW: Cyclic nucleotide levels in the gerbil cerebral cortex cerebellum and spinal cord following bilateral ischemia. In: Adv Exp Med Biol, 1977, 78, 287–298.
11. Mrsulja BB, Lust WD, Passonneau JV, Klatzo I: Post-ischemic changes in certain metabolites following prolonged ischemia in the gerbil cerebral cortex. J Neurochem, 1976, 25, 1–5.

12. Mrsulja BB, Ueki Y, Lust WD: Regional metabolite profiles in early stages of global ischemia in the gerbil. Metab Brain Dis, 1986, 1, 205–220.
13. Mrsulja BB, Djuricic BM, Ueki Y, Lust WD, Spatz M: Cerebral ischemia: Changes in monoamines are independent of energy metabolism. Neurochem Res, 1989, 14, 1–7.
14. Northup JK: Regulation of cyclic nucleotides in the nervous system. In: Basic neurochemistry. Mollecular, cellular and medical aspects. Eds. GJ Siegel, BW Agronoff, RW Albers, PB Molinoff. Raven Press, New York, 1989, pp 349–363.
15. Onodera H, Iijima K, Kogure K: Mononucleotide metabolism in the rat brain after transient ischemia. J Neurochem, 1986, 46, 1704–1710.
16. Pulsinelli WA, Brierley JB: A new model of bilateral hemispheric ischemia in the unanaesthetized rat. Stroke, 1979, 10, 267–272.
17. Pylova SJ: Adenilatcikaznaja sistema tkani gołownogo mozga pri kliniczeskoj smierti i w postreanimacjonnom pierjodie. Nejrochimja, 1988, 7, 39–46.
18. Robinson GA, Butcher RW, Sutherland EW: Adenyl cyclase as an adrenergic receptor. Ann NY Acad Sci, 1967, 139, 703–723.
19. Sikorska M: Metabolizm cyklicznego adenozyno-3′, 5′-monofosforanu w mózgu szczura w warunkach niedotlenienia. Ph. D. Thesis Medical Research Centre, Polish Academy of Sciences, Warsaw, 1978.
20. Spatz M, Maruki C, Karnushina I, Nagatsu I, Bembry J, Markel N: The relationship of monoamines to the blood-brain barrier. In: Adv Biosci, 1983, 43, 27–40.
21. Sutherland EW, Rall TW, Merion T: Adenyl cyclase. I. Distribution, preparation and properties. J Biol Chem, 1962, 237, 1220–1227.
22. Taylor MD, Palmer GC, Callahan AS: Kinetics of GTP-modulation of adenylate cyclase in gerbil cerebral cortex after bilateral ischemia. J Neurosci Res, 1984, 12, 615–621.

Author's address: Department of Neuropathology, Medical Research Centre, Polish Academy of Sciences, 3 Dworkowa Str., 00-784 Warsaw, Poland.

NEUROPAT. POL. 1991, 29, 1–2
PL ISSN 0028-3894

IZABELA KUCHNA[1], PIOTR B. KOZŁOWSKI[2]

SEQUELAE OF PERINATAL CENTRAL NERVOUS SYSTEM DAMAGE AFTER LONG-TERM SURVIVAL*

[1]Laboratory of Developmental Neuropathology, Medical Research Centre, Polish Academy of Sciences, Warsaw, [2]New York State Institute for Basic Research in Developmental Disabilities, Staten Island, New York

We presented the case of 78-year-old man with mental retardation and spastic paraparesis diagnosed early in life as cerebral palsy. Six years prior to demise he had post-traumatic subdural hematoma, which was removed surgically. The neuropathological examination revealed the sequelae of the recent trauma, superimposed on the extensive old lesions. Cavitary changes in the periventricular white matter and cortical ulegyria in the border zones of the major cerebral arteries vascularization were characteristic of perinatal hypoxic-ischemic lesions. Peculiar in the ulegyria were extensive areas with numerous corpora amylacea adjacent to the areas of fibrillar and cellular gliosis. Another sequelae of involution processes was the atrophy of brain hemispheres (secondary microcephaly). The case appears to be an example of the late degenerative involution changes developing on the background of lesions originated from the perinatal period.

Key words: *perinatal hypoxia, ulegyria, long-term survival.*

It is only rarely in routine neuropathological practice that we have an opportunity to evaluate a case of perinatal brain lesions with very long survival. Presented here is the case of a man with cerebral palsy and mental retardation diagnosed early in life. He spent almost his entire life in the institution where he was observed clinically, properly treated and died at the age of 78, after having suffered an additional brain trauma six years prior to demise.

CASE REPORT

Patient M.P. 78 years old at death, was for 62 years a permanent resident of Wassaic Developmental Center in New York. Early records indicate that his disabilities were birth related, but no details are available. He did not walk until

* Supported in part by New York State Office of Mental Retardation and Developmental Disabilities.

five years of age and was essentially nonverbal. He was diagnosed as microcephalic, with spastic paraparesis and profound mental retardation (I.Q. below 20, classified 318.2, DSM III). His clinical status never improved and his developmental age was equivalent to 1.7 years. At the age of 30, the patient had advanced tuberculosis with pleuritis. At age 72, he developed posttraumatic subdural hematoma, which was removed surgically. During the last six years of life, the patient was bedridden and fed *via* gastrostomy. He died of massive gastrointestinal bleeding at age 78.

General autopsy showed extensive esophageal ulcerations, hemorrhagic gastritis, and old pleural adhesions.

Neuropathological macroscopic examination revealed a small brain, 585 grams in total weight; the weight of the brain stem and cerebellum was 130 g. Bilateral areas with small and narrowed cortical gyri were noted on the surface of the frontal and parietal lobes. There was also a large cortical defect in the left fronto-temporal area involving the left superior and middle temporal gyri and the lower parts of the precentral and postcentral gyri. On coronal sections, there was almost symmetrical bilateral narrowing of the superior and middle frontal gyri (Fig. 1). The gyri of the parietal lobes were mushroom-shaped, shortened and flattened. The white matter underneath the affected cortex, as well as the deep periventricular white matter, were firm, had rubbery consistency, and showed multiple small, smooth-walled cavities (Fig. 2). The remaining central white matter appeared atrophic. The lateral ventricles, especially the posterior horns, were markedly dilated. In addition to these almost symmetrical lesions, there was an extensive defect of the cortex and the subcortical white matter involving the frontal and temporal operculum (Fig. 1). The basal ganglia, brain stem and cerebellum did not show gross abnormalities.

Microscopic examination was performed on paraffin embedded sections stained with hematoxylin and eosin (HE), Klüver-Barrera and Bielschowsky techniques.

In the sections taken from the narrowed and short frontal and parietal cortical gyri there was almost complete absence of neuronal cells. Neurons were replaced by proliferating glial cells. Prominent subpial fibrillary gliosis was noted (Fig. 3). Scattered among proliferating glial cells, in all layers of the cortex, were numerous *corpora amylacea* (Fig. 4). The density of *corpora amylacea* in any given area, seemed to be inversely proportional to the density of proliferating glial cells. In some areas of the cortex, bundles of thick myelinated fibers were noted (Fig. 5).

The white matter underneath the affected cortex showed inadequate myelination (Fig. 6) and diffuse glial proliferation. There was focal calcification in the subcortical white matter of the occipital lobes, and the small leptomeningeal blood vessels showed adventitial fibrosis. Some of these vessels also showed extensive adventitial calcification (Fig. 3). In the sections from the edge of the defect of the left hemisphere, there was an extensive, dense glial scar with numerous macrophages and with hemosiderin deposits. The sections from the grossly unaffected cortical areas showed diffuse loss of neuronal cells. The

Fig. 1. Coronal section of brain hemispheres. The cerebral gyri in the area bordering the areas of vascularization of frontal and medial cerebral arteries are damaged and narrowed. Note also a large defect of the frontal and temporal opercula

Fig. 2. Coronal section of the brain hemispheres at the parietal level. The gyri at the medial surface of the hemisphere are small and there are multiple cavities in the underlying white matter. The posterior horns of the lateral ventricles are markedly dilated

sections of the central white matter showed moderate pallor of myelin in the areas underneath the affected cortex. The brain stem showed moderate atrophy of the pyramidal tracts. No significant changes were noted in the sections of the cerebellum.

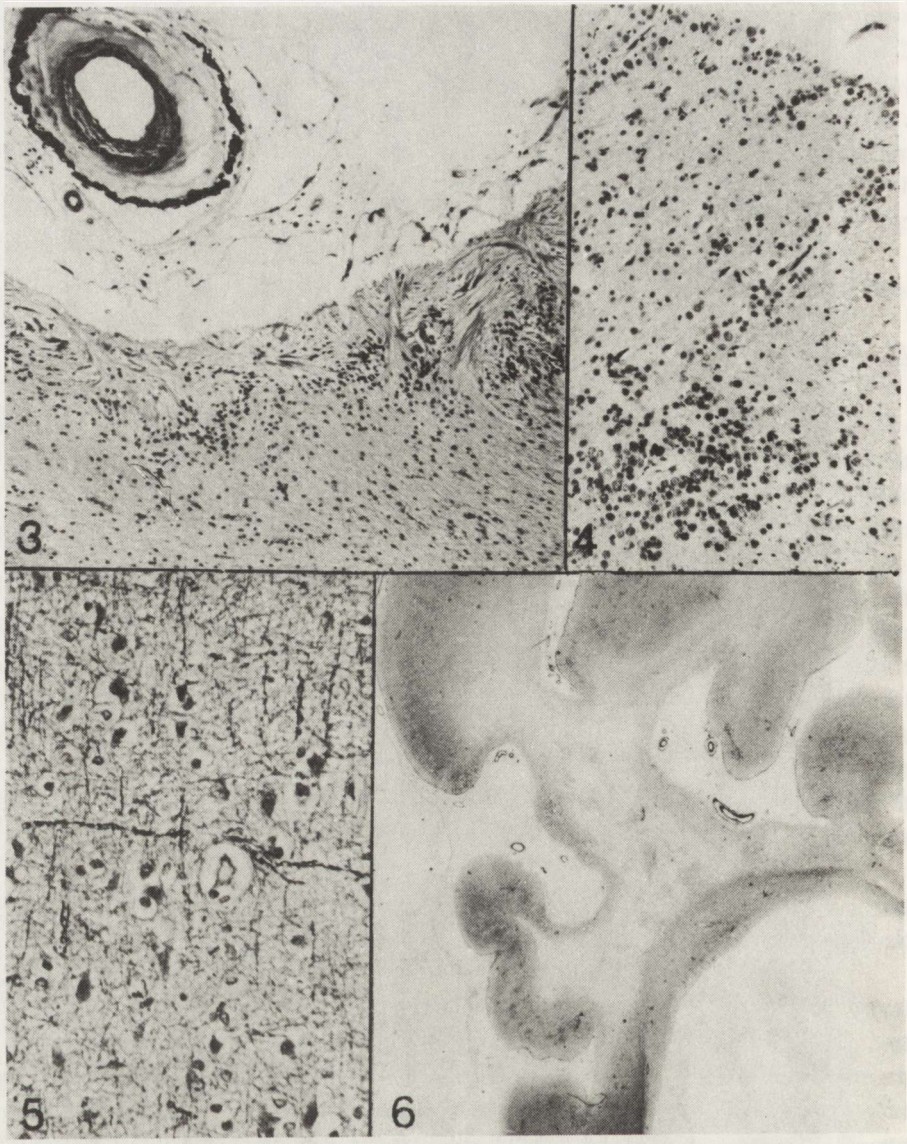

Fig. 3. Occipital cortex with glial scars of the superficial cortical layers and fibrotic leptomeningeal blood vessels showing calcification in the adventitia. HE, × 60

Fig. 4. The cortex of the medial frontal gyrus with almost complete loss of neurons. Multiple corpora amylacea are present in all cortical layers. Klüver-Barrera, × 100

Fig. 5. Frontal cortex with thick, intensely stained myelinated fibers among a few remaining neurons. Klüver-Barrera/PAS, × 200

Fig. 6. Coronal section of the occipital lobe at the level of the posterior horns of the lateral ventricles. Mushroom-shaped gyri and demyelination of the white matter are seen. Klüver-Barrera/PAS, magn. glass

DISCUSSION

In the presented case, the clinical picture of mental retardation and spastic paraparesis had stabilized at early infancy. The deterioration of the patient's clinical status in the last few years of life, was apparently the result of post-traumatic subdural hematoma. The neuropathological examination revealed the sequels of this relatively recent trauma, superimposed on the extensive old lesions, which were clearly the result of perinatal brain damage. Large cortical encephalomalacia in the area of vascularization of the left medial cerebral artery, originating from the perinatal period, was surrounded by an old glial scar. At the edge of this scar, there were scattered macrophages and hemosiderin deposits, which were the result of posttraumatic hematoma, removed surgically a few years prior to demise. The topography of the cavitary lesions in the white matter was characteristic of hypoxic-ischemic perinatal lesions, so-called multifocal cystic encephalopathy. This entity usually present multiple defects of the immature cerebral white matter, rimmed with gliosis, calcification and damaged axons (Aicardi et al. 1972; Friede 1975; Larroche 1977; Ferrer, Cervós-Navarro 1978).

The lesions found in the presented case, produced a typical clinical manifestation. Spastic diplegia, with paraparesis of the lower limbs, is usually the result of bilateral lesions in the periventricular white matter at the fronto-parietal level (Dąmbska et al. 1989; Saia et al. 1989). The distribution of lesions in the border zones of the areas of vascularization of the major cerebral arteries (anterior, medial and posterior) was particularly pronounced in the presented case. These lesions involved the white matter and cortex, in which there were focal lesions of ulegyria type. Ulegyria indicates atrophy of the gyri in which almost total loss of neurons with glial proliferation are characteristically found in the cortex in the depth of the sulci. This is usually accompanied by islands of preserved neurons in the cortex of the crowns of the gyri. These islands are usually separated by so-called "plaques fibromyeliniques" (abnormal and hypermyelinated fibers) (Bressler 1899; Norman et al. 1957; Friede 1975). In the presented case, the picture of ulegyria was modified with time, as the glial scars resulting from perinatal brain damage had time to "mature". Adjacent to the areas of fibrillar and cellular gliosis with thick, abnormal and hypermyelinated fibers, there were extensive areas with numerous corpora amylacea. These structures are usually found in the astrocytic processes (Ramsay 1965) and usually are a peculiar expression of the long lasting involution process. Another sequel of involution processes in the presented case was atrophy of brain hemispheres, which can be called secondary microencephaly.

The presented case appears to be an excellent example of the evolution of late involutionary lesions against background of typical anoxic-ischemic lesions originating from the perinatal period.

NASTĘPSTWA ZMIAN OKOŁOPORODOWYCH W OŚRODKOWYM UKŁADZIE NERWOWYM OCENIANE PO WIELOLETNIM PRZEŻYCIU

Streszczenie

Opisano przypadek 78-letniego chorego, u którego wcześnie po urodzeniu rozpoznano klinicznie zespół mózgowego porażenia dziecięcego i upośledzenie umysłowe, a w schyłkowym okresie życia doszło do pourazowego krwiaka podtwardówkowego ewakuowanego chirurgicznie. Badanie neuropatologiczne ujawniło następstwa tego względnie świeżego urazu, a przede wszystkim rozległe zmiany, które były wynikiem okołoporodowych uszkodzeń mózgu. Topografia obustronnych ognisk zwyrodnienia torbielowatego istoty białej półkul mózgu oraz korowej ulegyrii w obszarach granicznego unaczynienia tętniczego była charakterystyczna dla okołoporodowych uszkodzeń niedotlenieniowo-niedokrwiennych. Obraz ulegyrii korowej został zmodyfikowany przez czas. W miejscu rozległych ubytków neuronalnych zaznaczona była glejoza i widoczne były liczne ciała skrobiowate. Innym następstwem procesów inwolucyjnych był zanik mózgu, który można określić jako małomózgowie wtórne. Całość obrazu jest dobrym przykładem narastania zmian inwolucyjnych w typowym zespole uszkodzeń okołoporodowych.

REFERENCES

1. Aicardi J, Coutieres F, Hodebourg de Verbois A: Multicystic encephalomalacia of infants and its relation to abnormal gestation and hydrencephaly. J Neurol Sci, 1972, 15, 357–373.
2. Bresler J: Klinische und pathologisch-anatomische Beiträge zur Mikrogyrie. Arch Psychiat, 1899, 31, 566–573.
3. Dąmbska M, Laure-Kamionowska M, Schmidt-Sidor B: Early and late neuropathological changes in perinatal white matter damage. J Child Neurol, 1989, 4, 291.
4. Ferrer J, Cervós-Navarro J: Multicystic encephalomalacia of infancy. J Neurol Sci, 1978, 38, 179–189.
5. Friede RL: Developmental neuropathology. Springer-Verlag, Wien – New York, 1975.
6. Larroche JC: Developmental pathology of the neonate. Excerpta Medica, Amsterdam – London – New York, 1977, pp 399–441.
7. Norman RM, Urich H, McMenemey WH: Vascular mechanism of birth injury. Brain, 1957, 80, 49–58.
8. Ramsay HJ: Ultrastructure of corpora amylacea. J. Neuropathol Exp Neurol, 1965, 24, 25–39.
9. Saia OS, Vozzi A, Fiore A, Griffith P, Angonesse J, Zorzi C, Cantarutti F: Periventricular leukomalacia: ultrasound diagnosis and follow-up. Abstract, Ann Meet Europ Soc Pediat Res, Kraków, Poland, 1989.

Address for correspondence: I. Kuchna, Laboratory of Developmental Neuropathology, Medical Research Centre, Polish Academy of Sciences, 3 Pasteura Str., 02-093 Warszawa, Poland.

NEUROPAT. POL. 1991, 29, 1–2
PL ISSN 0028-3894

HALINA KROH

GANGLION CELLS AND THEIR SATELLITES IN EXPERIMENTAL TRIGEMINAL SCHWANNOMAS IN THE RAT

Department of Neuropathology, Medical Research Centre, Polish Academy of Sciences, Warsaw, Poland

Ten neurinomas of *ganglion semilunare nervi trigemini* induced in rats with ethylnitrosourea contained numerous neurons entrapped into solid neoplastic tissue. Ganglion cells were mostly well preserved and presented the receptors to the lectin Con A, i.e. the ability for its binding to α-glucose and α-mannose. Positive GFAP immunoreaction in neuronal satellite cells suggests that the function of satellites corresponds to that of intracerebral astrocytes and that the preservation of ganglion cells depends on their satellites.

Key words: *neurons, satellite cells, schwannomas, GFAP, Con A.*

Detection of damaged neurons in cerebral and spinal cord tissue caused by glioma infiltration is generally acknowledged, whereas incorporation of ganglion cells by solid, non-glial tumors, such as intracranial and paravertebral schwannomas in humans is uncommon (Zülch, Christensen 1956; Matyja, Kroh 1988). The purpose of this investigation is to characterize the neurons entrapped by experimental schwannomas and to determine the possible morphological conditions required for their survival in alien neoplastic tissue.

MATERIAL AND METHODS

Ten schwannomas originating from nine non-inbred Wistar rats were induced with ethylnitrosourea according to the previously published procedure (Kroh 1985). The tumors attached to the brains of seven dead or sacrificed animals (aged 170–375 days) were embedded in paraffin, the 7 μm thick sections were stained with hematoxylin and eosin, cresyl violet and according to Klüver-Barrera' and Gridley's methods. Brain sections together with the semilunar ganglion (*ganglion Gasseri*) and two upper cervical ganglia taken from an adult Wistar rat served as control material. Glial fibrillary acidic protein (GFAP) was immunohistochemically investigated with the use of polyclonal antiserum

(Dakopatts, Copenhagen), dilution 1:500, on paraffin sections by the ABC method. Paraffin sections served also for direct reaction with the lectin, *Concavalia ensiformis* (Con A), labelled with peroxidase (Sigma, USA), 20 μg/ml (Figols et al. 1990).

RESULTS

The tumors were compact, some contained small cysts. Their diameter was 0.5–1.5 cm and they were attached to the trigeminal roots. Bilateral localization occurred in one animal only. In each case the tumor caused a distinct indentation in the cerebral tissue, without any infiltration. Single or multiple oligodendrogliomas of the brain were associated with schwannomas in six animals.

The neoplastic tissue consisted of small densely packed hyperchromatic cells, with some loose areas in 5 schwannomas. Classification into Antoni A and B types could not be established. Mitotic figures were absent. Reticulin fibers were scarce and could be traced intercellularly and perivascularly. The vascularization of tumors was moderate with prevalence of thin-walled vessels of large diameter. Large cysts and necrotic foci were present in five tumors. Fragmented myelin fibers, best preserved at the periphery were present in nine tumors.

Ganglion cells scattered among neoplastic cells were of various size and exhibited normal or pathological appearance, including ghost cells (Fig. 1). Pathological changes included intracytoplasmic vacuolization, acute neuronal swelling, central tigrolysis. Chronic neuronal changes were less frequent. Some neurons of the semilunar ganglion outside schwannomas remained either normal or displayed chronic and ischemic cellular changes.

Con A receptors were best expressed as small irregular granules in the cytoplasm of well-preserved neurons, especially of the large ones and, in lesser amount, in those with pathological changes (Figs 2, 3). Neoplastic cells were negative for Con A.

GFAP immunostaining was assessed in five tumors as a narrow, irregular zone of strongly stained elements adhering to outer side of some normal ganglion cells (Fig. 4), but also around some presenting neuronal degeneration (Figs 5 and 6). Such GFAP immunoreaction was displayed also around neurons outside thick neoplastic infiltration. Edematous tissue at the border between the normal and infiltrated nerve root presented a strong positive cellular GFAP reaction. Neoplastic cells were GFAP-negative in all cases.

In the control animal, the large number of neurons of the semilunar ganglion and upper cervical ganglia expressed a strong intracytoplasmic, granular reaction with Con A, presented also by altered neurons (Figs 7a and b). The GFAP immunostaining was low and detected around the few neurons of the semilunar ganglion (Fig. 8). This reaction was difficult to trace around the neurons of cervical ganglia.

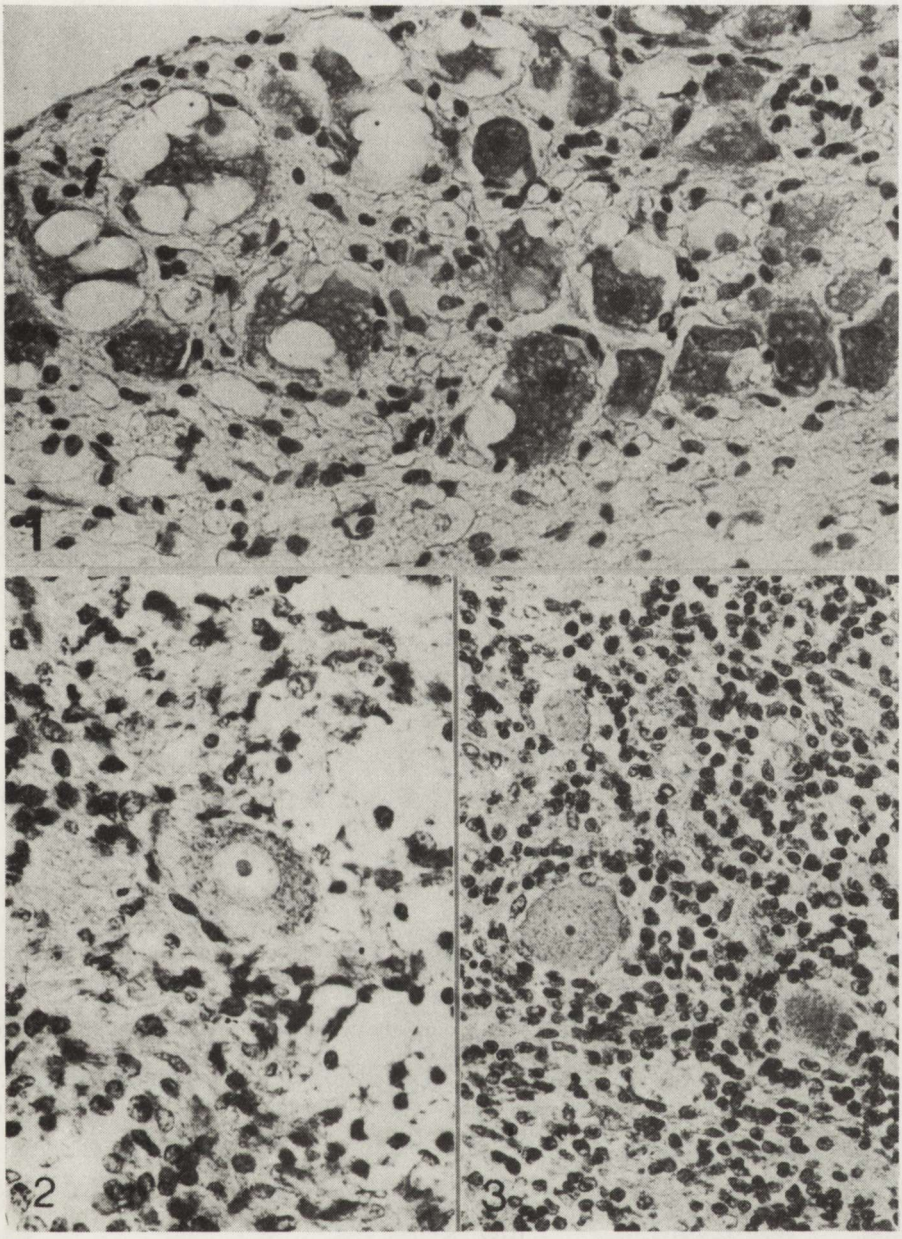

Fig. 1. Ganglion semilunare infiltrated with schwannoma cells. Vacuolization of ganglion cells. HE. ×132

Fig. 2. Schwannoma. Ganglion cell with blurred appearance of cytoplasm exhibits granular Con A acceptors. Direct PAP. ×160

Fig. 3. Schwannoma. All ganglion cells incorporated into the tumor express granular Con A acceptors. Direct PAP. ×100

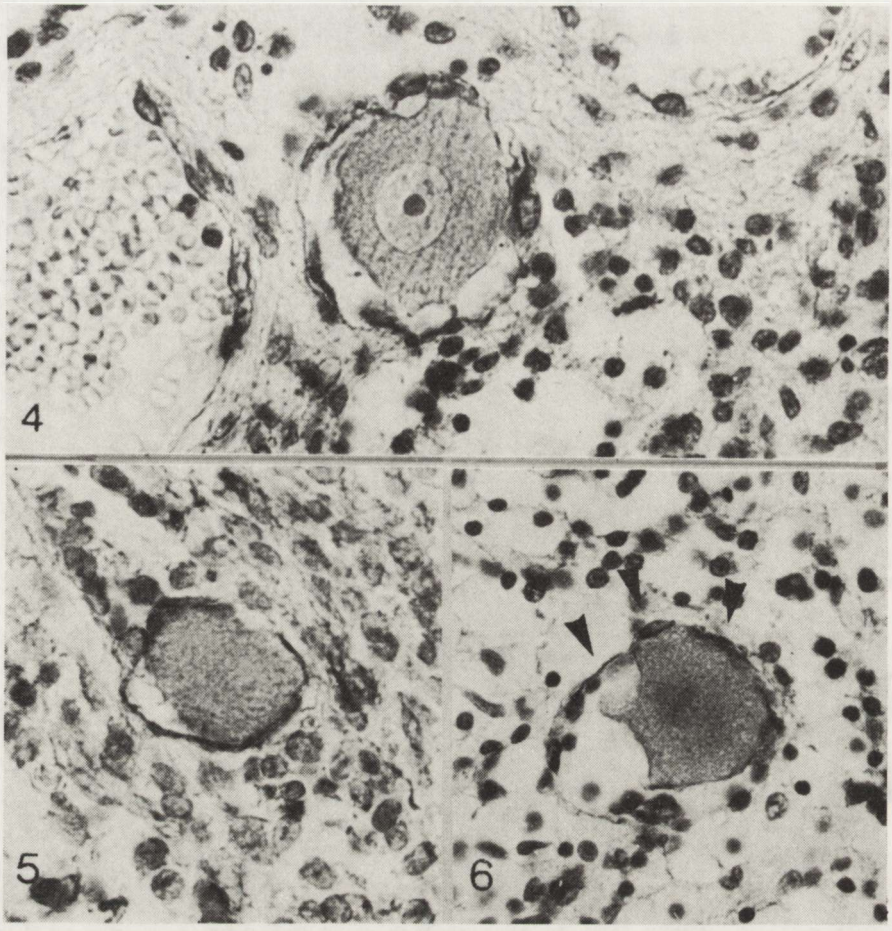

Fig. 4. Schwannoma. GFAP-positive cytoplasm of satellite cells around the unchanged ganglion cell. × 200

Fig. 5. Schwannoma. GFAP-positive reaction around the cytoplasm of pathological ganglion cell. × 200

Fig. 6. Schwannoma. GFAP-positive reaction surrounds segments of periphery of pathological neuron (arrows). × 160

DISCUSSION

Ganglion cells were often noticed in experimental schwannomas of the trigeminal nerve and spinal dorsal roots after involvement of their ganglia or autonomic trunk ganglia in the neoplastic tissue (Jänisch et al. 1967; Ivankovic, Druckrey 1968; Stavrou 1969; Zülch, Mennel 1971; Denlinger et al. 1973; Kleihues et al. 1976; Naito et al. 1981; Vinores, Koestner 1982; Kroh 1985), but only few authors paid attention to the well preserved morphology of neurons in spite

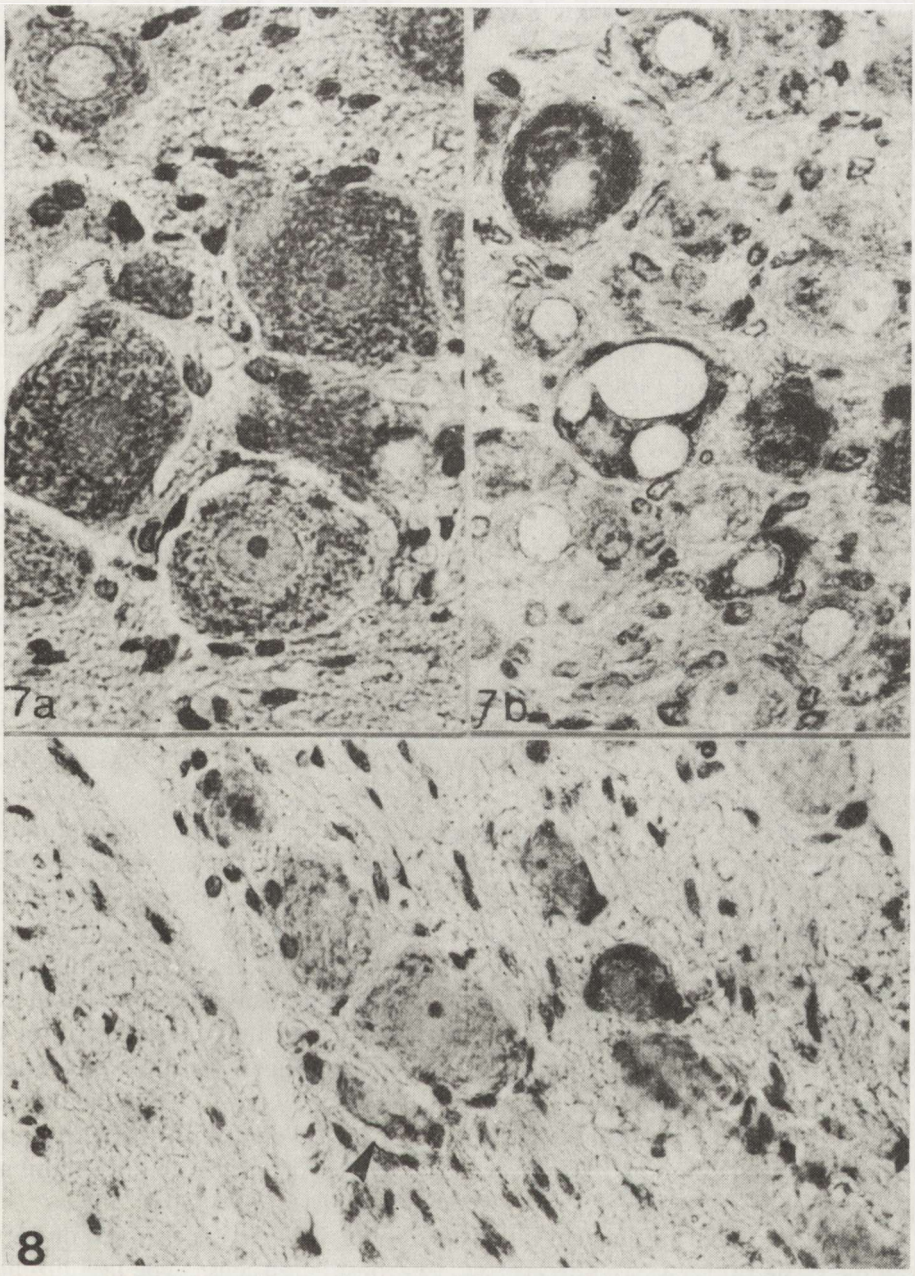

Fig. 7. Control rat: *a* — neurons of semilunar ganglion with fine Con A granules; *b* — neurons of upper cervical ganglion with Con A granules, visible also in vacuolized neuron. Direct PAP. ×160

Fig. 8. Control rat. Semilunar ganglion. Traces of GFAP immunostaining in satellite cells (arrow). ×160

of advanced damage to myelin fibers within the tumor area (Mennel, Ivankovic 1975). The presented material, chosen for its homogeneity as the tumor type and degree of anaplasia, displayed a wide range of neuronal changes. The generally accepted reasons for neuronal changes within experimental cerebral gliomas are mechanical pressure and chronic ischemia which can be also a result of abnormal vascularization and blood-brain barrier permeability (Lantos, Pilkington 1980). Abnormal permeability connected with fenestration of the endothelia in human and rat schwannomas support this view (Hirano et al. 1972a, b). Lantos and Pilkington (1980) associate the intensity of neuronal changes in gliomas with the size, type and degree of anaplasia of the tumor. Our material points only to the lack of direct relation between the intensity of neuronal alterations and their central or peripheral localization within schwannomas.

Investigations on dorsal sensory ganglia disclosed two types of neurons: type A which corresponds to the large, light, and type B corresponding to small, dark neurons (Andres 1961). The former display numerous neurofilaments, whereas the latter only a very scarce amount (Sharp et al. 1982). According to other authors (Parfianowicz et al. 1971) the large cells of the dorsal root ganglia are pure sensory neurons. These large cells increase their size in rat dorsal root ganglia parallel to the increase of body growth (Larson 1979), but there remain still some differences among the neurons of the peripheral nervous system, i.e. in the groups of neurons of cranial nerves ganglia, of dorsal roots sensory ganglia, of autonomic system ganglia, and as special subtype in the ganglion cells of the visceral organs (Smith 1961; D'Agostino 1964; Maxwell 1967; Moses 1967; Jessen, Mirsky 1980).

The binding of Con A by normal and degenerated neurons in schwannomas seems to be at variance, but was expressed mostly by the large neurons. The well-preserved neurons, like the control ones, display an intensity of reaction from strong to weak, whereas the degenerated ganglion cells show weak reaction or are deprived of it, pointing at the relationship of Con A expression with cellular metabolism of glycoproteins and glycolipids (α-mannose and α-glucose) in normal and damaged neurons. It was surmised before, that the intensity of the binding of Con A, in particular by the large neurons in the cortex, basal ganglia, anterior horns and semilunar ganglia depends mainly on the degree of differentiation of these neurons (Schwechheimer et al. 1984a, b, c). In the peritumoral area, the low differentiated neoplastic cells of neuronal origin do not exhibit any or only traces of Con A acceptors (Schwechheimer et al. 1984a).

According to early electron microscope observations, the neurons of dorsal ganglia in the rat are surounded by two typs of satellite cells: Type I (Hüllzellen) adhere to the cellular membrane as a narrow zone (150 μm–10 μ wide) and by type II cells (Schwann cells) associated with axons (Cervós-Navarro 1960). Many authors are of the opinion that both types of satellite cells contain some glial filaments (Maxwell 1967; Moses 1967; Dahl et al. 1982) and glycogen (Maxwell 1967). These data support the earlier view, that the function of satellite cells is similar to that of astrocytes in CNS (Cervós-Navarro 1960). The immunohis-

tochemical similarity of satellite cells to astrocytes has been lately confirmed by GFAP investigations though there exist several contradictory data resulting from anatomical and species differences in the peripheral and visceral neuron systems, demonstrated by poly-and monoclonal antibodies suggesting the presence of various GFAP epitopes (Achtstätter et al. 1986). It has been established that there are two types of Schwann cells which differ by their GFAP positivity (Hacker et al. 1985); the GFAP-positive Schwann cells are not associated with myelinated axons (Dahl et al. 1982; Field, Yen 1985). Therefore it seems clear, why satellite cells of sensory, sympathetic and visceral ganglia are GFAP-positive (Jessen et al. 1984). Our results prove that GFAP-positive satellite cells also adhere to the cellular membrane of some unchanged and some degenerated neurons of semilunar ganglia and in this aspect they do not diverge from other sensory ganglion cells.

Convergence of a distinct expression of the Con A by the large neurons entrapped into trigeminal schwannomas and the marked GFAP-positive immunoreaction in satellite cells points at them as the source of survival for these ganglion cells in unsuitable external conditions. It can only be surmised that as long as satellite cells are functioning, the ganglion cells preserve their function and morphology. GFAP-positivity assessed in satellite cells around the neurons with blurred appearance indicates a sustained cellular interaction. Enhanced GFAP reactivity of satellite cells around the neurons incorporated into neoplastic infiltration as compared with controls implies additional similarities to the reaction of cerebral astrocytes in pathological conditions and an analogy to the increased reaction in Schwann cells during Wallerian degeneration (Dahl et al. 1982). The distinct GFAP reaction in the trigeminal root at the boundary with neoplastic infiltration confirms this observation.

KOMÓRKI ZWOJOWE I SATELITARNE W DOŚWIADCZALNYCH NERWIAKACH NERWU TRÓJDZIELNEGO SZCZURA

Streszczenie

Na materiale 10 nerwiaków zwoju półksiężycowatego nerwu trójdzielnego wywołanych u szczurów etylonitrozomocznikiem stwierdzono, że liczne komórki zwojowe wśród zbitej tkanki nowotworowej zachowują prawidłowy wygląd histologiczny i zdolność wiązania lektyny Con A, co wskazuje na zachowane przyswajanie przez nie D-glukozy i D-mannozy. Identyfikacja GFAP w towarzyszących im komórkach satelitarnych pozwala przypuszczać, że funkcja komórek satelitarnych odpowiada czynności astrocytów względem neuronów śródmózgowych i wskazuje na zależność stanu morfologicznego komórek zwojowych od ich satelitów.

REFERENCES

1. Achtstätter T, Moll R, Anderson A, Kuhn C, Pitz S, Schwechheimer K, Franke W: Expression of glial filament protein (GFP) in nerve sheaths and non-neural cells reexamined using monoclonal antibodies, with special emphasis on the co-expression of GFAP and cytokeratins in epithelial

cells of human salivary gland and pleomorphic adenomas. Differentiation, 1986, 31, 206–227.
2. D'Agostino AN: An electron microscopic study of the trigeminal ganglion of the rat poisoned by plasmocide. Neurology, 1964, 14, 114–124.
3. Andres KH: Untersuchungen über den Feinbau von Spinalganglien. Z Zellforsch, 1961, 55, 1–48.
4. Cervós-Navarro J: Elektronenmikroskopische Untersuchungen an Spinalganglien. II Satellitenzellen. Arch Psychiat Nervenkr, 1960, 200, 267–283.
5. Dahl D, Chi NH, Miles LE, Nguyen BT, Bignami A: Glial fibrillary acidic (GFA) protein in Schwann cells: fact or artifact. J Histochem Cytochem, 1982, 30, 912–918.
6. Denlinger RH, Koestner A, Swenberg J: An experimental model for selective production of neoplasms of the peripheral nervous system. Acta Neuropathol (Berl), 1973, 23, 219–228.
7. Fields K, Shu-Hui Yen: A subset of Schwann cells in peripheral nerves contain a 50-kDa protein antigenically related to astrocyte intermediate filaments. J Neuroimmunol, 1985, 8, 311–330.
8. Figols J, Madrid JF, Cervós-Navarro J: Lectins in gliomas. Histology, Histopathology, 1990 (in press).
9. Hacker GW, Polak JM, Springall DR, Ballesta J, Cadieux A, Gu J, Trojanowski JQ, Dahl D, Marangos PJ: Antibodies to neurofilament protein and other brain proteins reveal the innervation of peripheral organs. Histochemistry, 1985, 82, 581–593.
10. Hirano A, Dembitzer H, Zimmerman H: Fenestrated blood vessels in neurilemmoma. Lab Invest, 1972a, 27, 305–309.
11. Hirano A, Hassoun' J, Zimmerman H: Some new fine structural observation of ethylnitrosourea-induced nerve tumors in rats. Lab Invest, 1972b, 27, 555–560.
12. Ivankovic S, Druckrey H: Transplazäntare Erzeugung maligner Tumoren des Nervensystems. I Athyl-nitroso-harnstoff (ANH) an BD IX Ratten. Z Krebsforsch, 1968, 71, 320–360.
13. Jänisch W, Schreiber D, Spengel R, Steffen V: Die Induktion von experimentellen Hirngeschwülsten bei Ratten mit Methylnitroscharnstoff. Exp Pathol, 1967, 1, 243–255.
14. Jessen KR, Mirsky R: Glial cells in the enteric nervous system contain glial fibrillary acidic protein. Nature, 1980, 286, 736–737.
15. Jessen KR, Thorpe R, Mirsky R: Molecular identity, distribution and heterogeneity of glial fibrillary acidic protein: an immunoblotting and immunohistochemical study of Schwann cells, enteric glia and astrocytes. J Neurocytol, 1984, 13, 187–200.
16. Kleihues P, Lantos PL, Magee PN: Chemical carcinogenesis in the nervous system. Int Rev Exp Pathol, 1976, 15, 194.
17. Kroh H: Multifocal neoplasms of the nervous system induced with ethylnitrosourea in Wistar rats. Neuropatol Pol, 1985, 23, 389–410.
18. Lantos P, Pilkington J: Neuronal changes in experimental gliomas. Neuropathol Appl Neurobiol, 1980, 6, 255–266.
19. Lawson SN: The postnatal development of large light and small dark neurons in mouse dorsal root ganglia: a statistical analysis of cell numbers and size. Neurocytology, 1979, 8, 279–294.
20. Matyja E, Kroh H: Atypical morphological components in a tumor of the cerebellopontione angle. Neuropatol Pol, 1988, 26, 558–581.
21. Maxwell D: Fine structure of the normal trigeminal ganglion in the cat and monkey. J Neurosurg, 1967, 26, 127–131.
22. Mennel HD, Ivankovic S: Experimentelle Erzeugung von Tumoren des Nervensystem. In: Handbuch der allgemeinen Pathologie. VI Band, 7 Teil-Geschwülste, Springer, Berlin – Heidelberg – New York, 1975, pp 33–104.
23. Moses HL: Comparative fine structure of the trigeminal ganglia, including human autopsy cases. J Neurosurg, 1967, 26, 112–126.
24. Naito.M, Naito Y, Ito A: Spinal tumors induced by neonatal administration of N-ethyl-N-nitrosourea in Wistar rats. Gann, 1981, 72, 30–37.
25. Parfianowicz J, Hawryłko S, Pietrzak J, Kmieć B: Morfologia i cytochemia komórek nerwowych zwojów rdzeniowych. Folia Morphol (Warsz), 1971, 30, 475–484.
26. Schwechheimer K, Weiss C, Möller P: Concanavalin A binding and neuronal differentiation. Virchows Arch (A), 1984a, 402, 297–306.

27. Schwechheimer K, Weiss G, Möller P: Concanavalin A target cells in human brain tumors. J Neurol Sci, 1984b, 63, 393–401.
28. Schwechheimer K, Weiss G, Schnabel P, Möller P: Lectin target cells in human central nervous system and the pituitary gland. Histochemistry, 1984c, 80, 165–169.
29. Sharp G, Shaw G, Weber K: Immunoelectronmicroscopical localization of the three neurofilament triplet proteins along neurofilaments of cultured dorsal root ganglion neurones. Exp Cell Res, 1982, 137, 403–413.
30. Smith KR: The fine structure of neurons of dorsal root ganglia after stimulating or cutting the sciatic nerve. J Comp Neurol, 1961, 116, 103–107.
31. Vinores S, Koestner A: Reduction of ethylnitrosourea-induced neoplastic proliferation in rat trigeminal nerves by nerve growth factor. Ca Res, 1982, 42, 1038–1040.
32. Stavrou D: Morphologische und enzymhistochemische Untersuchungen an experimentellen PNS-Tumoren der Ratte. Arch Geschwulstforsch, 1969, 34, 297–308.
33. Zülch KJ, Christensen E: Patologische Anatomie der raumbeengenden intrakraniellen Prozesse. Springer, Berlin – Heidelberg, 1956, p 377.
34. Zülch KJ, Mennel H: Die Morfologie der durch alkylierende Substanzen erzeugten Tumoren des Nervensystems. Zentralbl Neurochir, 1971, 32, 225–243.

Author's address: Department of Neuropathology, Medical Research Centre, Polish Academy of Sciences, 3 Dworkowa Str., 00-784 Warsaw, Poland.

NEUROPATOLOGIA POLSKA
V. 29, No. 1–2, 1991

Cena zł 11 000,—

CONTENTS

Indeks 36668